# Alluvial Stratigraphy and Depositional Environment of the Gangetic Plains near Kanpur using Sedimentary and Magnetic Mineralogy

By

**Partha Sarathi Bhattacharjee**

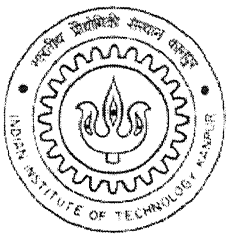


**Department of Civil Engineering**

**INDIAN INSTITUTE OF TECHNOLOGY KANPUR**

July, 2004

# Alluvial Stratigraphy and Depositional Environment of the Gangetic Plains near Kanpur using Sedimentary and Magnetic Mineralogy

A thesis submitted
In partial fulfillment of the requirements
for the degree of

**Master of Technology**

By

Partha Sarathi Bhattacharjee

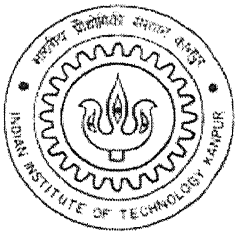


**Department of Civil Engineering**

**INDIAN INSTITUTE 0F TECHNOLOGY KANPUR**

July, 2004

# CERTIFICATE

It is certified that the work presented in this thesis entitled "**Alluvial stratigraphy and depositional environment of Gangetic plain near Kanpur using sedimentary and magnetic mineralogy**" has been carried out by Mr. Partha Sarathi Bhattacharjee (Roll No. Y210324) under our supervision and has not been submitted elsewhere for a degree.

Dr. B.C.Raymahashay
Professor
Department of Civil Engineering
Indian Institute of technology
Kanpur – 208016

Dr. Rajiv Sinha
Associate Professor
Department of Civil Engineering
Indian Institute of Technology
Kanpur- 208016

# ACKNOWLEDGEMENTS

I take this opportunity to express my deep sense of gratitude and sincere thanks to my supervisor, Dr. Rajiv Sinha for providing me consistent support and encouragement to make this thesis possible. Special thanks are due to him for providing me excellent modern laboratory facilities. The guidance and technical expertise and suggestions rendered by my co-supervisor Dr. B.C.Raymahashay, in the real time need and during the progress of this project is highly acknowledged. Particular thanks are due to both of my supervisors for painstaking reading through various drafts of my thesis and for suggesting significant improvements.

I am indebted to Dr. S.Sangode for granting me the permission and also helping me to use the Rock Magnetic facilities at Wadia Institute of Himalayan Geology, Dehradun during this work. I wish to thank Prof. M.Gibling and Prof. S.K.Tandon for their valuable suggestions during my thesis work. I am also grateful to Dr. R.P.Singh and Dr. J.N.Malik for their constant encouragement and support.

Mr. Umashankarji of X-Ray lab, Mr. S. Pal of ACMS and Mr. Girish Kumar of Engineering Geosciences laboratory helped me in various ways during the laboratory work. Special thanks is due to Kripashankarji for his timely help.

Dr. Vikrant Jain is specially thanked for his constant encouragement, valuable guidance and friendliness throughout the period of thesis work. I would like to acknowledge the help and support received from Nanida, Amlanda, Priyanka, Sagnikda, Chandrada, Anandada, Somsubhra, Subirda, Rajneesh, L.K.G Singh, Chirashree and Baral. I would also like to thank my juniors for their help. Finally, my parents and other members of my family deserve special thanks for their constant encouragement which helped me reaching this far.

Date: 12/07/04

Place: I.I.T Kanpur

Partha Sarathi Bhattacharjee

# Abstract

The Gangetic plains constitute the world's largest alluvial tract, covering an area of 8.5 million $km^2$. The major rivers in the Southern Gangetic Plains are characterized by narrow incised valleys bordered by cliffs along the southern bank and active floodplains few km wide along the northern bank. The present work focuses on the parts of the Ganga plain around Kanpur-Bithur region in Uttar Pradesh. The main aim of this work is to establish a stratigraphic framework of the area and also to understand the depositional environment of the alluvial sediments spanning about 25-30 ka. Three shallow subsurface drill cores (at IITK, Jagadishpur and Firozpur) and one exposed section (at Bithur) have been studied. Integrated laboratory and field techniques are employed to study all sections. Detailed stratigraphic logging of exposed section and the drill cores was followed up by mineralogical and environmental magnetism studies. Sediment mineralogy was studied by X-ray diffraction of powder for bulk samples and oriented slides with heating and glycolation experiments for the fine fraction. Environmental magnetic studies involved the measurement of magnetic susceptibility and magnetic mineralogical studies through induced magnetization experiments.

Startigraphic and sedimentological data suggest that the Bithur section and IITK core represent a proximal and distal floodplain environment whereas the Jagdishpur and Firozpur cores represent valley fills. Clay mineralogy and magnetic mineralogy of the sediments suggest that the alluvial successions at all sites are marked by strong discontinuities manifested in moderate pedogenesis and calcrete development. The proximal site such as the Bithur has been 'attached' and 'detached' to the main river during the last ~25-30 ka and the detachment phases are represented by swamp or eolian facies over the floodplain. Geochronological data (OSL and $^{14}C$ ages) suggest that Jagdishpur and Firozpur were sites of active channel deposition between ~26 ka and 6 ka and the area around Bithur kept accumulating floodplain sediments through overbank flooding. During this phase, the river level went down, perhaps during the Last Glacial Maximum (LGM) period represented by development of swamp and eolian facies.

Around 6 ka, the depocenter of the river shifted from the Jagdishpur-Firozpur to the preset-day position at Bithur. The river started incising the valley at Bithur in response to increased water budget between 5-6 ka thereby producing the high cliffs at Bithur. This observation is at variance with the present understanding that the dominant controls of cliff incision is tectonics and not climate and that the present-day position of the Ganga river at Bithur is ~1ka old. The area around IIT Kanpur, which forms an upland area today, remained in the distal floodplain setting at least since ~86 ka albeit with varying rates of sedimentation.

# CONTENTS

# LIST OF TABLES

# LIST OF FIGURES

# Chapter 1

# Introduction

Fluvial landforms and deposits provide one of the most readily available continental records to study environmental change. The studies on Quaternary sedimentation pattern with a view to reconstruct paleoenvironments, paleoclimates and past global changes have been recognized as active areas of research across the globe. The Indo-Gangetic plains represent the world's largest area of modern alluvial sedimentation and are of great cultural, historical interest for long time. Topographically, the plains are homogeneous, with only floodplain bluffs and other related features of river erosion and changes in river channels forming important natural features. The Ganga plain occupies a central position in the Indo-Gangetic Plain, roughly between Longitude $77^0$E and $88^0$E, and Latitude $24^0$N and $30^0$N, and shows a variety of landforms and drainage system. The Ganga river with sub-parallel drainage pattern of the main tributaries such as the Yamuna is the axial river following the regional slope towards SE in the Gangetic plain. The Ganga plain extends from Siwalik foothills in the north to the Bundelkhand craton in the south; from Aravalli-Delhi ridge in the west to the Rajmahal hills in the east. Fluvial landforms and alluvial sediments in the Gangetic plain are important Quaternary continental records, which are helpful to examine tectonic, climatic and lithological controls over their formation.

The present work focuses on parts of the Ganga plain around Kanpur-Bithur region, Uttar Pradesh representing the Central Ganga plain (Fig. 1.1). The Ganga river is flowing SE in this study window and the city of Kanpur is located at the western bank of the river. The river is braided in most parts with low sinuosity. At Bithur and Jajmau area bank sections up to 15m are exposed along the southern bank extending for nearly 2 km in SE-NW direction. Figure 1.2 shows a False color composite (FCC) (from IRS-1C LISS III imagery of May, 1997) of the study area on to which major geomorphic units after Sinha et al. (2002) and Babu (2003) has been superimposed. A large meander scar on the northern bank of the river is a prominent feature. This work is aimed at understanding

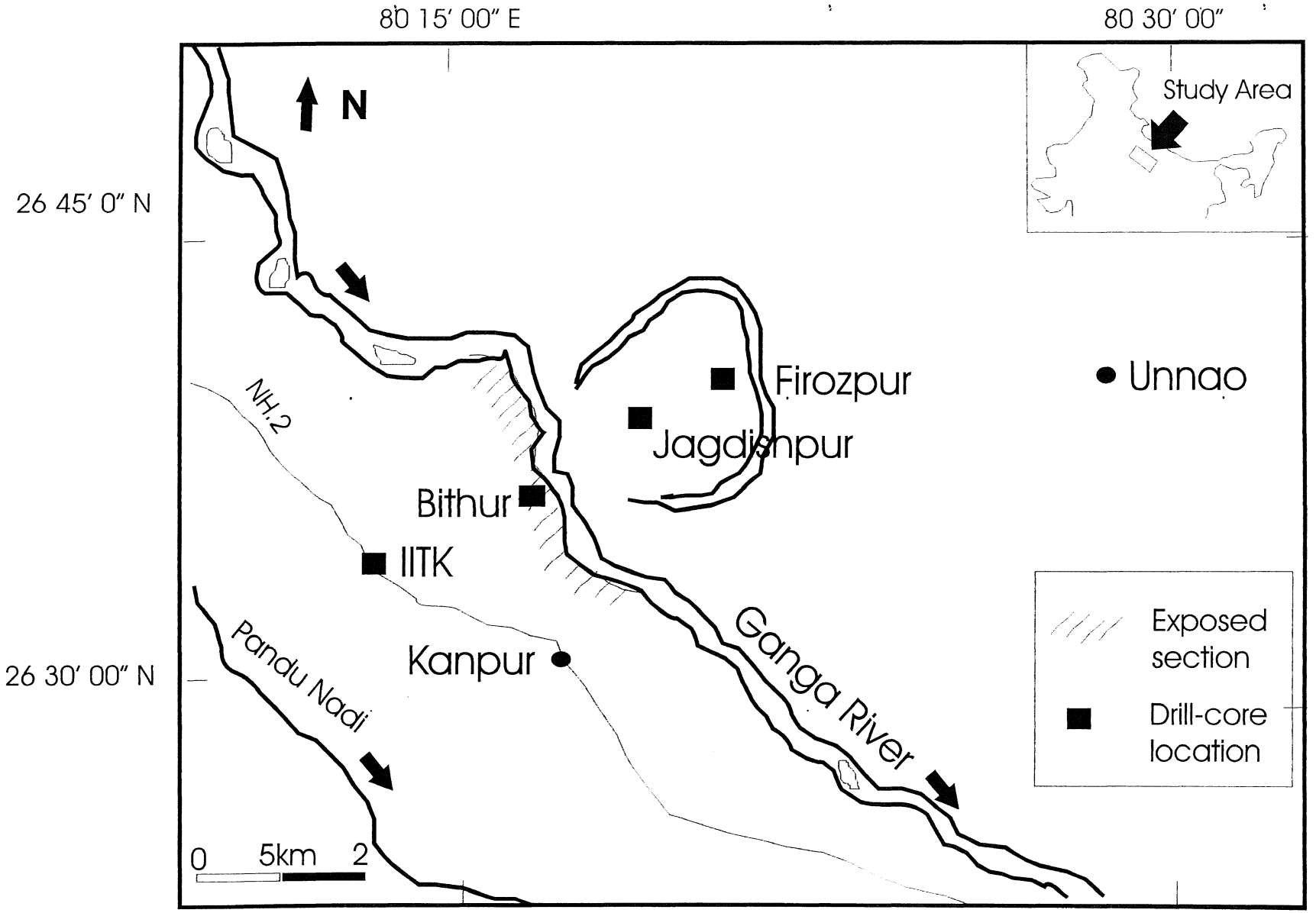


Fig. 1.1. Location map of the study area.

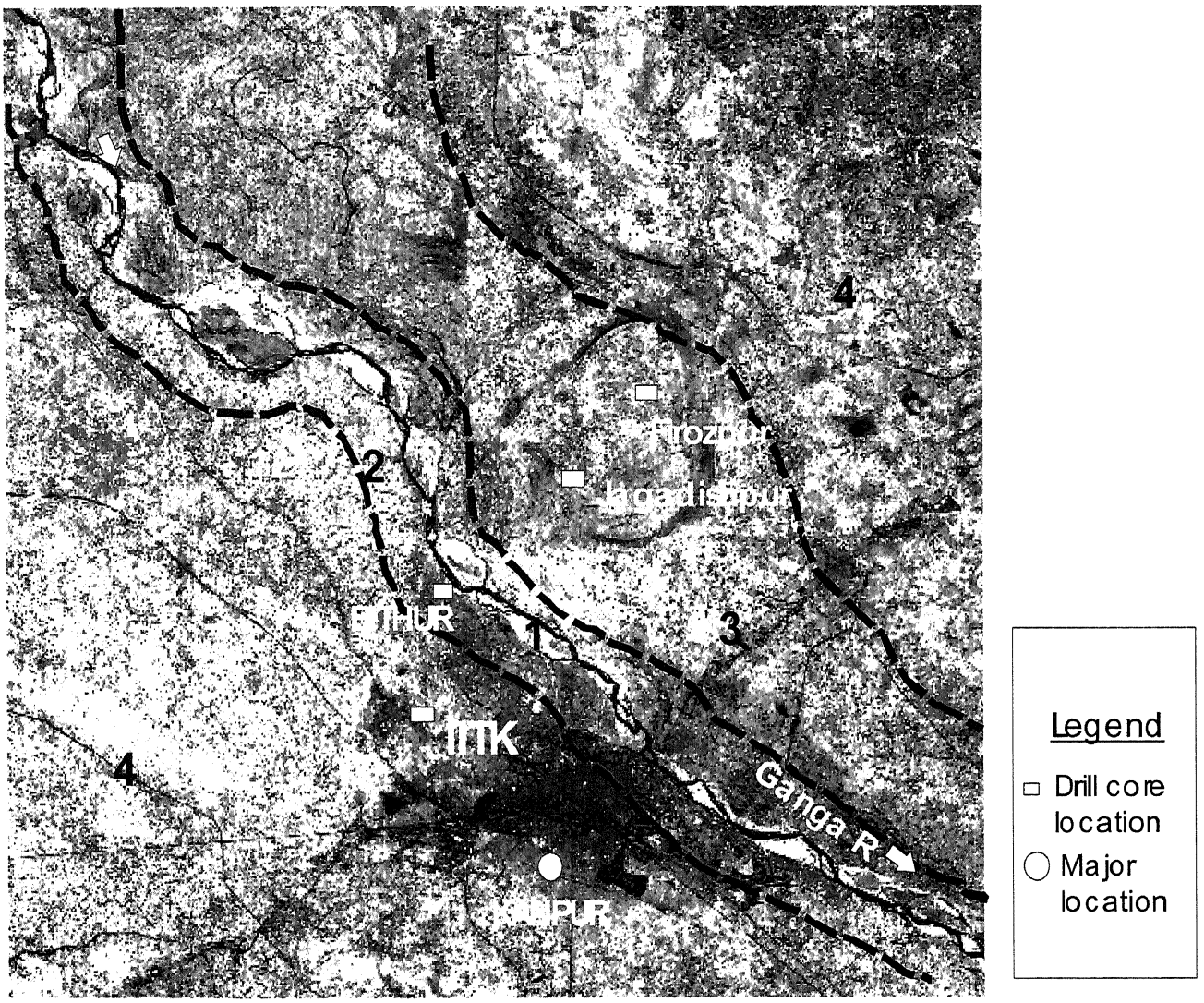


Figure 1.2 Geomorphic map of the study area; with locations of drill cores shown
Unit-1: present day channel,, unit-2: Upland section, Unit-3 : Channel fill, Unit-4 : interfluve

stratigraphic development in this region using exposed sections and shallow subsurface drill-cores.

## 1.2 Specific objectives of this work

The present work was formulated with the following objectives:

- Establish a stratigraphic framework in the Ganga plain around Kanpur and identify major discontinuities through exposed sections and drill cores.
- Identify and characterize the sedimentary facies using sedimentologic and mineralogic criteria.
- Investigate the magnetic mineralogy of the alluvial sediments in the Ganga plains to characterize post-depositional processes
- Integrate all data to understand the stratigraphic development and depositional environment in the region.

## 1.3 Approach

Figure 1.3 shows a flow diagram outlining the methodology followed in this work and the data used. Major staratigraphic units were identified in the exposed section an drill cores based on detailed logging. Sediment samples were collected from different units and were analysed for grain size, organic matter content, mineralogy and magnetic characteristics. All data was then integrated for interpreting the depositional environment and facies development at each site. A regional correlation was established to understand the general stratigraphic development in the study area.

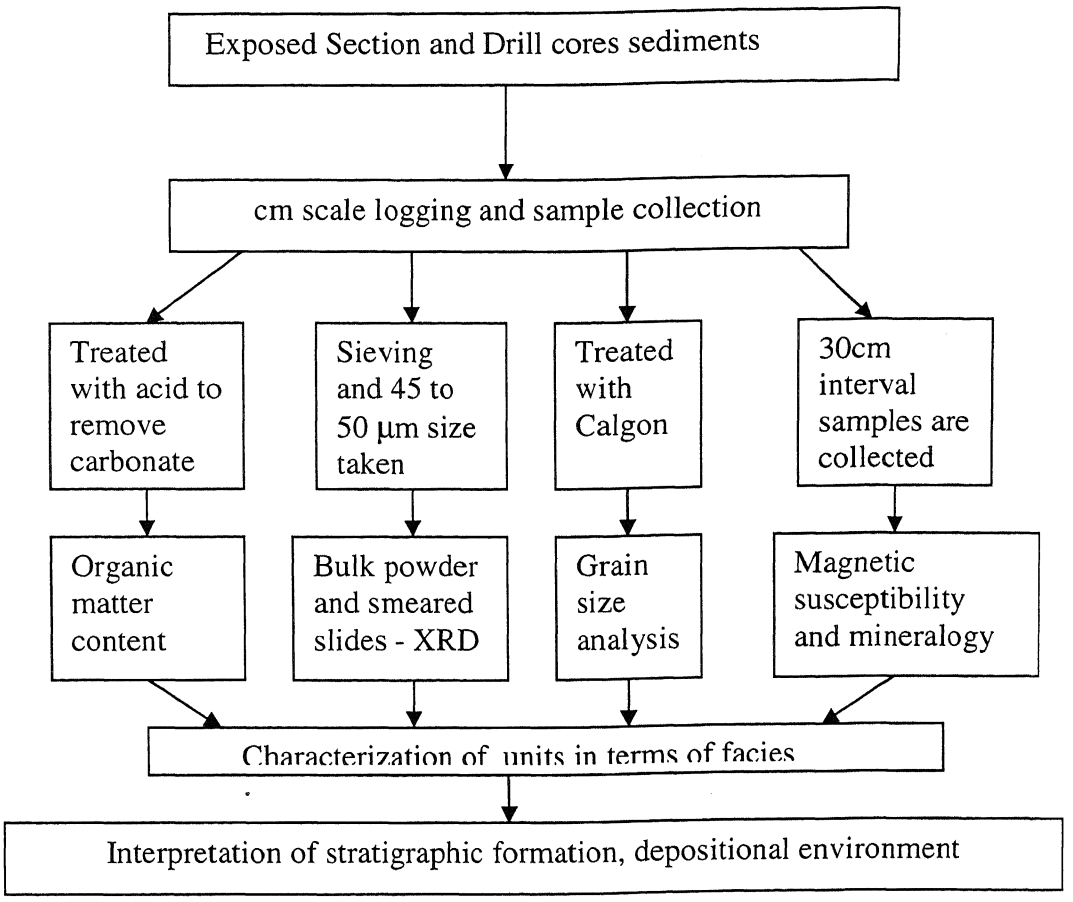


Figure 1.3 Flow diagram showing methodology followed in present study

## 1.4 Organization of thesis

The thesis has been organized into five different chapters. Chapter 1 gives the introduction of the study area, objective of the present work and Chapter-2 presents the literature review. Chapter 3 presents the various field and analytical methods used for this study. In Chapter 4, stratigraphy and sedimentology of the exposed section at Bithur and the three drill cores have been discussed. Finally, Chapter 5 presents the summary and conclusion of the thesis.

# Chapter-2

## Literature Review

### 2.1 General Geology

The Indo-Gangetic plains are the large alluvial plains of the Ganga, Indus and Bramhaputra rivers and their tributaries, and separate the Himalayan range from the Peninsular India. These plains in the world cover an area of about 1.75 million $km^2$ and form a major part of an active foreland basin with an east-west elongated shape. The basin formed in response to the uplift of Himalaya after the collision of India and China plates (Dewey and Bird, 1970). The sedimentation in the basin is considered to have started with shallow marine environment, gradually changing into estuarine and deltaic with time. By Mid-Miocene, the sedimentation was dominated by fluvial environment and continued to the Recent. The southern margin of the Ganga plain is irregular, showing outcrops of rocks in the alluvium, while the northern margin is marked by the exposure of Siwalik rocks; the contact is marked by a thrust (Himalayan Frontal Thrust). Tectonic processes have affected its evolution through time (Prakash and Kumar, 1991) From north to south, the Ganga plain is divided into three geomorphic divisions; piedmont zone, bordering the Himalayan front, central alluvium plain and marginal alluvial plain bordering the peninsular hills (Singh, 1996). Geographically it is divided into upper middle and lower Ganga plain (Singh and Ghosh, 1994).

A number of regional geophysical studies have been carried out over the Gangetic plain, including aeromagnetic, seismic, gravity and magnetic surveys. The thickness of alluvium is 6 km near the foothill zone and decreases gradually towards south (Rao, 1973). The Ganga plain is characterized by three subsurface ridges, i.e. Delhi-Hardwar ridge in the west, Faizabad ridge in the middle and Monghyr-Saharsa ridge in the east (Rao, 1973; Prakash and Kumar, 1991). The Ganga plain is traversed by several transverse and oblique subsurface faults (Dasgupta, 1987 and 1993; Valdiya, 1976) and the seismic data showed that most of these faults are active in nature. The seismic data

also indicate a profound unconformity at varying depths in the Bareily –Lucknow shelf, which is relatively shallow in the southern portion near peninsular shield and slopes towards north gently at first and then deeper near the foothills.

## 2.2 Neotectonics and Fluvial Geomorphology

A number of studies focused on the neotectonic influence on channel movements in the Gangetic plains in Uttar Pradesh (U.P) using remote sensing and field data started in early 70's. Singh and Rastogi (1973) inferred E-W and WNW-ESE running weak zones on the basis of flow direction of tributaries and river entrenchment, presence of escarpments and extension of floodplains. They were also of the opinion that the Ganga river in Uttar Pradesh is flowing along a weak zone, causing subsidence along the northern bank of the river and subsequent uplift along the southern bank. Gokhale and Bajpai (1986) and Bajpai (1989) produced some of the early geomorphic maps of this region based on Landsat images and related the N-NE flowing drainage in the southern marginal part of the Gangetic plain with the basement lineaments. A subsurface evidence of neotectonism along the Ganga river in Kanpur –Unnao region is represented by sudden deepening of the granite basement towards north. Above the basement, there is a succession of sediments derived from the peninsular source, dominated by the pink colored arkosic sand. This zone is overlain by a sequence of sediments of Himalayan source, which are gray colored micaceous sub-graywacke type. Singh and Bajpai (1990) inferred the NW-SE trending lineaments in the area around Kanpur on the basis of the variation in sedimentation pattern, thickness on both side of lineaments. Later work (Singh et al., 1990; Singh and Ghosh, 1994; Singh, 1996) recognized regional geomorphological features in the Gangetic plains and related these to climatic fluctuations in the Quaternary period. Three regional scale terrace surfaces in the Central Gangetic plain, marked as $T_0$, $T_1$ and $T_2$ were identified. The $T_0$ surface is marked by narrow active floodplain surface characterized by channel bars, levees, meander cutoffs, oxbow lakes and is the youngest geomorphic horizon. The $T_1$ surface located several meters higher than the $T_0$ surface, is marked as river valley terrace, and shows extensive development of abandoned channels, meander cutoffs and other floodplain features. The $T_2$ surface is the upland terrace surface and the oldest geomorphic surface. It has been

argued that these geomorphological features are related to climatic and sea level changes in during Pleistocene-Holocene period (Singh et al, 1990). However, recent workers on the Ganga plain (Sinha et al., 2002; Sinha and Jain. 2002; Jain and Sinha, 2003) are of the opinion that sea-level fluctuation will have little influence on the geomorphic development in the Ganga plain in U.P. Work by Schumm, (1993), Blum and Tornquist, (2000) emphasized that sea-level influence on the river systems are restricted to less than 400 Kms, ruling out its influence in parts of the Ganga plain in UP which is 1200 Kms inland from the sea. Schumm (1993) also pointed out that the delivery of large amounts of sediment to a shoreline probably reflects not only base level lowering, but also significant uplift of the sediment-source area and climate change. Singh et al. (1990) have also suggested that the $T_1$ surface is an older surface formed by a paleo-Ganga river during 25-30 Ka and during this time interval, the river underwent a distinct change form meandering type to present day braided type due to decrease in water budget along with increase in sediment load. However, a recent study based on luminescence chronology of the Kanpur area by Srivastava et al. (2002) has concluded that this change or metamorphosis in the Ganga river occurred between 1.5 and 0.5 Ka.

## 2.3 Stratigraphy and Sedimentology

Several studies of the Gangetic plain have focused on the geomorphology of the plain along with sedimentology, stratigraphic, paleoclimatic study to record the climatic variations and depositional characteristics of the alluvium. Gokhale (1971) used the subsurface bore hole data in the IIT Kanpur campus for hydro- geologic information. He reported presence of pink garnet, zircon, tourmaline and hornblende as the heavy mineral assemblage in the shallow, laterally discontinuous aquifers (between 45m to 60m). In the deeper aquifers between 100 to 110m, hornblende was absent. Large concretions of carbonate composition (Kankars) were reported from both upper and lower aquifer. Singh (1973) carried out mineralogical and petrographical studies of the samples from the subsurface alluvium near Lucknow and characterize sediments on the basis of the heavy mineral and clay mineral assemblages. He suggested the Himalayan origin of the sediments and a quick deposition rate of the sediments supplied. Singh (1997) observed the cliff section along the Senegar river, exposed for about 200m, showing two prominent

sets of fractures affecting the entire succession of the cliff. These fractures were interpreted to be the product of extensional processes in response to consistent tectonic stress conditions. Singh et al. (1999), Sinha et al. (2002) and Banerjee (2002) worked on the exposed section near Kalpi, on the Jamuna bank, identified stratigraphic horizons and paleosol layer. Clay mineral assemblages of a soil profile were used as potential indicator for paleoclimatic changes during Holocene in the Gangetic plain between Ramganga and Rapti rivers (Srivastava and Parkash, 1994). Srivastava et al. (2003) worked on the abandoned channel belts, ponds and point bar deposits of paleochannels in the interfluve regions of the Central Ganga plain, suggesting changes in the morpho-hydrologic conditions during the Pleistocene- Holocene. They concluded that the initiation of channels and abandonment, formation of ponds and their siltation, were controlled by the monsoon change and tectonic activity. Gibling et al. (in press) have proposed an attachment-detachment model for the southern Gangetic plain rivers using stratigraphic, sedimentological and geochronological data. According to the model, floodplains were attached to the major rivers prior to 27 ka BP, but later became detached and have since degraded or accumulated sediment locally. A comparison with proxy records of monsoon intensity suggests that the detachment reflects decreased precipitation around the Last Glacial Maximum. High precipitation during 15-5 ka period increased discharge of Himalayan and Cratonic rivers promoting cliff- line incision.

## 2.4 Carbonate concretion study

Carbonate concretion or 'kankars' are defined as near surface, terrestrial, secondary calcium carbonate accumulations in soil profiles, bedrocks and sediments introduced by displacive/replacive and passive modes of deposition (Tandon, 1999). Most of the kankar samples possesse pits and solution cavities on the outer surface. There are two principal types of kankars, namely, (a) cemented sands consisting of finely divided carbonate minerals in pore spaces and (b) carbonate nodules containing segregation of calcareous materials in lumps within the sandy and clayey sediments (Wadia, 1975). They commonly occur in both Quaternary and pre-Quaternary continental and marginal marine sequences and are of value in paleoenvironment and paleoclimatic interpretation

(Wright and Tucker, 1991). Kankars are widespread in semi-arid regions (rainfall zone of 400-600 mm), but groundwater kankars may however occur in annual rainfall zones of 1000-1500 mm (Seminuik and Searle, 1985). Kankars can form in near surface conditions by weathering processes (pedogenic), accumulation or replacement in subsoil by groundwater action (non-pedogenic) or by capillary water (capillary-fringe) (Carlisle, 1983). There are widespread surface and sub-surface occurrences of carbonate concretions (calcrete/ kankar) in the alluvium of the Gangetic plains. Deposition of Kankar is extensive in the central and southern part of the Ganga plain on the $T_2$ surface (Agarwal, 1992). It has been reported that the groundwater in the Gangetic plains is supersaturated with respect to carbonate minerals leading to precipitation of carbonates in pore spaces and formation of the concretions (Raymahashay & Chaturvedi, 1981). However, the non-pedogenic calcretes are difficult to distinguish from the pedogenic calcretes in the areas where water table fluctuation has taken place during different time period.

## 2.5 Magnetic Mineralogy and Susceptibility

During the last decade, the study of rock magnetism to reconstruct paleoclimate has gained much attention. More recently, the properties of magnetic minerals are used extensively to paleoclimate analysis (Mullins, 1977; Maher, 1998), paleo-oceanographic studies (Bloemendal and DeMenocal, 1989; Berger, 1988, Lean and McCave, 1998; Barthes et al., 1999), biomagnetism (Bazylinski and Moskowitz, 1997), studies of distribution and extent of anthropogenically induced pollutants (Flanders, 1994) and archeological studies (Dalan and Banerjee, 1998). Because of this extensive use of rock magnetism based on "non-directional" mineral characteristics, it is more popularly called as mineral magnetism (Maher, 1988). Various types of magnetic minerals are listed in Table 2.1.

**Table 2.1: Types of magnetic minerals**

| Magnetic minerals | Definition and characteristics | Examples |
|---|---|---|
| Diamagnetic | Magnetism in all materials- arising from the orbital motion of electrons | Quartz, Calcite |
| Paramagnetic | Magnetism arising from the spin of electrons | Siderite, Pyrite |
| Ferromagnetic | A form of magnetism characterized by strong interaction between atoms in the crystal lattice | Iron, Nickel, Cobalt |
| Antiferromgnetic | A form of ferromagnetism in which crystalline material involved contains two sub-lattices that are oppositely and equally magnetized leading to zero net magnetism | Hematite, Goethite |
| Ferrimagnetic | A form of ferromagnetism in which crystalline material involved contains two sub-lattices that are oppositely but unequally magnetized | Magnetite, Pyrrhotite ($Fe_7S_8$) |

Ferrimagnetic minerals are divided into small regions in which magnetization is uniform, but the magnetization vector within each region differs form that of its neighbors. These regions are called "magnetic domains" and they arise from the minimization of the overall energy budget of the sample. The direction of domain magnetization is determined by crystallographic structure (Evans and Heller, 2003). In all grains except very fine grains, the domains are mutually oriented so that the total magnetization of a ferrimagnetic body may have any value between zero and saturation, depending upon the fields to which it is exposed (Radhakrishnamurty, 1985). Various types of magnetic domains are listed in Table 2.2.

**Table 2.2. Various Magnetic domains**

| Magnetic Domains | Definitions |
|---|---|
| Multi-Domain (MD) | A state in which magnetic material is divided into several domains, the magnetization is uniform in each domain but differs in directions from domain to domain. (>70μm) |
| Pseudo Single Domain (PSD) | Magnetic structure and behavior is intermediate between SD and MD, in which particles contain more than one domain, but exhibit many of the properties typical to SD particles |
| Single Domain (SD) | A type of magnetic structure in which a particle is uniformly magnetized, i.e. all the atomic moments are aligned parallel (<0.2 μm) |
| Superparamagnetic (SP) | Very small particles have relaxation times on the laboratory timescale (<0.03μm) |

Mineral magnetic properties are sensitive, require little sample preparation, rapid, often grain-size indicative and non-destructive. Measurement of mineral magnetism in

sediments is highly specific to Fe and very sensitive to particular minerals especially strong ferrimagnets like magnetite. Magnetic minerals get into the soil, eolian deposit, and water laid-sediments in two major ways; (a) Detrital origin, where during weathering of igneous/metamorphic rocks, iron minerals is released from the rocks and are transported by wind, rivers into the current location and (b) they are created or transformed in-situ. Identification of ferrimagnetic minerals like magnetite ($Fe^{2+}O$, $Fe^{3+}{}_2O_3$), or antiferromgnetic mineral like hematite ($Fe_2O_3$) and goethite (FeO.OH) in fluvial sequence is important as they depict the changes in depositional conditions. In the fluvial environment, erosion in the upstream catchment gives rise to iron bearing ions (source mainly from Fe-pyroxenes, biotite) which are then carried by the river and deposited downstream and undergo chemical changes. Iron is released as ferrous state; undergo oxidation during transportation to ferric state and precipitate. Chemical reactions such as oxidation and hydration are responsible for the formation of hematite and goethite (Evans and Heller, 2003). During the time of water logging of soil/sediment, iron is leached out due to reduction, influenced by microbial activity (Borggard, 1997). Lowering of water table or sub aerial exposure of the soil or sediment causes oxidation of soil profile and subsequent precipitation of iron as iron hydroxide, $Fe(OH)_3$, which dehydrates to form goethite. Development of mottled zone thus indicates selective oxidation and reduction of iron.

$2Fe_3O_4$ (magnetite) + $0.5O_2$ = $3Fe_2O_3$ (hematite) (Oxidation)

2FeOOH (goethite) $\leftrightarrow$ $Fe_2O_3$ (hematite) + $H_2O$ (Hydration and dehydration)

The above chemical reactions occur during soil-forming processes in a sedimentary sequence. Alternatively, the presence of these minerals in sediments would indicate weathering of the sediments, break or hiatus in sedimentation and also presence of arid climatic conditions. Magnetite forms either from the pre-existing iron-bearing minerals by alteration or oxidation or precipitates directly form iron solutions. In the last case, biogenic mediation through bacterial activity is important (Evans and Heller, 2003). Magnetite in sediments, particularly SP particles size magnetites, may indicate high bacterial activity and more humid conditions. Mineral magnetic techniques would

therefore allow quantitative and qualitative analysis of Fe oxides and determination of sedimentary environments, degree of pedogenesis and detrital vs. authigenic composition (Verosub and Roberts, 1995). The mineral magnetic analysis has two components, one is determination of magnetic susceptibility and the other one is characterizing magnetic mineralogy by remanence study. These two components are then put together to characterize magnetic mineralogy and their grain size.

**Table 2.3: Magnetic parameters**

| Parameters | Definition | Possible Interpretation |
|---|---|---|
| K and $\chi$ | Magnetic Susceptibility: The ratio of induced magnetization to the applied magnetic field. | Bulk magnetic mineral content of the sample |
| $\chi_{fd}$ | Frequency dependable susceptibility: The variation of susceptibility between high field and low field. Indicates the presence of grains lying at the stable SD/SP boundary | High values (> 5%) indicate very fine ferrimagnetic grains (<0.02 μm) |
| $Bo_{cr}$ | Reverse field strength required to return a magnetized sample its saturation isothermal remanence to zero (unit- mT). | High values indicate anti-ferromagnetic minerals, whereas low values (<40) indicate ferrimagnetic minerals. |
| $\chi_{ARM}$ | Sample is subjected to strong alternative field decaying to zero in the presence of small steady field | Varies with Single Domain particles. |
| S-Ratio | Ratio between antiferromgnetic and ferrimagnetic minerals; obtained by using $IRM_{-300}$mTand Saturated IRM (SIRM2500 mT) | Indicates proportion of antiferromgnetic and ferrimagnetic minerals; Relative changes in the oxidative to reductive conditions |
| G/H | Represent Goethite/Hematite ratio; G is obtained from IRM $_{2.5-1}$ T field and H is obtained from IRM $_{1-0.5}$ T field | Relative hydroxylation to dehydroxylation conditions; |
| SIRM | Saturation Isothermal Magnetisation: the highest level of magnetic remanance induced in sample by application of a high field (2.5T). | Indicates Volume concentration of magnetic minerals in a sample |
| SIRM/$\chi_{lf}$ | Ratio between two parameters indicative of magnetic grain size | Very low value theoretically zero indicates presence of paramagnetic minerals, and higher values attributed to PSD/SD/SP particles. |

Magnetic susceptibility and mineralogy have been used successfully for interpretation of paleoclimatic fluctuations in loess-paleosol sequences, marine and lacustrine deposits. In China, alternating loess-paleosol strata show considerable variations in susceptibility, where in cold, dry glacial periods wind blown dust accumulated (low susceptibility) and

in the interglacial period, soils are formed (high susceptibility) (Evans and Heller, 1995). The variable magnetic mineralogy of the sediment cores of the Lake Manas points to changes between lacustrine and fluviatile depositions (Jelinowska et al., 1995). Peek et al. (1994) reported on the mineral magnetic properties of slowly deposited Quaternary sediments from Lake Baikal (Siberia) and correlated the record to the oxygen isotope time scale derived from the marine sediments. Magnetic properties of paleosols developed in Quaternary sequences of loess have been used for stratigraphic correlation with other terrestrial and deep sea sequences and paleoclimatic reconstruction (Maher, 1998). In loess/paleosol sequences role of magnetic enhancement and their dilution are investigated for a range of modern soil types. Magnetic enhancement is seen in the upper horizons of well-drained cambisols, whereas dilution of magnetic iron oxide is apparent in podsol profiles and waterlogged soils (Maher and Thompson, 1995; Maher, 1998). The mineral magnetic analysis of sediment cores recording recent soil history in central Tanzania reflects two different depositional environments. High antiferroamgnetic minerals and post-depositional dilution of ferrimangetic minerals indicating swamp type deposit and ferrimangetic assemblage characterizing lake sediments. The soil erosional history of catchments was reconstructed using mineral magnetic parameters (Eriksson and Sandgren, 1999). A correlation between pedogenic magnetic content and climate, particularly rainfall, is established from Quaternary loess/paleosol sequences of Central Asia (Maher et. al. 2003).

In India, pedogenic horizons from Upper Siwalik rocks were identified using rock magnetic parameters to investigate their climatic and stratigraphic significance (Sangode et al, 2001). Magnetic susceptibility analysis for sediments from the riverine, estuarine and marine environments in west coast of India is done to understand the behavior of magnetic minerals as they enter oceanic realm through estuary (Karbassi and Shankar, 1994). The results shows magnetic mineral content decreases from the river head to river mouth and in the riverine environment, magnetic minerals show bimodal distribution. Rock magnetic ratios in the Late Cenozoic fluvial sequences from NW Himalaya contain information on dynamic pedogenic transformation of magnetic minerals with time and use of magnetic susceptibility for basin source modeling has been demonstrated (Sangode

and Kumar, 2003). Spatial distribution of magnetic susceptibility in 13 cores from the western part of the Bengal sub-marine fan indicates predominance of Godavari river source during the late Quaternary and weakening of the Himalayan source after Last Glacial Maxima i.e. between 23-14 Ka BP (Sangode et al. 2001).

# Chapter 3

# METHODS

## 3.1 Stratigraphic analysis of the exposed section and drill cores

As discussed in the chapter 1, the main objective of the present work is to establish stratigraphical and sedimentological parameters for the near surface sections and shallow subsurface sections. The near surface stratigraphy in the region is generally made up of alluvial sediments deposited by the Ganga river its tributaries. One of best ways to establish vertical as well as lateral stratigraphic variation is to look at the bank sections along the rivers. Nearly 2 km long cliff section exposed along the southern bank of the river Ganga at Bithur trending SE-NW offers such an opportunity. The average height of the section is 10m, though at places it reaches up to 15m. The strata present at Bithur section are homogeneous and many of them are continuous over 1.5 km. Serial photos were used to prepare a photomosaic and individual sedimentary layers were traced along the cliffs. Three stratigraphic logs (from E-W) were made along the exposed section for documentation of lithological and sedimentological characteristics. The present-day water level of the river was taken as the base for each log. Detailed description of lithology, grain size, kankars, mottling of the each layer was recorded on cm scale and major stratigraphic units were identified in the section. Samples from each unit were taken for the analysis of grain size, mineralogy, organic matter, and magnetic susceptibility. Based on litho-logs and sedimentological analysis, each unit was characterized in terms of sedimentary facies and depositional environment.

Further, as a part of the continuing research programme at IIT Kanpur, we have carried out drilling at different locations in the Central and southern Ganga plain. Out of these, three drill cores in the study window were chosen for this work (see Fig.1.2 for locations of drill holes). One of the drill locations (BH-1) was located in the IIT Kanpur campus representing the 'upland' location in the interfluve south of the Ganga river (see Fig. 1.2). The other two drill hole locations (BH2 and BH3) are located at Firozpur and Jagdishpur respectively within the present-day valley of the Ganga river at the northern side. Both of these locations fall within the large meander scar at the north side of the Ganga river, the

Firozpur site being towards the edge of the meander loop while the Jagadishpur site located towards the center.

The drilling was done using a diamond core drilling bit involving a double barrel core tube. A PVC pipe was inserted inside the core tube. In a muddy sequence, a slow rotary method was used with close to 100% core recovery. In sandy sequences, a combination of rotary and percussion method was used to arrest the core with a slightly lesser core recovery (70-80%) including a slight compaction due to percussion. The core obtained in the PVC pipes were taken to the laboratory and split into two halves. One half was preserved and other half was used for logging and sampling. Total drill depths of IITK, Firozpur, Jagadishpur sites were 48.6m, 24m and 24.6m respectively. Core loss was estimated to be around 15%, but a slightly higher core loss occurred at the two latter sites being predominantly sandy.

Detailed logging of the cores at cm scale involved description of color, grain size, texture, kankars, mottling and other special features, if any. Munsell color chart and binocular microscope, grain size chart were used in describing cores. On the basis of the physical and sedimentological characteristics, the cores were divided into different lithostratigraphic units and further analyses were carried out to characterize these units.

## 3.2 Grain size Analysis

Samples collected from the exposed section and drill cores were air-dried and put in an oven for 6 hours at $80^0$ C for removing surface moisture. About 20gm of samples were treated with acetic acid to remove the carbonate fraction. Then, the samples were washed and put in 100ml of distilled water followed by treatment with 0.1N Calgon. Mechanical shaker was used to shake the samples for 24 hours before taking it to Fritsch Particle Sizer for grain size analysis. The grain size data was plotted as cumulative frequency curve. The coarse grains will lie to the left of abscissa and the fine grain to the right. Statistical techniques were used to characterize the grain size distributions. A brief description about the statistical parameters used is given below (from Tucker, 1988).

*Mean (M):* Measures the average grain size, computed form sizes of particles spread through a range of percentile values.

$$M = \frac{\phi_{16} + \phi_{5} + \phi_{84}}{3}$$

*Sorting ($\sigma$):* It measures the spread of particles about the average, to define the dispersion or sorting of the sediment. The best sorted sediments approximate to a single size and have low $\sigma$ values.

$$\sigma_I = \frac{\phi_{84} - \phi_{16}}{4} + \frac{\phi_{95} - \phi_{5}}{6.6}$$

*Skewness ($SK_I$):* In normal distribution with a bell-shaped curve, median and mean value will coincide. The tendency to deviate from the normality characterizes the asymmetry or skewness of the curve. The skewness has positive or negative value when more fine or coarse materials are present than in a normal distribution respectively.

$$SK_I = \frac{\phi_{16} + \phi_{84} - 2(\phi_{50})}{2(\phi_{84} - \phi_{16})} + \frac{\phi_{5} + \phi_{95} - 2(\phi_{50})}{2(\phi_{95} - \phi_{5})}$$

*Kurtosis* ($K_G$): Kurtosis is the ratio of the spreads of the tails and center of the distribution. It is related to the dispersion and normality of the distribution. Very flat curves of poorly sorted sediments or those with bimodal frequency curves are platykurtic, whereas very strongly peaked curves, in which there is exceptionally good sorting in the central part of the distribution, are leptokurtic.

$$K_G = \frac{\phi_{95} - \phi_{5}}{2.44(\phi_{75} - \phi_{25})}$$

## 3.3 Organic Matter Content

About 10g of sediment (between grain size fraction 50μm to 45 μm, ASTM sieve no. 270 and 325 respectively ) were taken in 50mL beaker and 1:1 suspension was made by mixing with distilled water. The suspension was heated below $80^0$ C and 30% $H_2O_2$ was added in small amounts at a time to control frothing. The suspension was evaporated to dryness, when no frothing occurred. Loss of weight was expressed as organic matter content in weight percentage.

## *3.4* Sediment Mineralogy

Mineralogy of the host sediments and carbonates (kankars) were analyzed separately using X-ray diffraction (XRD). The dried samples were ground and 50g of the sediment was sieved using ASTM sieve no. 270 and 325 (50 μm and 45 μm respectively). The fraction between 45 and 50 μm was used for XRD analysis. For kankars, samples were washed and crushed to fine powder. Both bulk powder and smeared slide method were used to analyse the major mineral and clay mineral component (Grim, 1953, 1968). For bulk mineralogy, powdered samples of both host sediments and calcretes were used; while for clay mineralogy a suspension was prepared by adding distilled water to the powdered samples and the fine grained top part was separated and smeared on the glass slide. Both powder and smeared slides were scanned under X-Ray diffractometer model ISO Deby flex 1001,1102 Rich-Scifert and Co. at 30 Ma, 40 KV, $3^0$ / min sweep, 5K CPM and 10s time constant using CrKα AND CuKα radiation. For smeared slides, each slide was heated to $550^0$ C for 1 hour in muffle furnace and also glycolated. For glycolation, ethylene glycol was taken in a silica crucible and heated till vaporization started. Then, it was kept in a desiccator with the slides kept over it for 24 hours before taking out for XRD. The X-rays peaks were identified by comparing the d-spacing (Å ) values of the each sample with diagnostic peaks of the standard minerals (Table 3.1). From the d-spacing values of calcite, $MgCO_3$ values in weight percent of the kankars were determined using (Chave, 1951) relations.

A semi-quantitative estimation of the relative concentrations of the bulk and clay minerals based on peak area method (Mann and Muller, 1980; Biscaye, 1965; Cook et al., 1975) was conducted. For bulk mineralogy, peak heights of the minerals, and in clay minerals, peak areas were chosen for quantitative study. The peak areas of individual

**Table 3.1: Diagnostic XRD peaks of selected minerals**

| **Minerals** | **Diagnostic peaks** (Å) |
|---|---|
| Quartz (Q) | **3.34**, 4.25, 2.45,2.28,2.1,1.98 |
| Feldspar (F) | 6.52, **3.19** |
| Mica/Illite (M/I) | **9.98**, 4.95 |
| Calcite (C) | 3.83, **3.03**, 2.28,2.12 |
| Goethite (G) | 4.18, **2.69**, 2.44 |
| Kaolinite (Kaol) | 7.1, 3.57 (on heating the 7.1Å collapses, indicate presence of kaolinite) |
| Chlorite (Chl) | 14.15, 7.1, **4.7** |
| Smectite (Sm) | 14 (expands on Glycolation to 17), 4.4 |
| Amphibole (Am) | 8.53 |
| Dolomite (Dol) | 2.89 |
| Aragonite (Ara) | 3.53, 3.19 |
| Siderite (Sid) | 2.79 |

minerals were first calculated by multiplying the peak height with half-peak width (Mann and Muller, 1980). In bulk mineralogy, 3.34Å peak of Quartz, 3.19Å peak for feldspar and 9.9Å peak for mica were chosen for the analysis. For clay minerals, 17Å peak for smectite (expanded glycolated peak), 10Å peak for Illite, 7Å peak for kaolinite/chlorite overlapping peaks and 4.7Å chlorite peak were chosen. In all samples kaolinite and chlorite peaks (of 3.57 and 3.53 Å) were indistinguishable and therefore the proportion of (kaolinite + chlorite) was taken together for 7.1 Å peak. The proportion of chlorite was calculated from peak height and half-peak width of the diagnostic 4.7 Å peak and the value was subtracted from 7.1 Å peak (chlorite + kaolinite) to estimate the proportion of

kaolinite. Then, the peak areas were multiplied by the weighting factors viz. 1.3 for quartz, 2 for feldspar, amphibole, calcite, chlorite, and kaolinite, and 4 for Illite (Mann and Muller, 1980). These values then normalized to 100% and individual mineral percentages were determined for all samples.

## 3.5 Magnetic Mineralogy and Susceptibility

For magnetic study, samples were taken at 30 cm interval from both exposed section and drill cores. Samples wrapped in thin paper were put in non-magnetic cylindrical pots. As the samples were not oriented, an imaginary north direction was assumed in each sample and all the analysis was done along that direction only. Magnetic susceptibility was measured using Bartington MS2B sensor for low frequency (0.465 KHz) and high frequency (4.65 KHz) applied fields. Magnetic susceptibility is measured as the ratio of magnetization acquired per unit field.

$$\kappa = M / H$$

where M is magnetization/volume (A/m) and H is magnetic field (A/m), giving rise to a dimensionless unit $\kappa$ (volume susceptibility). Mass susceptibility ($\chi$) is expressed as

$$\chi = \kappa / m$$

where m is the weight of the sample. In SI units, $\chi$ has units of $m^3/kg$. The magnetic susceptibility in a profile indicates bulk magnetic content in a sample, its variation with depth and is also sensitive to changes in grain size. From the variations of susceptibility between low (lf) and high (hf) frequencies, frequency dependent susceptibility ($\chi_{fd}$ %) is calculated from the following relation

$$\chi_{fd}\ \% = [(\chi_{lf} - \chi_{hf}) / \chi_{lf}] \times 100$$

The large value of this parameter indicates presence of ferromagnetic grains lying at the single domain (SD) / superparamagnetic (SP) boundary (~ 0.02 μm).

Anhysteretic remanence magnetization (ARM) was imparted by subjecting a sample to a strong alternating field decaying to zero in the presence of small steady field and is useful for characterizing magnetic particles. The ratio of ARM to 79.6 is termed as $\chi_{ARM}$

(susceptibility of anhysteretic remanence) varies with the quantity of the single domain grains. Isothermal remanent magnetization (IRM) was induced on samples at intervals of 20, 50, 100, 200 mT up to 2500 mT and backfield of 300 mT on ASC scientific impulse magnetizer (IM-10-30) and remanence was measured using Minispin Rock Magnetometer of Molspin at Wadia Institute of Himalayan Geology, Dehradun. Magnetic hysteresis curves were generated from the induced fields and magnetization values and additional parameters were computed.

# Chapter 4

# Results and Discussion

This Chapter presents the results of stratigraphic, sedimentological and magnetic analysis of sediments from the Bithur section and drill cores. The data from the Bithur section represent the near-surface (~12-13m) stratigraphy of the region while the drill cores go down to ~ 50 meters in the interfluve region at IIT Kanpur campus and ~25 meters in the valley fills at Jagdishpur and Firozpur. Data from each location have been interpreted for facies, depositional environment, and post-depositional changes. Finally, the results have been synthesized to develop a regional stratigraphic framework, and depositional environment for a period extending over 80 ka.

## 4.1 Bithur Section

Figure 4.1 shows a composite section for the Bithur cliffs and position of three logs. The units were continuous with only modest variation in the thickness along the 1.5 km long cliffs.

Figure 4.2a shows the details of the Log-1 with a total length of 10m positioned at a location 600m east of the Kalwari Ghat (Fig. 4.1). The lower part of the section (base to 3m) consists of yellowish brown clayey silt with increasing concretions (average diameter 3cm) in the upper part. Few drab mottles of 4 cm in diameter and very few rhizoconcretions were present. Reddish brown mottling present above it continued up to 4.5m. Carbonate concretions were sparse and small in size in the upper part. Dark brown clay was present between 5 and 6m with very few carbonate nodules and strong efflorescence. The clay layer was finely interbedded with grayish brown silty-clay. Pale yellow fine sand layer started at 6m from the base and continued up to 9.5m. Carbonate nodules with some surface efflorescence were present in the unit at 7m. At the top of the section, a 50cm thick unit of planar-bedded silt, with some reddish mottles was present. The layer has a prominent zone of rhizoconcretions of 1m thick with nodules present at the top.

Figure 4.2b shows the details of the Log-2 located at the Kalwari Ghat (Fig. 4.1) with log length of 11m. In the lowermost part (base to 1.5 m), brown colored clayey-silt

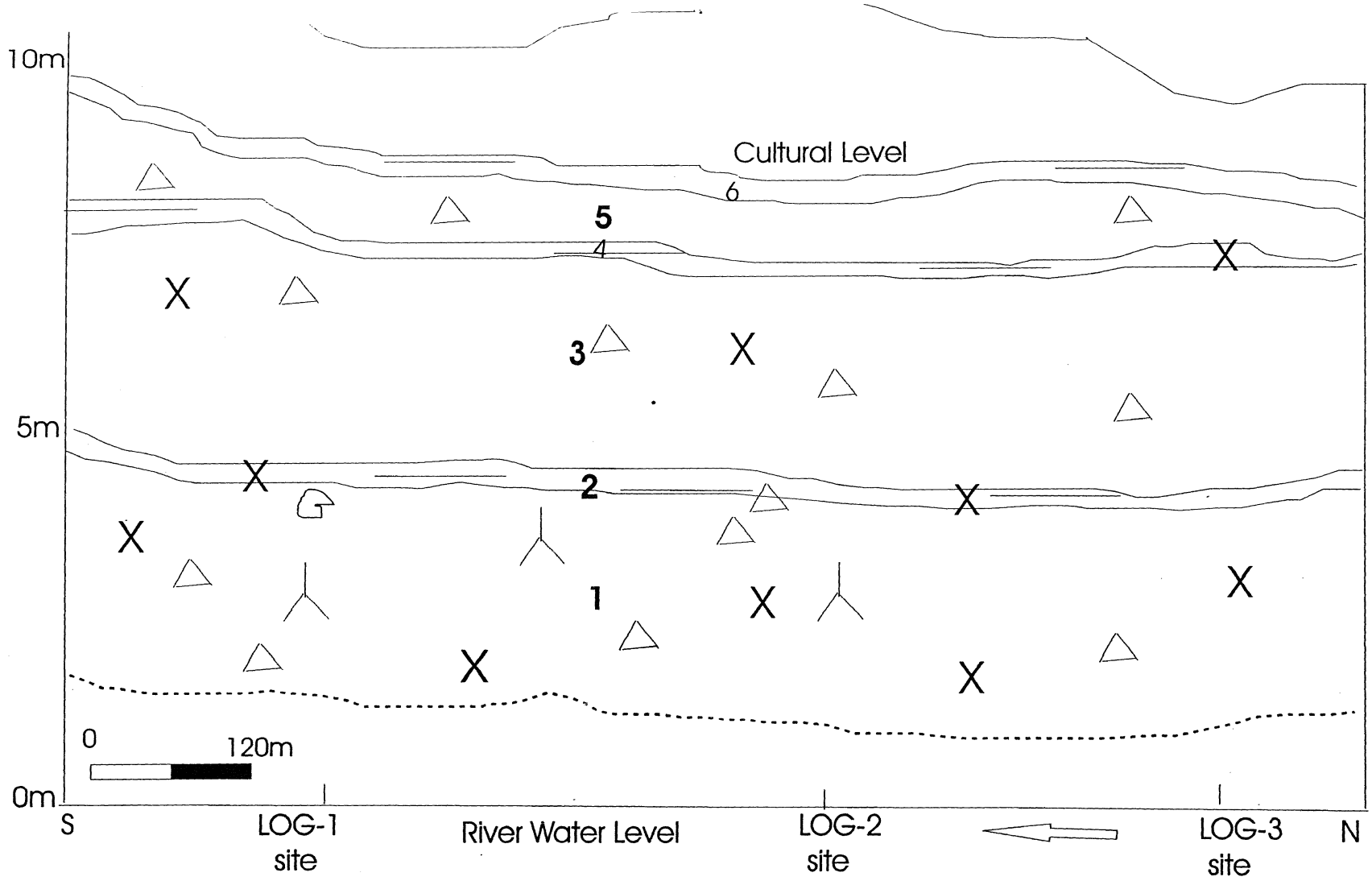


Figure 4.1. Log positions and composite section at Bithur

X - mottling, △ - Kankar, ⅄ - roots, —— Lamonation, ⌐ - organic shells

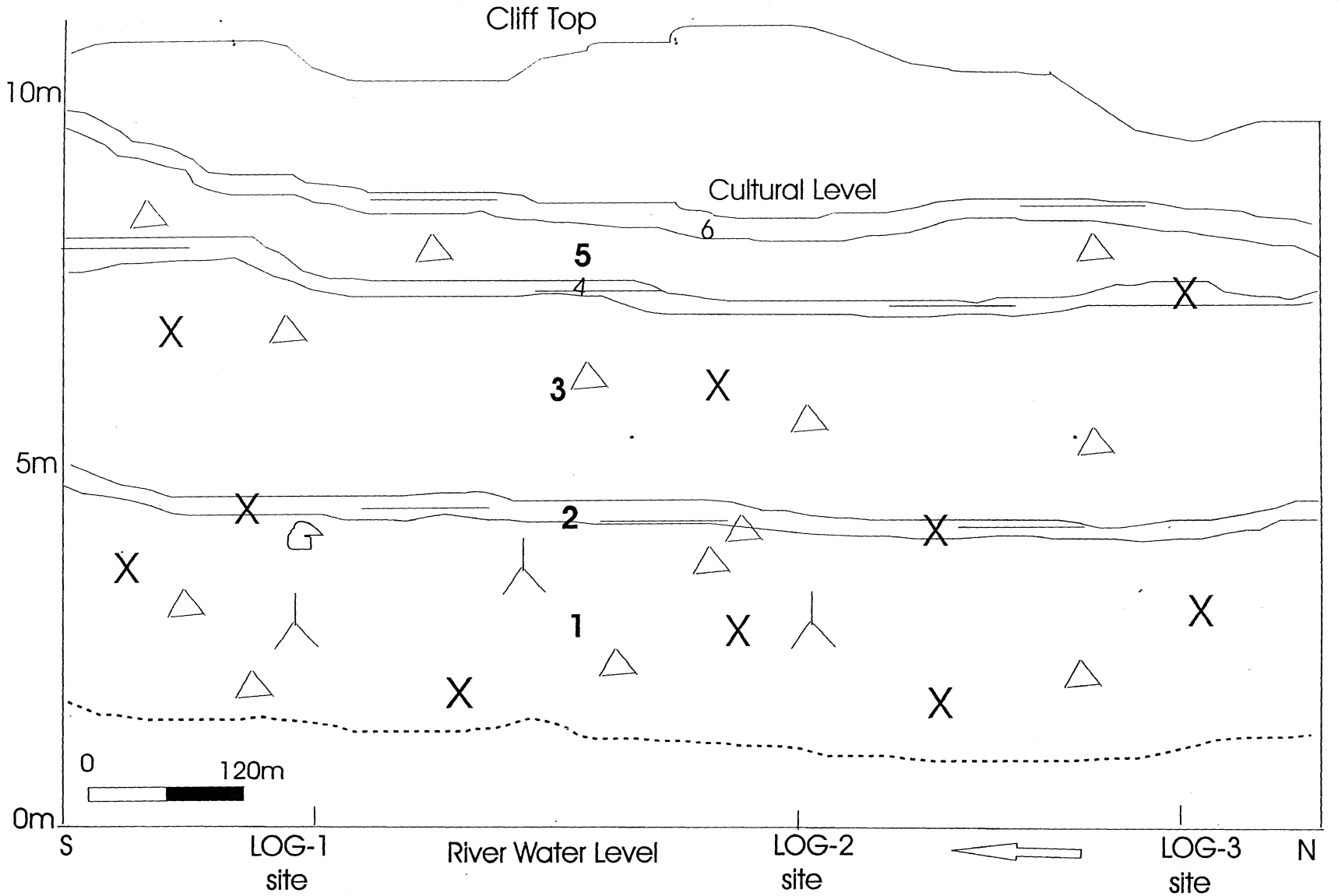


Figure 4.1. Log positions and composite section at Bithur

X - mottling, △ - Kankar, ⅄ - roots, —— Lamonation, ⌐ - organic shells

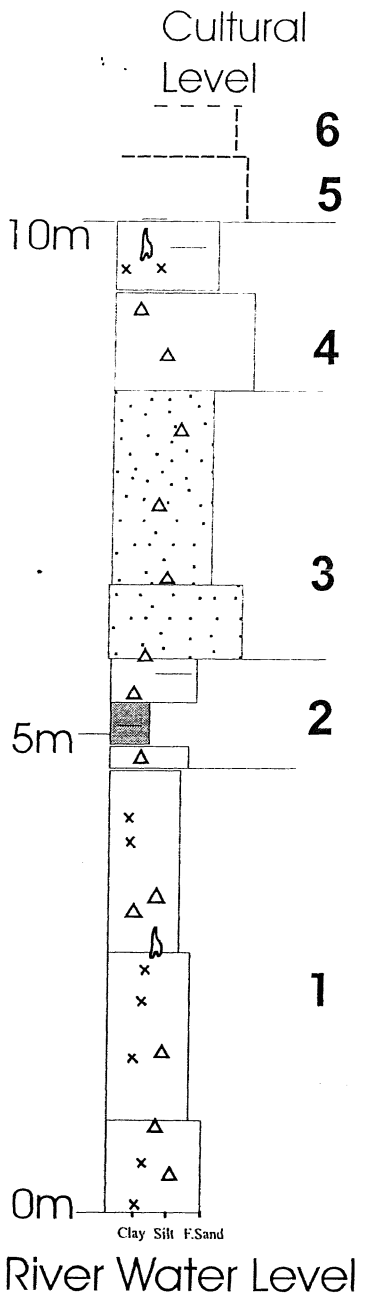


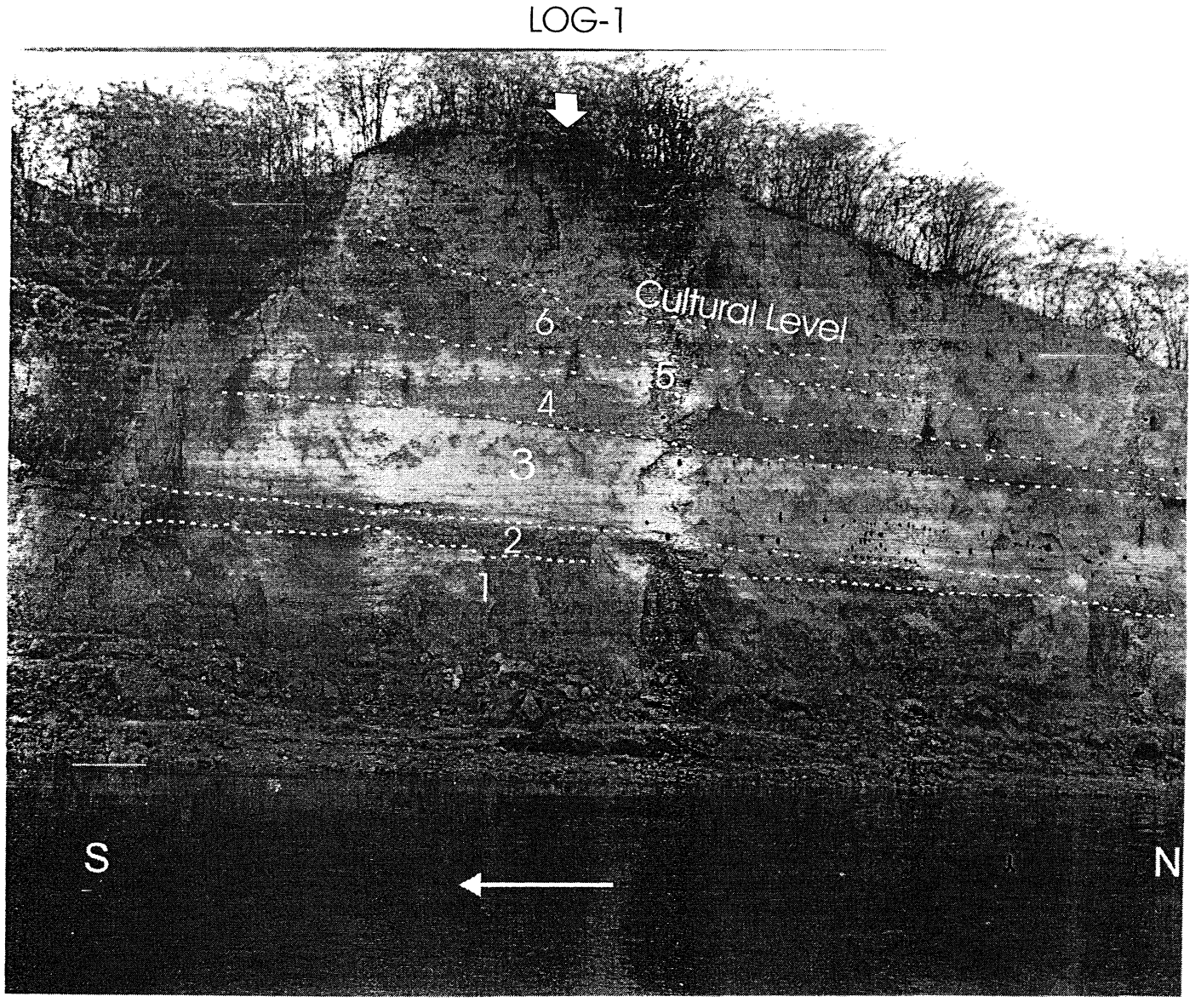


Figure 4.2a. Location of Log-1 at Bithur

Sand Silt Clay Lamination Kankar
X Mottling Rhizoconcretion

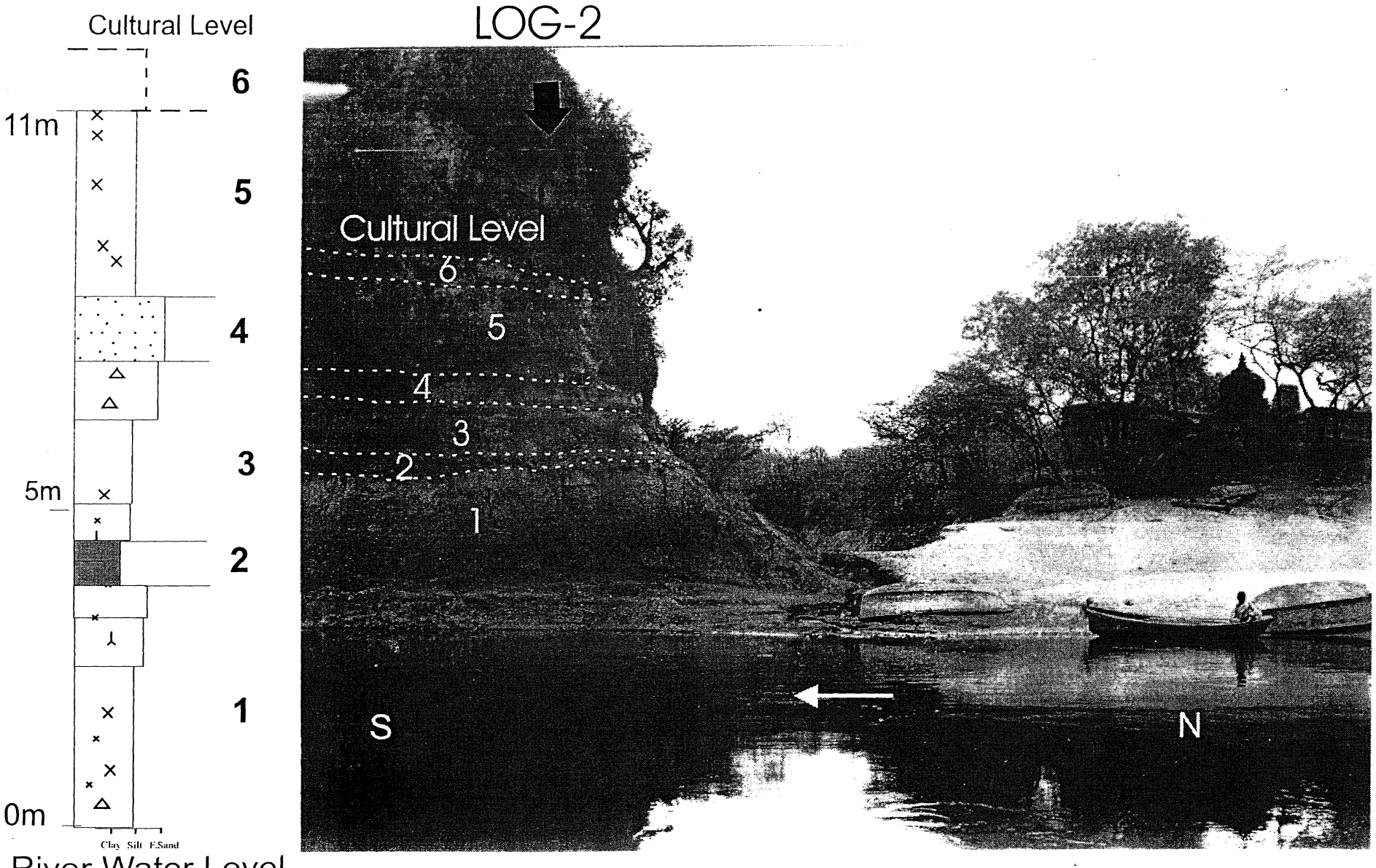


Fig.4. 2b: Location of Log-2 at Bithur Section

Sand Silt Clay Kankar X Mottling

Lamination Roots

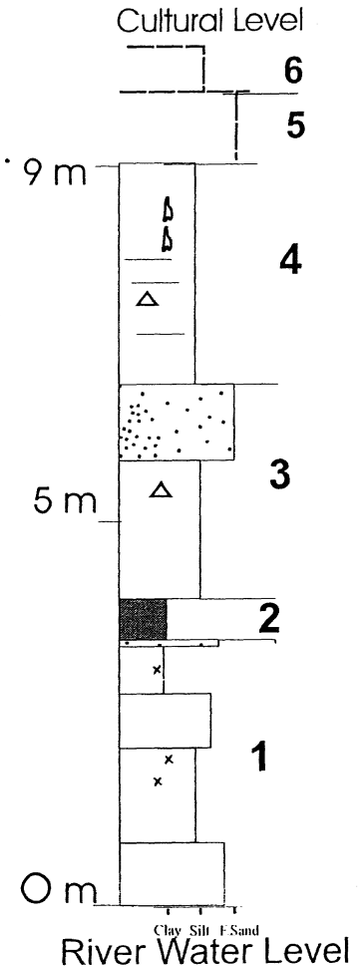


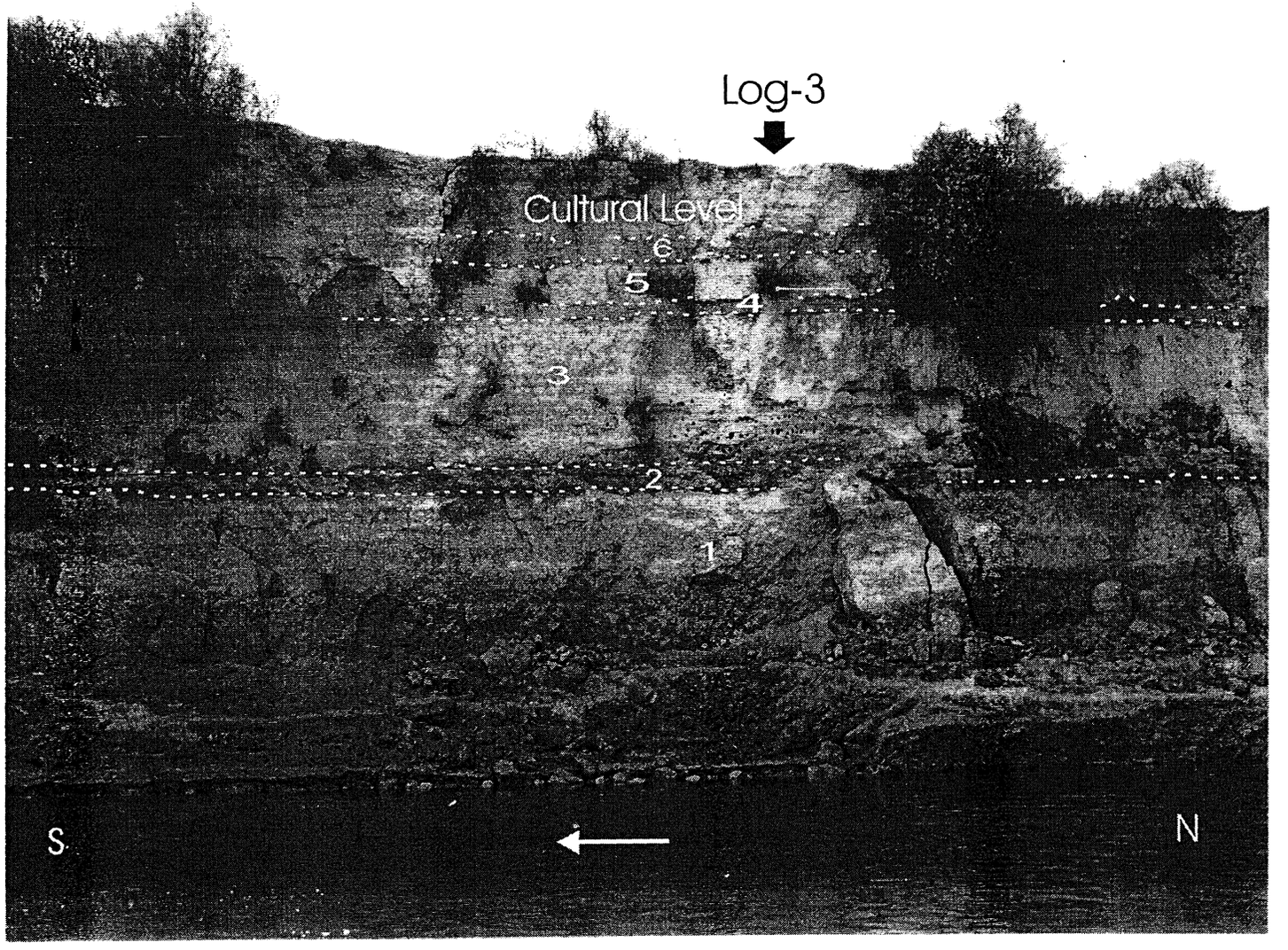


Figure 4.2c. Location of Log-3 at Bithur

Sand Silt Clay Lamination Kankar Mottling Rhizoconcretion

with dark brown mottling is present. Larger gray mottles are also present. Irregular kankars, mostly 2-3 cm in diameter, were recorded, though some were as large as 4cm. Reddish brown silt with red-brown mottles continued up to 4m from bottom. Kankars were rare in the upper part. Grey vertical pipes 30cm in height were present. A 50cm thick dark brown clay layer with abundant red brown mottles is present between 4 and 4.5m . Complete gastropod shells were recovered 20cm below the base of the clay layer. A very fine yellowish silt layer is present within the clay layer. A 3m thick (between 4.5m to 7.5m from bottom) yellowish silt with some fine sand was present above the clay unit. Red brown mottles became paler in this unit. Kankars are present with diameter ranging between 1-3cm. Between 7.5m and 8.5m a thinly laminated yellowish silt layer with reddish tinge was present. Yellowish gray mottles and kankars were present. At the top part of the section yellowish clayey silts with vertical gray mottling was reported. Kankars were sparse in this unit with most of them were in the upper part.

Details of log-3 located at Sunder Ghat (Fig. 4.1), around 500m west of Log-2, are shown in Fig. 4.2c. A 2m thick yellowish brown clayey-silt layer was present at the bottom, with abundant kankars at the lower level. Kankars were rare in the upper part and diameter was decreasing from 3-4cm in the lower part to less than 1cm in the upper part. A 60cm thick dark brown clay layer with yellow and gray mottling was present above it. Thick pale yellow silt to very fine sand layer was present between 3 and 6m measured from bottom. At the top of the log yellowish stratified silt to fine sand layer was present with some reddish mottles. Rhizoconcretions were prominent at the top, with 1m thick kankar rich zone.

### 4.1.1 Litho-Stratigraphic Units and age of the strata

Six major litho-stratigraphic units were identified on the basis of lithologs, field observations and mapping from photomosaics. Figure 4.3 shows a summary log for the Bithur section showing the stratigraphic units (taking the maximum thickness of each unit) which have also been transferred on logs 1, 2, and 3 shown in Fig. 4.2. A total of 4 radiocarbon dates are also available which are shown against each unit. A brief description of individual units is given below:

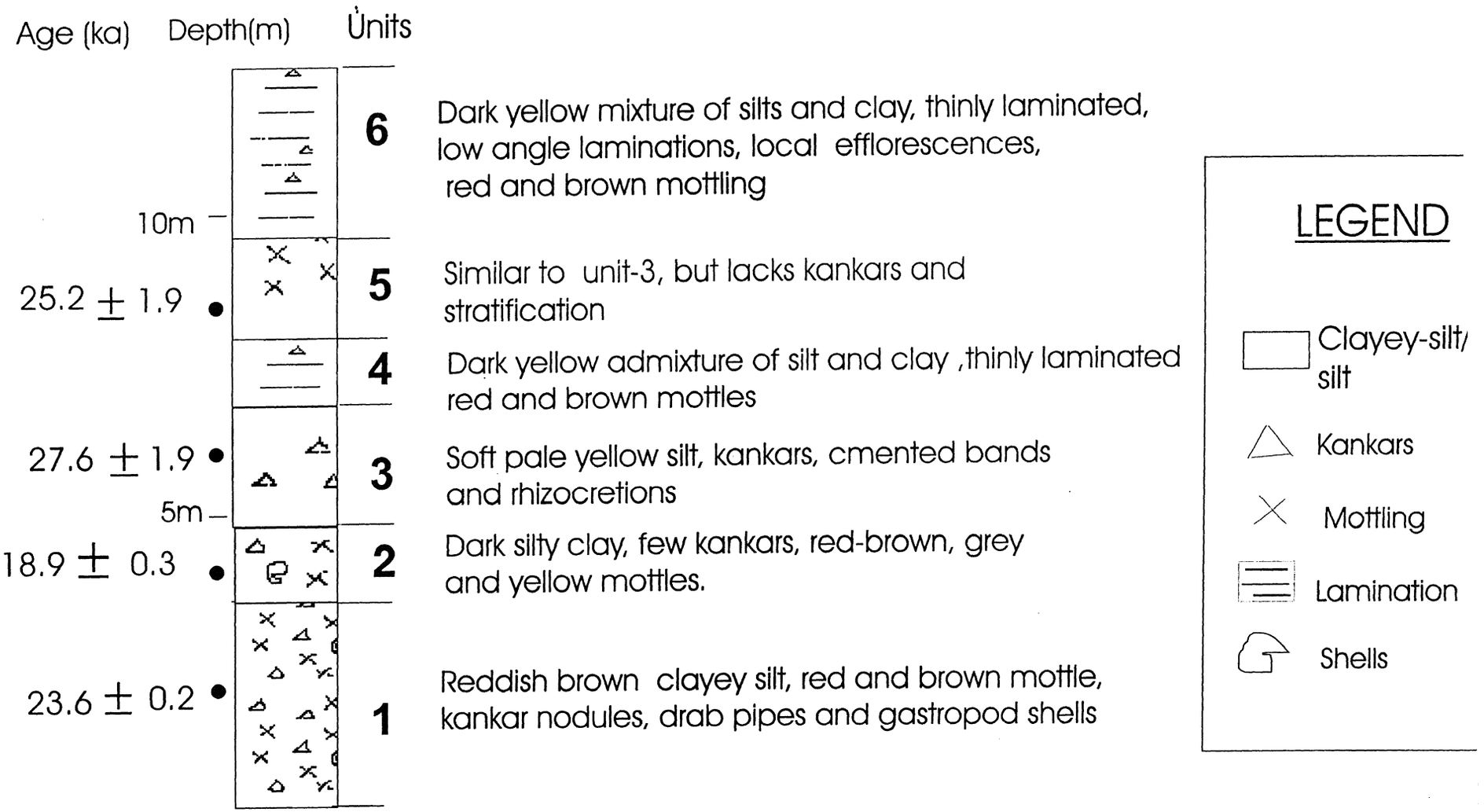


Figure 4.3 Summary log of the Bithur Section

The lowermost *Unit 1* is about 4m thick and consists of yellowish brown to reddish brown clayey silt, with gray and darker mottles, and rhizoconcretions. Kankars constitute about 20% of the sediments by volume, but become sparse in the upper part. The diameter of kankars is around 2-3cm in the lower part, decreasing to less than 1cm in the upper part. Vertical drab pipes and lens of gastropod shells are present in the top 30cm.

*Unit 2* commences abruptly with a dark silty-clay layer consisting of minor kankars, red-brown and yellow mottles. The unit is banded and maintains its thickness (around 1m) throughout the section. Strong efflorescence features were present in some parts. A 5cm thin band of yellow silt within the unit can be traced along the entire cliff section.

*Unit 3* comprises inter-bedded silt-rich and sand rich unit. The strata vary in thickness noticeably over a distance of few tens of meters and are massive in nature. The lower most part is yellowish silt, with some fine sand, becoming more whitish in the upper level. Carbonate nodules, cemented bands, rhizoconcretions are present.

*Unit 4* represents the top clayey-silt part of the logs. It contains thinly laminated yellowish clayey-silt with some dark and gray mottles. A kankar band, 1cm thick, is present in the lower part. Rhizoconcretions with scattered nodules are also reported.

Unit *5* is very similar to Unit-3, but kankars are less. The thickness of this unit is highly variable and in most of the logs this unit is absent. It consists of yellowish-white silt with very few mottling.

Unit 6 is the top most unit in the Bithur section consisting of yellowish thinly laminated silty-clay with dark mottles. The unit has a prominent one meter-thick band of rhizoconcretions and kankars present throughout the unit.

Available radiocarbon and OSL dates from Gibling et al. (in press) constrain the stratigraphic framework of this section. Gastropod shells at the top of Unit 1 yielded a radiocarbon date of 23.6±0.2 ka. (~27.5 ka cal BP). Total organic carbon from the

lowermost part of the Unit 2 yielded a radiocarbon date of 18.9±0.3 ka, and there seems to be some younging due to atmospheric contamination. The OSL dates from Units 3 and 5 range from 27.6±1.9 ka to 25.2±1.9 ka.

### 4.1.2 Grain size

Tables 4.1 lists the statistical grain size parameters and Figure 4.4 shows the cumulative frequency distribution for samples from different units at Bithur. These Data suggest that the grain size distributions of all units are fairly uniform. The mean grain size of all the Bithur units averages around 7ϕ, which corresponds to medium to fine silt as per the Udden and Wentworth scale. The sorting of all samples is poor. The asymmetry or skewness of the grain size curve, showed positive values indicating more fine materials present than in a normal distribution. Only in Unit-3, the skewness is near symmetrical indicating near-normal distribution of grain size. Kurtosis values suggest that samples from all units except from Units 3and 5 are mesokurtic, or near normal distribution of grain sizes. Samples from Unit 3 and 5 kurtosis are platykurtic as evident from very flat curve of poorly sorted sediments.

**Table 4.1. Grain size parameters for Bithur section sediments**

| Units | Mean | Sorting | Skewness | Kurtosis | Interpretation |
|---|---|---|---|---|---|
| 6 (n=1) | 7.819 | 1.11 | 0.25 | 0.928 | Medium to fine silt, poor sorting and positively skewed, Mesokurtic |
| 5 (n=1) | 7.76 | 1.05 | 0.21 | 0.8419 | Medium to fine silt, poor sorting and positively skewed, Platykurtic |
| 4 (n=1) | 7.79 | 1.17 | 0.28 | 0.9952 | Medium to fine silt, poor sorting and positively skewed, Mesokurtic |
| 3 (n=1) | 7.59 | 1.419 | 0.091 | 0.8923 | Medium to fine silt, poor sorting and near symmetrical, Platykurtic |
| 2 (n=1) | 7.796 | 1.19 | 0.27 | 0.956 | Medium to fine silt, poor sorting and positively skewed, Mesokurtic |
| 1 (n=1) | 7.887 | 1.218 | 0.467 | 0.9796 | Medium to fine silt, poor sorting and positively skewed, Mesokurtic |

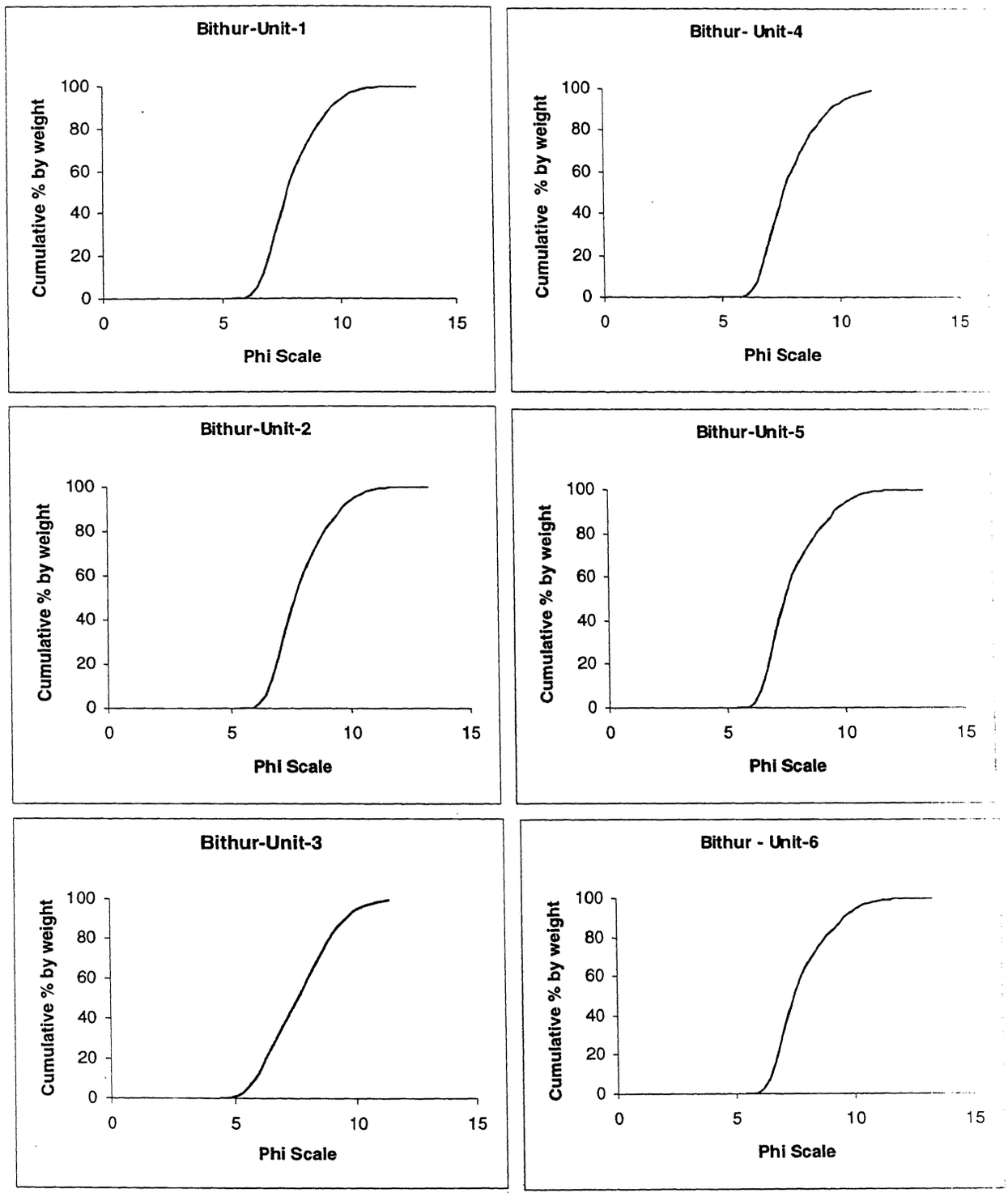


Fig.4.4. Grain size plots for different stratigraphic units at Bithur

### 4.1.3 Organic Matter Content and Sediment Mineralogy

The $H_2O_2$ reactive organic matter content (OMC) of the six units was determined and the results are listed in Table 4.2. The variation in OMC among different units is quite small. Most units show a value around 2-25% except Unit 2 which shows a slightly higher value of ~4.5 %.

Table 4.2 summarizes the qualitative mineralogical data for the Bithur section. The bulk mineralogy is represented by quartz, feldspar, mica, calcite in variable amounts. Amphiboles are present in trace amounts in units 1, 2 and 3 but are absent in upper units. Goethite is present only in the lower most unit. Clay mineral assemblage is represented by Illite, Kaolinite, Chlorite and Mixed layer clays. The presence of chlorite and kaolinite was confirmed by heat treatment. On heating to 550°C, the 7.1Å peak collapsed suggesting presence of kaolinite in the sample. Glycolation expansion did not show the characteristic 17 Å smectite peak in any sample, ruling out presence of expandable clay mineral in the section. The mixed-layer clays were present in all the units mainly represented by 11 Å peak. The carbonate fraction (kankars) showed presence of siderite apart from calcite in the Unit-1. The $MgCO_3$ content of the concretions were 6%, taken from Chave (1951) relation.

**Table 4.2: Organic matter and sediment mineralogy for the Bithur section**

| Units | Organic Matter Content (wt%) | Bulk mineralogy | | | | | Clay mineralogy | | | | Concretion mineralogy |
|---|---|---|---|---|---|---|---|---|---|---|---|
| | | Q (3.34Å) | F (3.19 Å) | M (10 Å) | Cc (3.03 Å) | Others | I (10 Å) | Ch (14.4 Å) | K (3.57 Å) | Mx (11 Å) | |
| 6 (n=2) | 2.52 | ++++ | ++ | ++ | + | | ++ | | ++ | | – |
| 5 (n=2) | 2.19 | ++++ | ++ | ++ | + | | ++++ | ++ | ++ | + | – |
| 4 (n= 2) | 2.42 | +++ | ++ | ++ | + | A+ | ++++ | | ++ | + | – |
| 3 (n= 2) | 2.25 | ++++ | ++ | +++ | | A+ | +++ | ++ | ++ | + | Cc |
| 2 (n=2) | 4.47 | ++++ | ++ | +++ | + | A+ | +++ | | ++ | + | – |
| 1(n=2) | 2.4 | ++++ | + | +++ | ++ | A+,G+ | ++ | ++ | ++ | | Cc, Sid. |

Q- Quartz, F-Feldspar, M-Mica, A- Amphibole, G-Goethite, Cc-Calcite, I-Illite, Chlorite, K-Kaolinite, Mx-Mixed layer clay; Sid- Siderite

++++ High; +++ Moderate; ++ Minor; + Trace

Results of semi-quantitative estimation of the relative concentrations of the bulk and clay minerals based on Peak area method (Mann and Muller, 1980; Biscaye 1965; Cook, 1975) are listed in Table 4.3 and plotted in Fig. 4.5. Quartz is the most dominant mineralogical constituent throughout the section, showing highest abundance in the Units 2 and 5. High abundance of feldspar is observed in Units 1, 3, 4 and the lowest abundance is observed in Unit 2. Illite is the most dominant (~90%) clay mineral. Chlorite is absent in some samples from unit 2, 4, and 6. Figure 4.5 shows the major bulk and clay mineral abundance, Quartz/Feldspar ratio and (Illite + chlorite)/kaolinite ratio for all the units. (I+C)/K ratio showed a decrease in the value (due to rise in kaolinite content) at the top of the unit-2 (2.1m from base) compared to lower horizons. The increase in cation-deficient kaolinite value indicates leaching of cations (more weathering) in the horizon compared to lower horizons (Grim, 1953). The lower units are rich in cation-rich illite and chlorite indicating poor drainage and less leaching. A sudden rise in the feldspar content and corresponding low value of kaolinite in the unit-3 indicates this to a zone of poor chemical weathering. A similar decrease in kaolinite content is also observed in unit-5 which would again indicate poor chemical weathering.

**Table 4.3. Relative abundance of bulk and clay minerals in Bithur section sediments**

| | | Bulk powder | | | | Smeared fine fraction | | | |
|---|---|---|---|---|---|---|---|---|---|
| Units | Height (m) | Q% | Felds% | Mica (%) | Q/F | Illite% | Chl % | Kaol % | (I+C)/K |
| 6 | 5.7 | 50.27 | 11 | 38.67 | 4.57 | 89.2 | 0 | 10.71 | 8.33 |
| 5 | 5.1 | 67.63 | 8.09 | 24.27 | 8.36 | 94.52 | 2.73 | 2.73 | 35.62 |
| 4 | 4.5 | 61.45 | 6.73 | 31.82 | 9.13 | 93.45 | 1.34 | 5.21 | 18.19 |
| | 4.2 | 56.9 | 20.2 | 22.89 | 2.82 | 88.54 | 0 | 11.45 | 7.73 |
| 3 | 3.9 | 45.94 | 8.31 | 45.73 | 5.53 | 94.65 | 3.47 | 1.88 | 52.19 |
| | 3 | 50.74 | 26.02 | 23.23 | 1.95 | 95.23 | 3.71 | 1.06 | 93.34 |
| 2 | 2.1 | 57.3 | 6.88 | 35.81 | 8.33 | 90.9 | 0 | 9.09 | 10.00 |
| | 1.8 | 65.17 | 4.22 | 30.6 | 15.44 | 94.56 | 1.8 | 3.64 | 26.47 |
| 1 | 1.2 | 76.1 | 5.97 | 17.92 | 12.75 | 92.23 | 2.38 | 5.39 | 17.55 |
| | 0.3 | 67 | 8.24 | 24.74 | 8.13 | 89.71 | 2.99 | 7.28 | 12.73 |

I-Illite, C-Chlorite, K-Kaolinite

### 4.1.4 Magnetic susceptibility and Mineral Magnetic Analysis

Magnetic susceptibility and mineral magnetic analyses were carried out for samples from the exposure at Kalwari Ghat (Log 2) collected at 30 cm interval covering all the units. Figure 4.6 shows the magnetic susceptibility profile for the Bithur section.

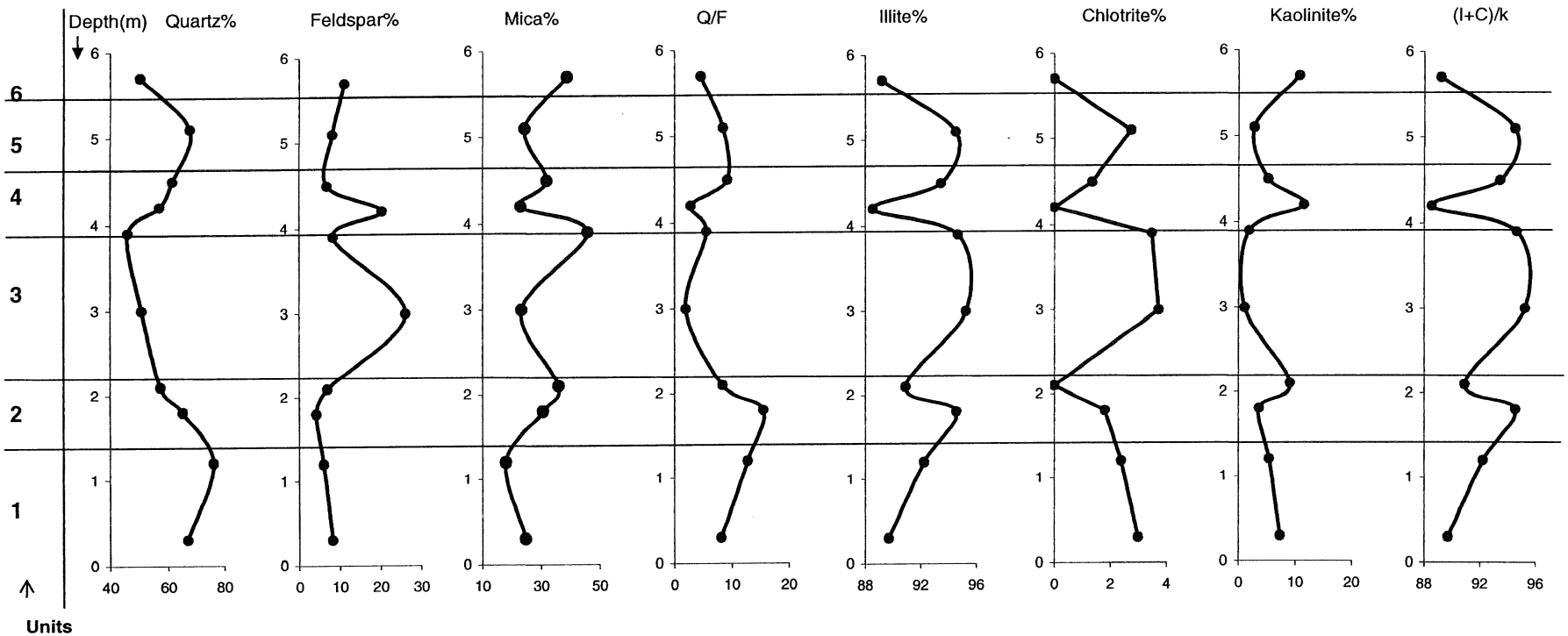


Figure 4.5. Major bulk and clay mineral abundance in percentage in Bithur section

The magnetic susceptibility is generally quite low and uniform with $\chi_{lf}$ value < 20 x $10^{-8}$ $m^3$/kg except for Unit 2 where it reaches up to 69 x $10^{-8}$ $m^3$/kg (Table 4.4 and Fig. 4.6). The frequency-dependent susceptibility is also low (~2-3%) in most of the units but it reaches up to ~12% in Unit 2, ~8% in lower parts of Unit 1 and 7% in Unit 4.

**Table 4.4. Magnetic susceptibility data for Bithur samples**

| Unit | Sample depth (m) | Corrected weight (gm) | $\chi_{lf}$ (*$10^{-8}m^3$/kg) | $\chi_{hf}$ (*$10^{-8}m^3$/kg) | $\chi_{fd\%}$ |
|---|---|---|---|---|---|
| 6 | 5.4 | 9.92 | 12.70 | 12.39 | 2.38 |
| | 5.1 | 11.18 | 15.47 | 15.34 | 0.80 |
| 5 | 4.8 | 10.52 | 12.92 | 12.83 | 0.73 |
| | 4.5 | 11.04 | 12.53 | 12.04 | 3.901 |
| 4 | 4.2 | 9.73 | 10.89 | 10.89 | 0 |
| | 3.9 | 9.07 | 13.23 | 12.3 | 7 |
| 3 | 3.6 | 11.53 | 14.39 | 14.01 | 2.65 |
| | 3.3 | 9.27 | 10.78 | 10.78 | 0 |
| | 3 | 8.95 | 16.20 | 15.97 | 1.37 |
| | 2.7 | 9.91 | 15.29 | 15.13 | 1.05 |
| | 2.4 | 7.52 | 13.51 | 13.51 | 0 |
| 2 | 2.1 | 12.11 | 15.02 | 14.99 | 0.21 |
| | 1.8 | 4.26 | 69.48 | 64.92 | 6.55 |
| | 1.5 | 6.62 | 24.16 | 21.14 | 12.5 |
| 1 | 1.2 | 9.18 | 11.06 | 11.06 | 0 |
| | 0.9 | 9.37 | 10.13 | 9.92 | 2.1 |
| | 0.6 | 11.35 | 9.69 | 9.69 | 0 |
| | 0.3 | 10.24 | 11.38 | 11.23 | 1.37 |
| | 0 | 10.14 | 9.861 | 9.03 | 8.4 |

$\chi_{fd\%} = \{(\chi_{lf} - \chi_{hf}) / \chi_{lf}\} * 100$

Additional mineral magnetic parameters for Bithur section sediments are listed in Table 4.5 and plotted in Fig. 4.6. Distinct peaks of ARM, in Units 2, 4 and 6 are noticeable. SIRM shows a very high value in the unit-2 and 6, while in other units it is uniformly low. The $Bo_{Cr}$ values show significant variation; Units 2 and 4 show low $Bo_{Cr}$ values and Unit 1 has comparatively high values. S-Ratio values are low throughout the section, except in Unit 2.

**Table 4.5. Mineral magnetic data for Bithur Samples**

| Unit | Sample depth (m) | $\chi_{ARM}$ (*$10^{-5}m^3$/kg) | SIRM/ $\chi_{lf}$ (*$10^3$A/m) | SIRM ($Am^2Kg^{-1}$) | BoCr (mT) | S-ratio |
|---|---|---|---|---|---|---|
| 6 | 5.4 | 0.026 | 7.938 | 102.87 | 52 | -0.771 |
| | 5.1 | 0.039 | 9.951 | 155.23 | 50 | -0.836 |
| 5 | 4.8 | 0.019 | 6.433 | 83.77 | 38 | -0.703 |

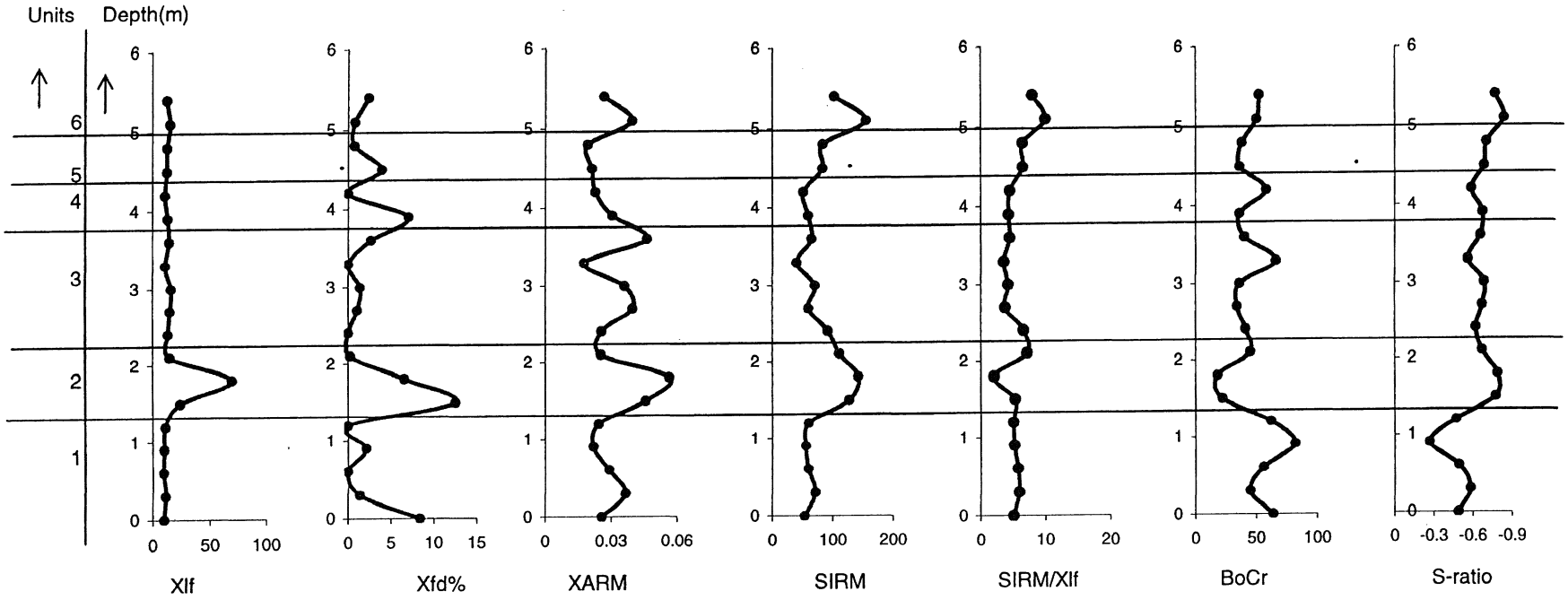


Figure 4.6. Bithur magnetic suceptibility and mineral magnetic parameters and results

| | | | | | | |
|---|---|---|---|---|---|---|
| | 4.5 | 0.021 | 6.495 | 82.92 | 36 | -0.685 |
| 4 | 4.2 | 0.022 | 4.469 | 51.28 | 58 | -0.589 |
| | 3.9 | 0.030 | 4.28 | 58.99 | 36 | -0.675 |
| 3 | 3.6 | 0.046 | 4.416 | 64.64 | 40 | -0.657 |
| | 3.3 | 0.017 | 3.53 | 39.8 | 66 | -0.561 |
| | 3 | 0.035 | 4.221 | 70.5 | 36 | -0.687 |
| | 2.7 | 0.039 | 3.753 | 59.56 | 34 | -0.67 |
| | 2.4 | 0.025 | 6.546 | 91.481 | 41 | -0.622 |
| 2 | 2.1 | 0.025 | 7.117 | 110.94 | 45 | -0.669 |
| | 1.8 | 0.056 | 2.047 | 142.35 | 18 | -0.787 |
| | 1.5 | 0.045 | 5.283 | 127.34 | 22 | -0.774 |
| 1 | 1.2 | 0.024 | 5.031 | 60.264 | 62 | -0.473 |
| | 0.9 | 0.021 | 5.158 | 55.565 | 82 | -0.267 |
| | 0.6 | 0.029 | 5.752 | 59.518 | 56 | -0.491 |
| | 0.3 | 0.036 | 5.905 | 70.784 | 45 | -0.581 |
| | 0 | 0.025 | 5.084 | 53.382 | 64 | -0.489 |

$\chi_{ARM}$ = ratio of ARM to 79.6; S-ratio is the ratio of IRM at –300mT to IRM at 2500 mT; BoCr is the remanence coercivity; SIRM is the saturated IRM (IRM at 2500mT)

A bivariate plot of SIRM/$\chi_{lf}$ vs. ARM/$\chi_{lf}$ ratio (Figure 4.7a) shows most of the sample lying between magnetite and titanomagnetite zone, while one sample of Unit-2 falls in magnetite zone(Maher and Thompson, 1995). The SIRM/$\chi_{lf}$ vs. $Bo_{Cr}$ plot (Fig. 4.7b) shows that most samples are characteristic of Multi Domain (MD) domain size (Bradshaw and Thompson, 1985). The SIRM vs. $k_{lf}$ plot (Fig. 4.7c) shows clustering of samples with increasing magnetic content in the Unit 2 samples (Thompson and Oldfield, 1986).

The low $Bo_{Cr}$ values indicate presence of ferrimagnetic minerals in the samples, like magnetite. The bulk powder XRD of samples failed to indicate presence of magnetite, may be present in minor amount and more advanced technique like Mossabauer Spectroscopy method is needed to confirm the presence of magnetite. The high values of $Bo_{Cr}$ may indicate presence of anti-ferromagnetic minerals, like hematite/goethite. S-Ratio values are very low in the unit-2 indicating presence of ferrimagnetic minerals like magnetite, while in the unit-1, 3 and 4 anti-ferromagnetic minerals like hematite is present. The bottom of the unit-2 indicated enrichment of the ferrimagnetic minerals. However the upper part, (at 2.1m) of unit-2 shows relatively high BoCr and S-ratio values indicating presence of antiferromagnetic minerals. The change from ferrimagnetic to antiferromagnetic minerals is related to the change in the anoxic-oxic conditions. More sub aerial exposure and subsequent oxidation of sediments in the

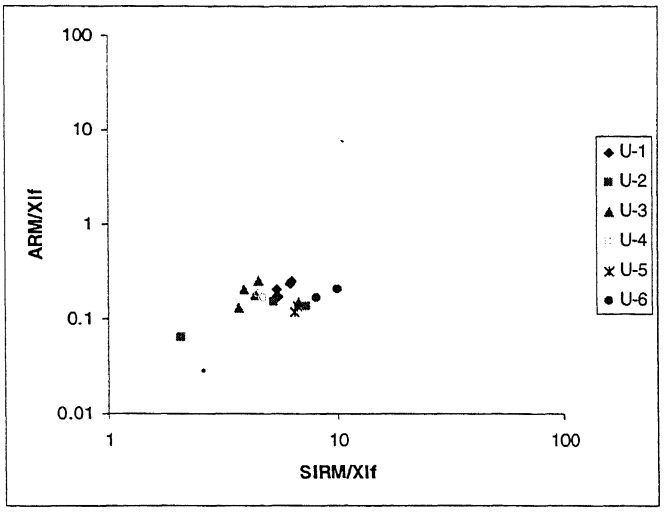


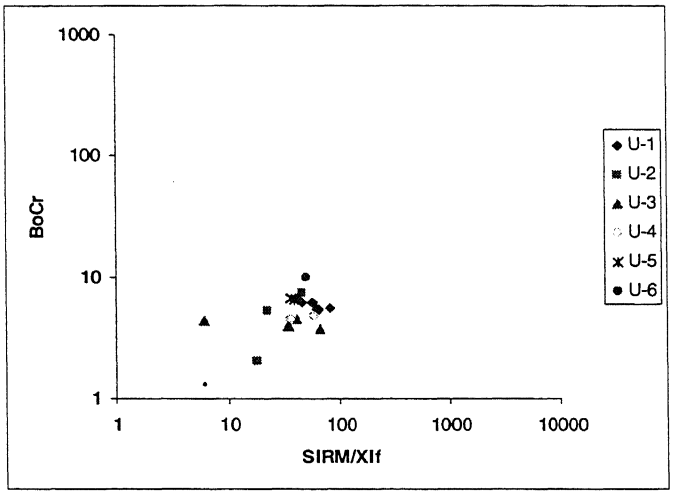


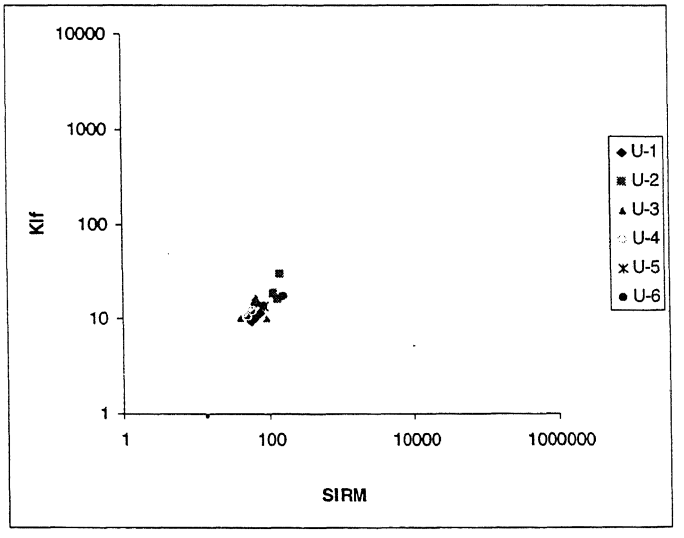


Figure. 4.7 Bi-variate plots of Magnetic parameters of Bithur samples

upper part, might have resulted in the formation of hematite/goethite. The SIRM values indicating volume concentration of magnetic minerals in horizons shows a high value in Unit-2, whereas in other units the value is uniformly low. The overall magnetite grain sizes are SD and PSD indicating coarser domains except in the Unit-2 where SP particles are present. Presences of SP magnetite in unit-2 may indicate in-situ production of magnetite by bacterial activity (Lovely, 1987).

### 4.1.5 Data Interpretation

Based on lithological, sedimentological and sediment magnetic data, the stratigraphic units of the Bithur section has been interpreted in terms of their depositional environment and facies. Table 4.6 summarizes all data on mean grain size, major bulk and clay mineralogy and rock magnetic parameters for different units.

The basal **Unit 1** consisting of reddish brown clayey-silt (mean grain size 7.887ϕ) with dominant mottling, kankars and localized gastropod shell in the topmost parts is interpreted as **floodplain deposit** with a modest to intense degree of pedogenesis, although individual soil horizons are not apparent. Kaolinite is present in significant amount and feldspar content is fairly low. Significant iron segregation has taken place in an oxidizing environment manifested as extensive mottling and presence of goethite in XRD charts. Siderite rich concretions are present. High coercivity and S-ratio values also suggest the presence of hematite/goethite in the unit by oxidation and hydration reactions (converting ferrous ions to ferric). A very low SIRM and $\chi_{lf}$ indicate absence of magnetic flux, and suggests a post-depositional changes in sediments. There is a complete lack of stratification and organic matter content is comparatively low.

Dark silty-clay sediments (mean grain size 7.796ϕ) of **Unit 2** with minor kankars, brown mottling and higher organic matter content are interpreted as **swamp deposits**. This unit can be traced for more than 1.5 km, but becomes more banded in nature between Log-2 and Log-3. Significant chemical weathering is indicated by high-kaolinite, low-feldspar assemblage particularly in the upper parts. The magnetic characteristics of Unit 2 are significantly different from the rest of the section. High $\chi$fd% values (~12%) characterize fine Super-Paramagnetic (SP) particles, and indicate magnetic enhancement i.e. enrichment of the strongly magnetic ferrimagnetic mineral

such as magnetite (figure 4.6). High $\chi$lf, low BoCr, S-ratio also characterize the presence of ferrimagnetic component. A very high SIRM along with high $\chi$lf and $\chi_{fd}$% value indicate increase in SP ferrimagnetic concentration, which may have formed in-situ. It is suggested that the anaerobic condition in swampy environment might have favored the formation of pedogenic magnetite through bacterial activity producing extracellular ultra fine grains (Lovely et al., 1987). In the upper part of Unit-2, a gradual change to more oxidizing environment is observed indicated by the presence of antiferromagnetic minerals (as evident by high $Bo_{Cr}$ and high S-ratio). Relative rise in kaolinite content (at the expense of feldspar) in the upper part indicates change of swampy water-logged condition to a good drainage and leaching condition.

**Unit 3 is** a fine-silt unit (mean grain size 7.59$\phi$) with a distinct band of calcrete. Highest values of (I+C)/K ratio and high feldspar content suggest little chemical weathering. The magnetic properties are characterized by very low $\chi_{fd}$% and a distinctly high G/H ratio, and high S-ratio suggesting an anti-ferromagnetic assemblage. **Unit 5** is quite similar to Unit 3 but lacks kankar and is not stratified. This Unit is enriched in quartz, illite, ferrimagnetic minerals, but the grain size is a little finer than in unit-3. Both these units are interpreted as **eolian** deposits and a poor sorting of sediments suggests short distance transport of riverine sediments during drier periods.

**Units 4** and **6** are similar to Unit 2 with clayey and thinly laminated sediments with fewer mottling and kankars in the upper part of the unit. Coercivity and S-ratio values are low suggesting presence of magnetite. Kaolinite content is high in both unit 4 and 6 indicating chemical weathering activity. A relatively high SIRM value and low $\chi_{fd}$% indicate SD-MD magnetic grain influx of sediments in Unit-6 .However, no variations in $\chi_{lf}$ is observed in Unit-6, and therefore, the possibility of ferrimagnetic influx is ruled out.

**Table 4.6: Summary table for Bithur Section**

| Units | Mean Grain Size and Characteristics Of units | Organic Matter Content (Wt %) | XRD-Bulk mineralogy | XRD- Clay mineralogy | Magnetic mineralogy | Interpretation |
|---|---|---|---|---|---|---|
| 6 (4.8-5.4) | Medium to fine silt, sitly-clay laminated, | 2.52 | Quartz, feldspar, mica | Illite> Kaolinite | Slightly higher SIRM, MD grains. | Swamp deposit |
| 5 (4.2-4.8m) | Medium to fine silt, Yellowish silt | 2.19 | Quartz, feldspar, mica | Illite>chlorite= kaolinite | Slight increase in SD Ferrimagnetic Mineral | eolian deposit |
| 4 (3.6-4.2) | Medium to fine silt laminated silty clay kankars | 2.42 | Quartz, feldspar, Mica, amphibole | Illite> kaolinite >chlorite | SD particle, Anti-ferroma gnetic Minerals | Swamp Deposit (repeated wet and dry cycle) |
| 3 (2.1-3.6m) | Medium to fine silt yellowish silt with kankar bands | 2.25 | Quartz, feldspar, Calcite. High feldspar content | Illite> chlorite >kaolinite | Uniform Susceptibility, Anti-ferrima gnetic minerals | eolian deposit (with distance of transportation is less) |
| 2 (1.5-2.1m) | Medium to fine silt, dark laminated clay | 4.47 (very high) | Quartz, feldspar, Mica, amphibole | Illite> kaolinite >chlorite | High Susceptibility, SIRM, $\chi_{fd\%}$ - Ferrimagne tic SP particles, at lower level changes to anti-ferroma gnetic minerals at top | Swamp Deposit (prolong anaerobic condition changes to oxidizing environment at top) |
| 1 (0-1.5m) | Medium to fine silt with reddish brown mud, concretion and red and brown mottling | 2.4 | Quartz, feldspar, Goethite, amphibole | Illite> kaolinite >chlorite | Low Susceptibility, Low SIRM, More anti-ferromagnetic minerals | Floodplain deposit |

## 4.2 IIT Kanpur drill core

Figure 4.8 shows the detailed log for the IITK drill core along with positions of samples for OSL dating. Yellowish brown clayey-silt with abundant roots and some brick particles are present from surface to 1.2m. Some of the clay in the top part shows presence of cross-lamination. Yellowish brown silty clay with concretions (average diameter 2cm) and mottling continued to 6m. Few dark nodules were recorded between 1.2-1.8m measured from top. Yellowish silt layer with patches of clays are present from 6 to 10m and concretions are sparsely distributed. Some of the intervening clay layers are thinly laminated. Alteration of yellowish brown clayey silt and grayish brown silty clay with sparse concretions are present between 10 to 13m. Red and brown mottles are present mostly in clay rich parts. Between 13.30m to 13.68 m, reddish brown silty clay with abundant concretions and mottling is present. A pale tough clay layer is present between 13.72m and 14.05m, with numerous concretions (average diameter. few mms to 1cm). Olive brown silty clay and sparsely distributed concretions is present down to 16.47m. Light olive brown clays with patches of silts are present from 18m to 22m. Concretions and mottling are sparse in this horizon. A thick olive brown clay layer with occasional silty patches is present up to 30m. Reddish brown clay layer with concretions and dark nodules (average diameter. 1-3mm) are present between 26.25m to 28.12m. Olive brown clay with high concentrations of concretions and dark nodules (average diam.3-6mm) and red and brown mottles are present at 29.47m and 30.61m. Light olive brown silty clay with occasional silty patches is recorded between 32.57m to 36.54m. Kankars are sparse and some red and brown mottling was observed. Red brown and dark brown silty clay with kankars increasing down depth, are present from 37.88m to 40m. The kankar diameter increases from 5-6 mm at the 38m to 4-5cm at the 39.15m level. High abundance of kankars (nearly 40% of the matrix) with some red and brown mottling is present at this level. Some of the kankars show black coatings. Yellowish brown silty clay with occasional silty patches are present from 40m onwards till the bottom of the core. A reddish brown clay layer with numerous concretions (average diameter. 3-5mm) and red and brown mottling are present between 43.73m to 44.85m. Some of the clay layers are thinly laminated. Concretions were sparse in the bottom part, with presence of some dark nodules and red and brown mottling.

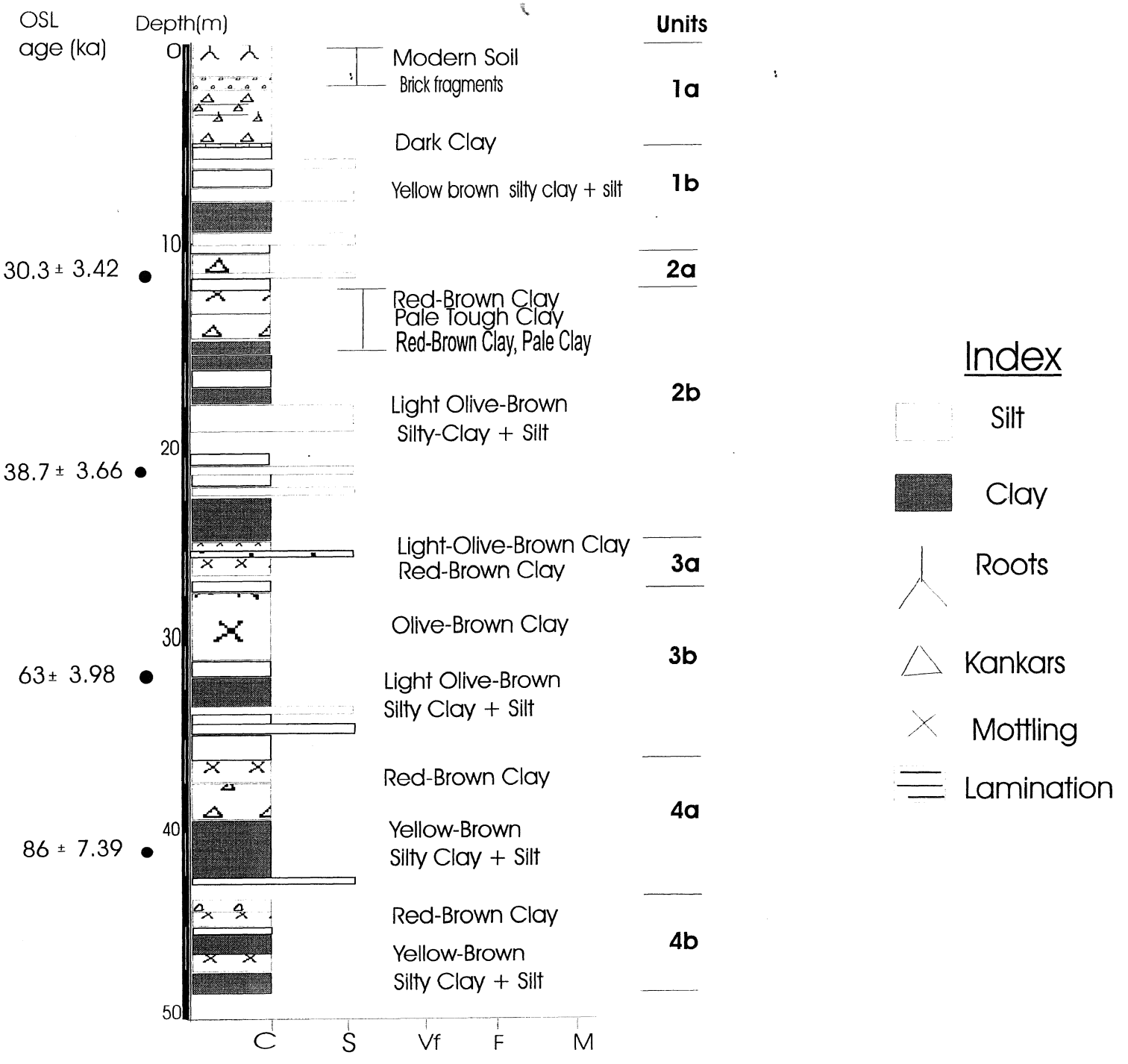


Figure 4.8 Summary Log of IITK Core

### 4.2.1 Litho-Stratigraphic Units

Four litho-stratigraphic units have been identified on the basis of physical parameters (grain size, texture, compositional variations) and a summary log is presented in Fig. 4.8. A brief description of the individual units is given below:

*Unit-1* (surface – 10m) comprises of two parts, viz. 1a & b. The top most layer 1a (surface-5.40m) mainly contains the modern soil and partly disturbed strata. It consists of yellowish brown clay-silt alterations, with abundant roots down to 2m and some brick fragments. Some dark nodules are also recorded, mostly between 1.2 and 2m. A dark clay layer is present at 5.40m marking the end of 1a. Abundant concretions are present between 2-3.5m with some red and brown mottling. Unit 1b (5m-10m) consists mainly of micaceous silty patches with silty-clay layers in between. Concretions are absent in Unit 1b.

*Unit-2* (10-24.85m) comprises of two sub-divisions, 2a and 2b. The upper part, Unit 2a (10- 12.80m) consists of light olive-brown silty clay layer with few occasional silt bands. Concretions are present, and their concentration increases towards the bottom of the unit. At the top of the unit, red and brown mottling are present. *Unit-2b* (12.8-24.85m) consists of light olive brown silty clay and thick patches of silt layers. A red brown clay layer, about 1m thick, with abundant concretions and red and brown mottling, is recorded at 12.8m. Immediately below, a pale tough clay layer is recorded with abundant concretions (2-7mm average diameter). Silty patches are present from 19m downwards. Silty bands are mostly 60cm to a meter thick. Concretions are mostly absent in silty layers, and sparse in the clay horizons. Both red-brown and yellow white mottling are present in the clay layers.

*Unit-3* (24.85-36.75m) is further sub-divided into Units 3a (24.85 -28.6m) and 3b (28.6 – 36.75m). Light olive brown-to-brown clay layer with very few silty patches is present at the top of the Unit 3a. Concretions are sparse and red and brown mottling is present at places. Another red-brown clay layer, < 1 m thick, with abundant concretions and red and brown mottling is recorded at 24.85m. Presence of dark nodules is recorded in the lower

parts of the unit accompanied by increase in red and brown mottling. *Unit-3b* (28.6-36.75m) comprises of light olive brown silty clay layers with silt patches. The silt patches are 40-70 cm thick with sparse kankars. Few dark nodules and red and brown mottling are present in the top part and some concretions are recorded in the clayey layers.

*Unit-4* (36.75-48.6m) comprises of two sub-divisions, i.e. 4a & b. Unit 4a (36.75-43.5m) consists of yellow brown silty clay with very few silty patches. A third red brown clay layer, <1m thick, with abundant kankars and red and brown mottling is recorded in this unit at 38.15m. Some of the kankars show presence of dark coatings on their surface. In the middle part of this unit (~ 38m), kankar concentration increases downward and an increase in the average diameter of the kankars (from 4-5mm to 3-4cm) is also recorded. *Unit-4b* (43.5-48.6m) comprises of yellow brown silty clay with few silty patches. At the top part of this unit, a 1.5m thick red-brown clay layer with abundant concretions and red and brown mottling are present. Some black nodules are present between 45.47m to 47.36m.

The OSL ages from IITK core (Fig. 4.8) suggest that the Unit 4 is > 80, 000 years old whereas Unit 3 falls in the age bracket of 60-80ka. Unit 2 was deposited between 30-40ka and the strata falling in Unit 1 is younger than ~30ka.

### 4.2.2 Grain size

Table 4.7 lists the statistical grain size parameters and Figure 4.9 shows the cumulative frequency distribution for samples from different units at IITK drill core. The mean grain size of the drill core sample varies between fine silt to coarse silt (after Udden & Wentworth scale). The silty patches present in the Unit-2 fall in coarse silt grade, whereas the overall mean grain size is fine silt. All samples are poorly sorted except the sample from Unit-4, which is moderately well-sorted. The skewness or asymmetry of the grain size curve shows positively skewed values indicating more fine materials present than in a normal distribution. However, the sample from Unit-2 shows very negatively skewed values indicating more coarse material present than in a normal distribution.

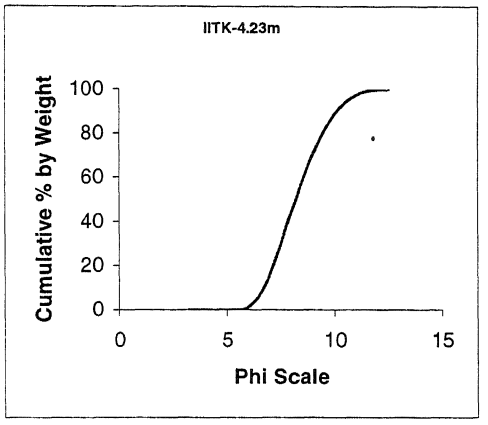


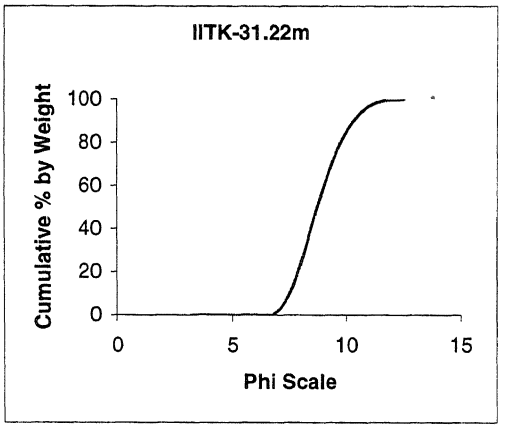


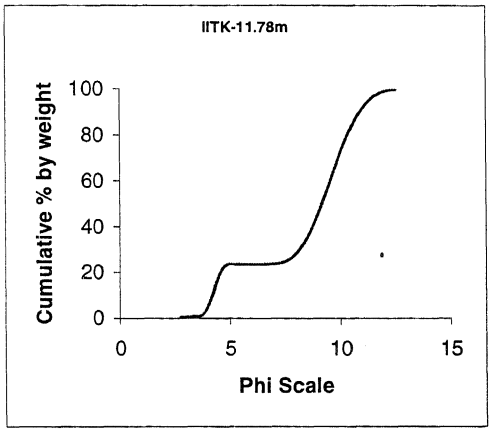


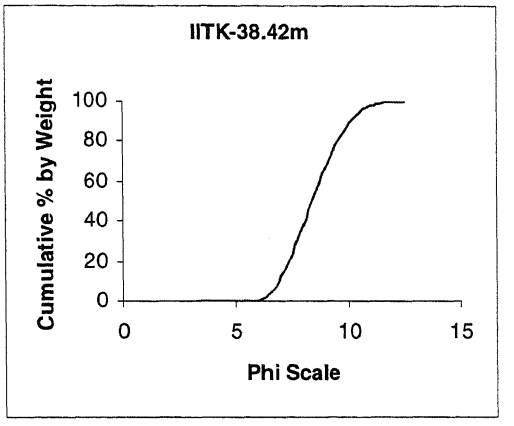


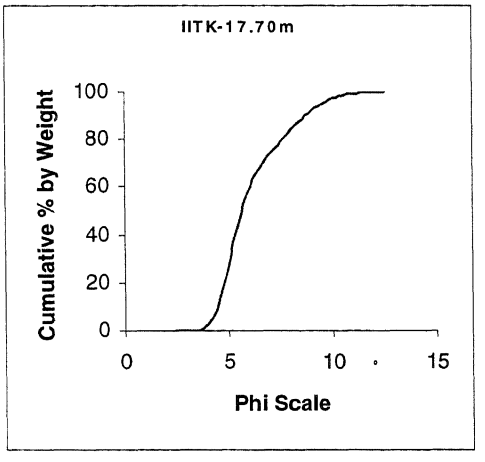


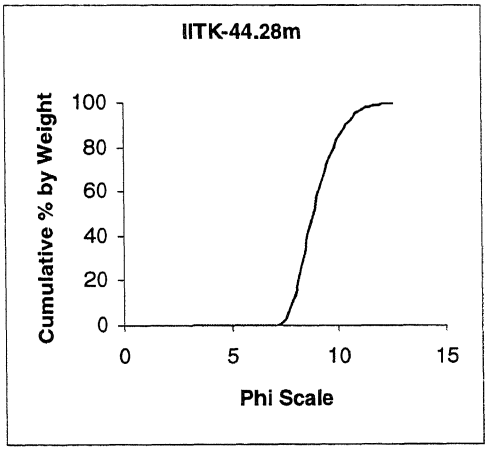


Fig.4.9. Grain size plots for different units of IITK drill core

Units 3 and 4 samples show near symmetrical distribution representing near normal distribution of grain size. The samples from all units are mesokurtic.

**Table 4.7. Grain size parameters for IITK core samples**

| Depth (m) | Units | Mean | Sorting | Skewness | Kurtosis | Interpretation |
|---|---|---|---|---|---|---|
| 4.23 | 1 | 7.65 | 1.366 | 0.109 | 0.949 | Medium to fine silt, poorly sorted, positively skewed and mesokurtic |
| 11.78 | 2 | 6.22 | 2.6 | -0.509 | 1.1 | Medium silt, very poorly sorted, very negatively skewed and mesokurtic |
| 17.7 | 2 | 5.396 | 1.653 | 0.45 | 0.977 | Very coarse silt, poorly sorted, very positively skewed, mesokurtic |
| 25.7 | 3 | 8.6 | 1.045 | 0.042 | 0.933 | Very fine silt, poorly sorted, symmetrical and mesokurtic |
| 31.22 | 3 | 8.25 | 1.13 | 0.17 | 0.98 | Fine silt to very fine silt, poorly sorted, positively skewed and mesokurtic |
| 38.42 | 4 | 8.53 | 0.98 | 0.297 | 0.917 | Very fine silt, poorly sorted, symmetrical and mesokurtic |
| 44.28 | 4 | 7.8 | 1.26 | 0.05 | 0.949 | Medium to fine silt, moderately sorted, Positively skewed and mesokurtic |

### 4.2.3. Organic matter content and Sediment Mineralogy

The $H_2O_2$ reactive organic matter contents of representative samples from all seven units are shown in Table 4.8. The organic matter content generally shows a decrease in values down depth, with high values in near surface horizons. The bulk mineralogy of core sediments determined by XRD is represented by quartz, feldspar and mica in variable amounts (Table 4.8). Calcite is present in trace in bulk in all the units, while amphiboles are identified in Units 4, in trace. Quartz is the dominant mineral in all the units, ranging from 60-80% of the bulk samples (Table 4.9 and Fig. 4.10). Feldspar content is variable and is distinctly high in Units 2 and 4 and these units also show a higher mica content. Quartz/feldspar ratio show uniformly constant value throughout the units. Increase in mica content is observed in the silty patches of unit-2. Carbonate concretions are represented by calcite and minor amounts of aragonite and dolomite in the upper ~25m (Units 1 and 2). Siderite presence recorded at unit-4. $MgCO_3$ content lies between 3-8% in most samples, only few samples of Unit-1 and 3 show 13-18% of $MgCO_3$ in samples.

**Table 4.8: Qualitative mineralogical data for the IITK drill core**

| Units | Organic Matter (wt%) | Bulk mineralogy | | | | | Clay mineralogy | | | | Concretion mineralogy |
|---|---|---|---|---|---|---|---|---|---|---|---|
| | | Q (3.34Å) | F (3.19 Å) | M (10 Å) | Cc (3.03 Å) | Others | I (10 Å) | Ch (14.4 Å) | K (3.57 Å) | Mx (11 Å) | |
| 1 | 4.8 | ++++ | ++ | ++ | + | | ++ | ++ | ++ | + | Calcite, aragonite |
| 2 | 1.5 | +++ | ++ | ++ | + | | ++++ | ++ | ++ | + | Calcite, Aragonite, dolomite |
| 3 | 2.3 | ++++ | ++ | +++ | + | | +++ | ++ | ++ | + | calcite |
| 4 | 2.2 | ++++ | ++ | ++ | + | A+ | +++ | ++ | ++ | | Calcite, siderite |

Q-Quartz, F-Feldspar, M-Mica, A- Amphibole, G-Goethite, Cc-Calcite, I-Illite, Chlorite, K-Kaolinite, Mx-Mixed layer clay
++++ High; +++ Moderate; ++ Minor; + Trace

Clay mineral assemblage is represented by illite, kaolinite, chlorite and mixed-layer clays. Illite is the most dominant clay mineral, corresponding to ~ 80-90% of the clay fraction (Table 4.9 and Fig. 4.10). Chlorite and kaolinite are two other major clay minerals. The relative abundance of chlorite averages around 5% with just one exception of a sample from Unit 1 where it reaches a value of 15%. Kaolinite shows significant variation and some samples from upper part of Unit-2 show high values (>15% of the clay fraction). Both chlorite and kaolinite are present in all the units except for a few exceptions where chlorite is absent. (Illite +Chlorite/Kaolinite) ratio shows particularly low values at 12.47m indicating more leaching and weathering condition. A very high value of kaolinite content is recorded from Unit-2b. But as the feldspar content does not show much change in this unit, it is inferred that the origin of kaolinite may not be related from feldspar breakdown only compared to the lower horizons. Trace amounts of mixed layer clays (11Å) are recorded , in unit 1, 2 and 3.

**Table 4.9. Relative abundance of minerals computed by normalization in IITK Core**

| Bulk powder | | | | | | | Smeared fine fraction | | | | |
|---|---|---|---|---|---|---|---|---|---|---|---|
| Units | Depth (m) | Q% | Felds% | Mica% | Q/F | Units | Depth (m) | Illite% | Chl % | Kaol % | (I+C)/K |
| 1 | 3.93 | 62.13 | 15.14 | 22.71 | 4.10 | 1 | 2.95 | 95.34 | 0 | 4.65 | 20.50 |
| | 5.83 | 56.06 | 20.5 | 20.5 | 2.73 | | 3.93 | 94.08 | 0.98 | 4.93 | 19.28 |
| | 9.64 | 57.97 | 14.57 | 27.44 | 3.98 | | 4.99 | 91.3 | 3.62 | 5.07 | 18.72 |
| 2 | 11.18 | 64.49 | 10.92 | 24.57 | 5.91 | | 5.83 | 81.75 | 15.32 | 2.91 | 33.36 |
| | 12.47 | 61.9 | 10.76 | 27.32 | 5.75 | | 8.32 | 89.23 | 1.76 | 9 | 10.11 |
| | 13.8 | 76.47 | 8.55 | 14.97 | 8.94 | | 9.64 | 86.95 | 7.6 | 5.43 | 17.41 |

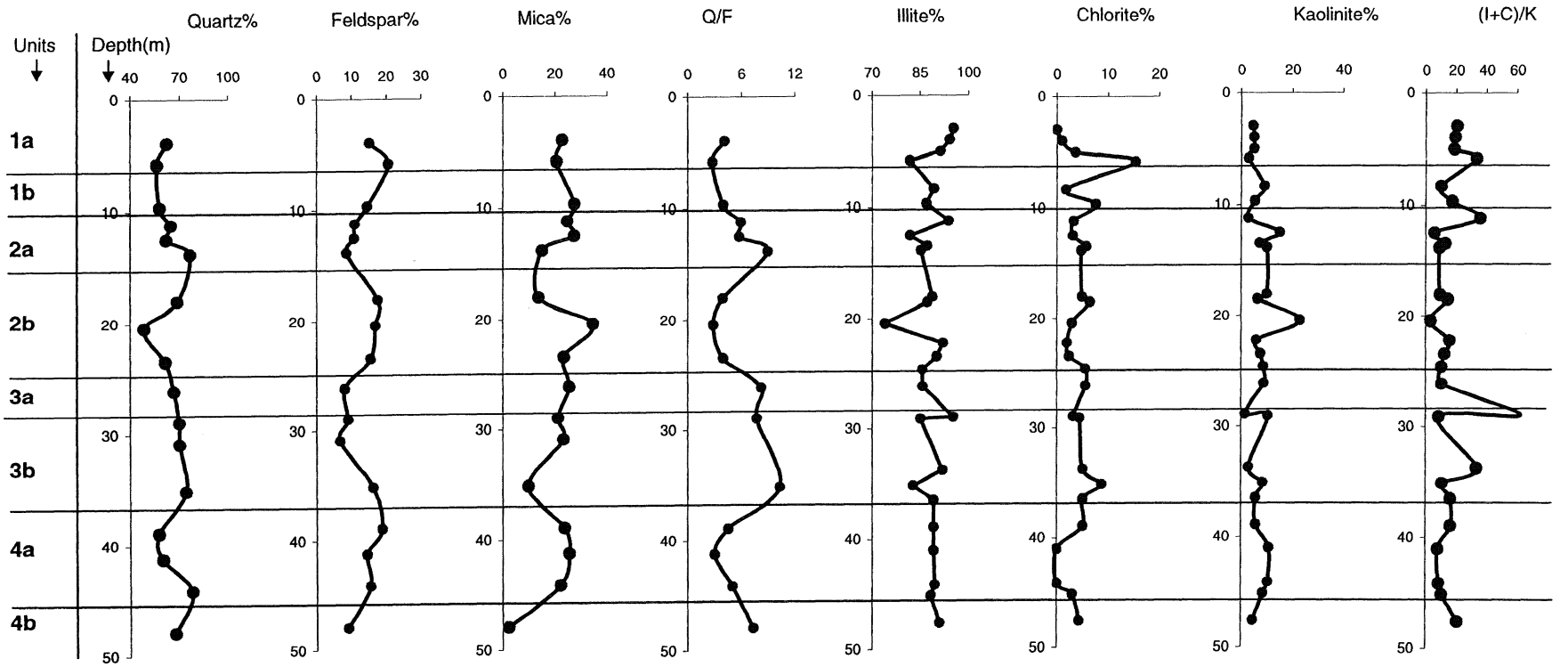


Figure 4.10. bulk and clay mineral abundance in percentage in IITK core section

| | | | | | | | | | | | |
|---|---|---|---|---|---|---|---|---|---|---|---|
| | 18 | 68.68 | 17.61 | 13.69 | 3.90 | | 11.18 | 93.73 | 3.26 | 2.72 | 35.66 |
| | 20.4 | 48.39 | 16.95 | 34.64 | 2.85 | | 12.47 | 81.81 | 3.11 | 15.06 | 5.64 |
| | 23.4 | 61.15 | 15.57 | 23.3 | 3.93 | | 13.43 | 87.1 | 5.73 | 7.16 | 12.97 |
| 3 | 26.1 | 66.54 | 8.1 | 25.34 | 8.21 | 2 | 13.8 | 85.2 | 4.73 | 10.05 | 8.95 |
| | 28.95 | 69.86 | 9.04 | 21.09 | 7.73 | | 18 | 88.78 | 4.9 | 10.05 | 9.32 |
| | 30.9 | 69.94 | 6.76 | 23.26 | 10.35 | | 18.42 | 87.17 | 6.41 | 6.41 | 14.60 |
| | 35.1 | 73.98 | 16.26 | 9.75 | 4.55 | | 20.4 | 74.07 | 2.96 | 22.96 | 3.35 |
| 4 | 38.92 | 57.41 | 18.92 | 23.65 | 3.03 | | 22.18 | 92.1 | 1.97 | 5.92 | 15.89 |
| | 41.21 | 59.87 | 14.59 | 25.53 | 4.10 | | 23.4 | 90.12 | 2.35 | 7.53 | 12.28 |
| | 44.1 | 77.81 | 15.51 | 22.16 | 5.02 | | 24.6 | 85.71 | 5.55 | 8.73 | 10.45 |
| | 47.9 | 67.55 | 9.17 | 23.84 | 7.37 | | 26.1 | 85.71 | 5.56 | 8.78 | 10.40 |
| | | | | | | | 28.95 | 95.23 | 3.17 | 1.58 | 62.28 |
| | | | | | | 3 | 29.1 | 85.1 | 4.43 | 10.46 | 8.56 |
| | | | | | | | 33.76 | 91.91 | 5.05 | 2.91 | 33.32 |
| | | | | | | | 35.1 | 82.8 | 8.75 | 8.43 | 10.86 |
| | | | | | | | 36.8 | 89.18 | 5.06 | 5.74 | 16.42 |
| | | | | | | | 38.92 | 89.18 | 5.06 | 5.74 | 16.42 |
| | | | | | | | 41 | 89.19 | 0 | 10.96 | 8.14 |
| | | | | | | 4 | 44.1 | 89.55 | 0 | 10.44 | 8.58 |
| | | | | | | | 45.1 | 88.37 | 3.05 | 8.57 | 10.67 |
| | | | | | | | 47.55 | 91.05 | 4.35 | 4.6 | 20.74 |

I-Illite, C-Chlorite, K-Kaolinite

### 4.2.4. Magnetic susceptibility and Mineral Magnetic Analysis

Tables 4.10 and 4.11 show data on magnetic susceptibility and mineral magnetic parameters respectively for the IITK drill core. The magnetic parameters indicate presence of magnetic minerals in the entire section. Magnetic susceptibility ($\chi_{lf}$) is quite low with exceptions at 6.9 12.9, 17.4, 20.4, 25.8, 30, 31.2, 36.6 and 45m where high susceptibility is recorded (Fig.4.11). $\chi_{fd}$% value is low (~2-3%), except in Unit 2b and 3a where $\chi_{fd}$% reaches to ~6-7% indicating presence of SP particles.

**Table 4.10. Magnetic susceptibility data for IITK Drill core samples**

| Unit | Sample depth (m) | Corrected. Weight ($*10^{-3}$kg) | $\chi_{lf}$ ($*10^{-8}m^3$/kg) | $\chi_{hf}$ ($*10^{-8}m^3$/kg) | $\chi_{fd\%}$ |
|---|---|---|---|---|---|
| | 0 | 10.76 | 22.28 | 21.61 | 2.7 |
| | 0.3 | 9.83 | 19.28 | 18.67 | 3.3 |
| | 0.6 | 12.56 | 14.27 | 13.98 | 1.35 |
| | 0.9 | 11.98 | 10.68 | 10.20 | 4.44 |
| | 1.2 | 14.34 | 5.98 | 5.86 | 1.92 |
| | 1.5 | 11.27 | 10.56 | 10.54 | 0.19 |
| | 1.8 | 9.5 | 9.16 | 9.084 | 0.83 |
| | 2.1 | 9.48 | 7.55 | 7.46 | 1.02 |
| | 2.4 | 11.02 | 15.42 | 15.06 | 2.39 |
| | 2.7 | 11.51 | 11.03 | 10.72 | 2.74 |

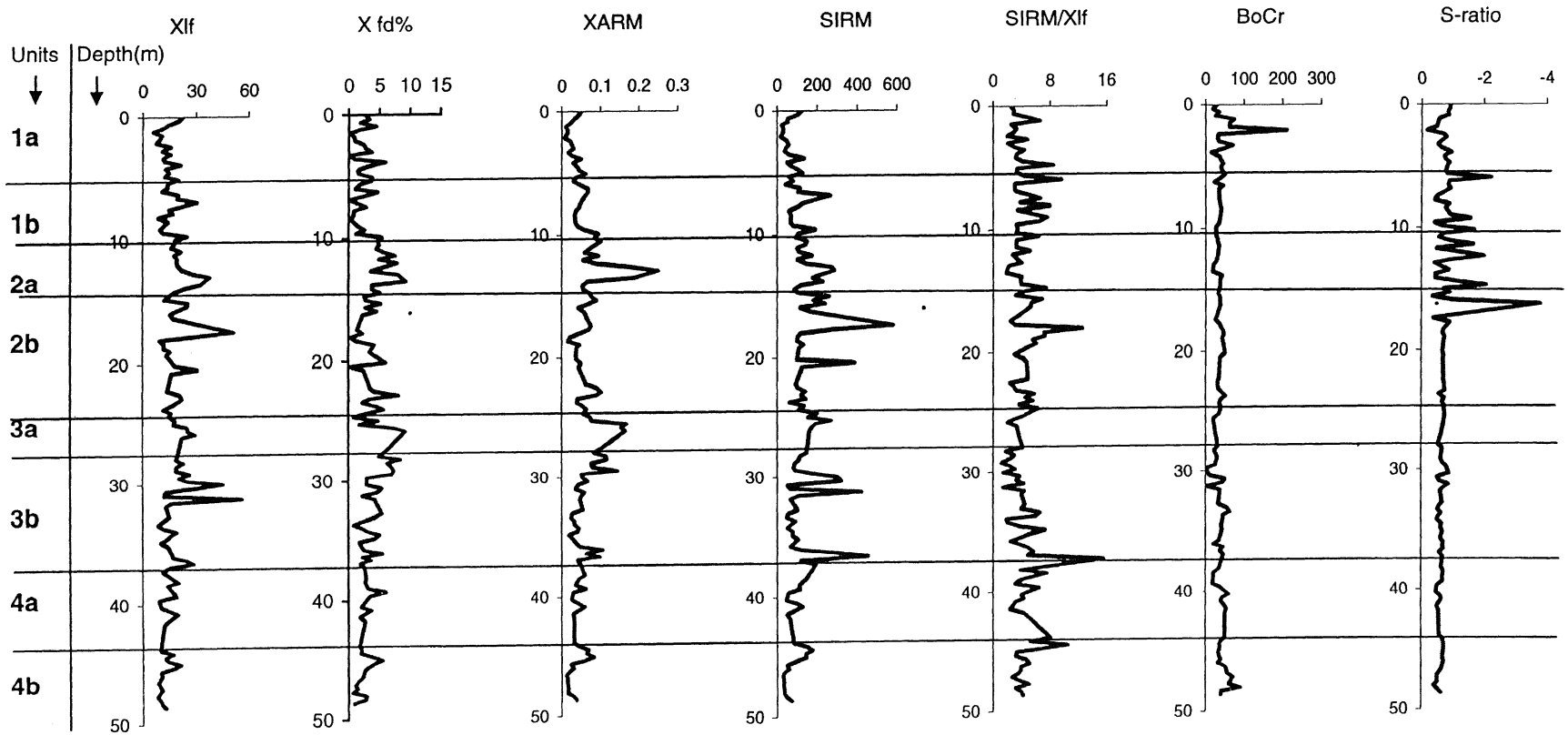


Figure 4.11. Mangetic sucseptibility and mineral magnetic plottings of IITK drill core

| | | | | | |
|---|---|---|---|---|---|
| 1 | 3 | 10.09 | 15.3 | 14.7 | 3.67 |
| | 3.3 | 9.35 | 11 | 11.3 | 0.019 |
| | 3.6 | 10.66 | 12.12 | 12 | 0.99 |
| | 3.9 | 11.61 | 20.93 | 19.68 | 5.94 |
| | 4.2 | 12.3 | 12.86 | 12.46 | 3.08 |
| | 4.5 | 8.58 | 14.58 | 14.35 | 1.466 |
| | 4.8 | 12.86 | 12.34 | 12.13 | 1.65 |
| | 5.1 | 12.08 | 19.86 | 19.10 | 3.81 |
| | 5.4 | 9.41 | 13.85 | 13.34 | 3.66 |
| | 5.7 | 10.99 | 13.90 | 13.65 | 1.741 |
| | 6 | 11.1 | 10.77 | 10.20 | 1.04 |
| | 6.3 | 10.44 | 19.54 | 18.63 | 4.66 |
| | 6.6 | 10.17 | 19.22 | 18.74 | 2.5 |
| | 6.9 | 11.74 | 30.3 | 30.34 | 0.16 |
| | 7.5 | 11.68 | 14.45 | 14.04 | 2.79 |
| | 7.8 | 9.75 | 16.69 | 16.57 | 0.79 |
| | 8.1 | 10.61 | 8.77 | 8.699 | 0.83 |
| | 8.4 | 11.86 | 14.08 | 14.04 | 0.29 |
| | 9 | 12.58 | 9.53 | 9.38 | 1.55 |
| | 9.3 | 12.88 | 11.14 | 10.85 | 2.58 |
| | 9.6 | 10.34 | 24.80 | 24.49 | 1.208 |
| | 9.9 | 10.37 | 17.94 | 16.97 | 5.38 |
| 2 | 10.2 | 10.16 | 17.43 | 16.59 | 4.75 |
| | 10.5 | 12.41 | 15.85 | 15.06 | 4.97 |
| | 10.8 | 10.51 | 21.2 | 20.31 | 4.47 |
| | 11.1 | 10.37 | 17.6 | 16.61 | 5.69 |
| | 11.4 | 9.79 | 18.9 | 18.16 | 7.51 |
| | 11.7 | 11.77 | 18.77 | 17.84 | 4.96 |
| | 12 | 11.04 | 19.56 | 18.03 | 7.8 |
| | 12.3 | 11.42 | 21.54 | 20.31 | 5.66 |
| | 12.6 | 13.39 | 27.65 | 26.10 | 3.587 |
| | 12.9 | 14.01 | 37.40 | 34.42 | 7.94 |
| | 13.5 | 10.94 | 32.84 | 29.7 | 9.3 |
| | 13.8 | 9.31 | 24.33 | 23.41 | 3.78 |
| | 14.1 | 10.55 | 17.81 | 17.13 | 3.77 |
| | 14.4 | 9.2 | 14.83 | 14.07 | 5.08 |
| | 14.7 | 13 | 12 | 11.69 | 2.54 |
| | 15 | 12.08 | 25.1 | 24.40 | 2.79 |
| | 15.3 | 14.83 | 24.65 | 23.36 | 5.19 |
| | 15.6 | 12.01 | 19.28 | 18.74 | 2.78 |
| | 15.9 | 10.36 | 15.11 | 14.43 | 4.51 |
| | 16.2 | 10.18 | 16.85 | 16.46 | 2.3 |
| | 17.4 | 11.99 | 51.15 | 50.44 | 1.37 |
| | 17.7 | 10.51 | 31.30 | 30.5 | 2.24 |
| | 18 | 14.56 | 9.581 | 9.53 | 0.42 |
| | 18.3 | 11.34 | 11.798 | 11.64 | 1.26 |
| | 18.6 | 11.33 | 11.518 | 11 | 4.13 |
| | 18.9 | 12.79 | 15.246 | 14.6 | 3.8 |
| | 19.2 | 12.84 | 13.247 | 12.79 | 3.39 |
| | 20.1 | 8.92 | 18 | 16.9 | 5.97 |
| | 20.4 | 11.74 | 30.36 | 30.2 | 0.46 |
| | 20.7 | 12.32 | 16.05 | 15.64 | 2.489 |
| | 22.2 | 9.65 | 13.68 | 13.21 | 3.45 |

| | | | | | |
|---|---|---|---|---|---|
| | 22.5 | 9.1 | 20.7 | 19.86 | 4.2 |
| | 22.8 | 8.93 | 21.72 | 19.96 | 8.08 |
| | 23.1 | 9.52 | 19.27 | 17.64 | 3.42 |
| | 23.4 | 9.25 | 15.90 | 15.54 | 2.22 |
| | 23.7 | 12.48 | 11.45 | 10.94 | 4.44 |
| | 24 | 13.53 | 15.67 | 14.78 | 5.65 |
| | 24.3 | 11.68 | 14.75 | 14.28 | 3.14 |
| | 24.6 | 12.14 | 17.89 | 17.75 | 0.81 |
| 3 | 24.9 | 12.59 | 17.1 | 16.29 | 4.77 |
| | 25.2 | 10.72 | 24.7 | 24.4 | 1.77 |
| | 25.5 | 10.65 | 25.1 | 23.36 | 7.18 |
| | 25.8 | 11.79 | 29.2 | 26.5 | 9.15 |
| | 26.1 | 12.3 | 21.81 | 19.9 | 8.75 |
| | 27.9 | 10.78 | 18.70 | 17.7 | 4.93 |
| | 28.2 | 13.78 | 22.6 | 18.5 | 8.43 |
| | 28.5 | 11.97 | 18.8 | 17.66 | 6.32 |
| | 28.8 | 10.58 | 18.52 | 17.23 | 6.96 |
| | 29.1 | 10.73 | 25.93 | 24.02 | 7.35 |
| | 29.4 | 11.41 | 20.34 | 18.91 | 7.01 |
| | 29.7 | 10.94 | 24.66 | 23.91 | 2.95 |
| | 30 | 10.74 | 45.1 | 43.78 | 2.93 |
| | 30.3 | 12.14 | 29.8 | 29.07 | 2.93 |
| | 30.6 | 14.11 | 12.45 | 11.78 | 5.37 |
| | 30.9 | 11.28 | 11.99 | 11.41 | 4.77 |
| | 31.2 | 11.15 | 55.81 | 54 | 2.21 |
| | 31.5 | 9.34 | 15.74 | 15.07 | 4.28 |
| | 31.8 | 11.02 | 12.84 | 12.25 | 4.49 |
| | 32.7 | 12.17 | 14.85 | 14.05 | 5.4 |
| | 33 | 11.55 | 11.47 | 10.9 | 4.37 |
| | 33.3 | 12.1 | 8.479 | 08.23 | 2.56 |
| | 33.6 | 12.27 | 12.08 | 11.9 | 0.79 |
| | 33.9 | 8.99 | 18.75 | 18.353 | 2.13 |
| | 34.2 | 9.75 | 15.64 | 15.13 | 3.21 |
| | 34.5 | 12.65 | 13.97 | 13.2 | 5.06 |
| | 34.8 | 11.94 | 10.11 | 9.68 | 4.23 |
| | 35.1 | 13.8 | 14.173 | 13.92 | 1.75 |
| | 35.7 | 10.25 | 16.27 | 15.85 | 2.56 |
| | 36 | 10.75 | 16.8 | 15.8 | 5.51 |
| | 36.3 | 11.9 | 24.68 | 24.1 | 2.24 |
| | 36.6 | 13.78 | 28.41 | 27.36 | 3.66 |
| 4 | 36.9 | 11.29 | 15.24 | 14.95 | 1.9 |
| | 37.2 | 14.24 | 11.2 | 10.94 | 2.64 |
| | 38.1 | 12.41 | 20.8 | 19.4 | 2.86 |
| | 38.4 | 14.55 | 13.9 | 13.53 | 2.71 |
| | 39 | 11.17 | 17.21 | 16.6 | 3.18 |
| | 39.3 | 10.99 | 18.63 | 17.49 | 6.07 |
| | 39.6 | 11.62 | 9 | 8.71 | 3.48 |
| | 40.2 | 10.55 | 10.37 | 10.10 | 2.56 |
| | 40.5 | 11.08 | 15.07 | 14.75 | 2.06 |
| | 40.8 | 11.81 | 19.39 | 18.67 | 3.68 |
| | 41.4 | 12.37 | 13.95 | 13.70 | 1.87 |
| | 41.7 | 11.46 | 11.86 | 11.54 | 2.71 |
| | 43.8 | 11.37 | 9.9 | 9.71 | 1.8 |

| | | | | | |
|---|---|---|---|---|---|
| | 44.1 | 9 | 16.86 | 16.5 | 2.15 |
| | 44.4 | 12.77 | 12.76 | 12.49 | 2.03 |
| | 44.7 | 11.38 | 13.84 | 13.29 | 3.98 |
| | 45 | 12.41 | 20.854 | 19.70 | 5.5 |
| | 45.3 | 10.44 | 17.29 | 16.58 | 4.12 |
| | 45.6 | 10.78 | 10.18 | 9.86 | 3.15 |
| | 45.9 | 10.65 | 10.70 | 10.42 | 2.59 |
| | 46.2 | 14.41 | 9.58 | 9.34 | 2.46 |
| | 46.5 | 10.8 | 8.48 | 8.29 | 2.15 |
| | 46.8 | 12.43 | 9.63 | 9.49 | 1.54 |
| | 47.1 | 11.4 | 10.87 | 10.75 | 1.1 |
| | 47.4 | 10.6 | 9.16 | 9.01 | 1.49 |
| | 47.7 | 11.96 | 8.09 | 8.03 | 0.71 |
| | 48 | 13.67 | 10 | 9.72 | 2.95 |
| | 48.3 | 12.77 | 10.67 | 10.36 | 2.75 |
| | 48.6 | 12.25 | 12.86 | 12.7 | 0.93 |

$\chi_{fd\%} = \{(\chi_{lf} - \chi_{hf}) / \chi_{lf}\} * 100$

**Table 4.11. Mineral magnetic data for IITK Drill Core Samples**

| Unit | Sample depth (m) | $\chi_{ARM}$ ($*10^{-5}m^3/kg$) | SIRM/ $\chi_{lf}$ ($*10^3A/m$) | SIRM ($Am^2Kg^{-1}$) | BoCr (mT) | S-ratio |
|---|---|---|---|---|---|---|
| 1 | 0 | 0.048 | 2.52 | 56.29 | 28 | -0.9008 |
| | 0.3 | 0.042 | 2.91 | 56.20 | 18 | -0.904 |
| | 0.6 | 0.031 | 2.84 | 40.59 | 35 | -0.8458 |
| | 0.9 | 0.023 | 4.85 | 51.89 | 26 | -0.863 |
| | 1.2 | 0.010 | 6.55 | 39.21 | 73 | -0.5600 |
| | 1.5 | 0.013 | 2.55 | 27.01 | 62 | -0.509 |
| | 1.8 | 0.013 | 3.26 | 29.90 | 63 | -0.4818 |
| | 2.1 | 0.007 | 2.91 | 21.99 | 210 | -0.170 |
| | 2.4 | 0.021 | 2.02 | 31.29 | 33 | -0.683 |
| | 2.7 | 0.026 | 4.80 | 52.97 | 30 | -0.782 |
| | 3 | 0.029 | 2.05 | 31.404 | 35 | -0.634 |
| | 3.3 | 0.016 | 2.89 | 32.90 | 70 | -0.5183 |
| | 3.6 | 0.026 | 4.35 | 52.80 | 47 | -0.654 |
| | 3.9 | 0.049 | 3.38 | 70.91 | 15 | -0.943 |
| | 4.2 | 0.029 | 3.16 | 40.67 | 35 | -0.721 |
| | 4.5 | 0.040 | 4.25 | 61.974 | 40 | -0.769 |
| | 4.8 | 0.045 | 8.42 | 103.97 | 45 | -0.882 |
| | 5.1 | 0.061 | 3.39 | 67.37 | 40 | -0.8264 |
| | 5.4 | 0.037 | 3.32 | 46.02 | 43 | -0.774 |
| | 5.7 | 0.0303 | 4.45 | 61.87 | 50 | -0.8090 |
| | 6 | 0.0484 | 9.56 | 103 | 37 | -2.224 |
| | 6.3 | 0.0667 | 3.08 | 60.2 | 22 | -0.905 |
| | 6.6 | 0.0669 | 3.03 | 58.2 | 45 | -0.854 |
| | 6.9 | 0.059 | 3.12 | 94.9 | 34 | -0.935 |
| | 7.5 | 0.047 | 6.5 | 95.2 | 35 | -0.513 |
| | 7.8 | 0.04 | 3.83 | 64.07 | 36 | -0.428 |
| | 8.1 | 0.036 | 7.95 | 69.78 | 38 | -0.889 |
| | 8.4 | 0.033 | 3.44 | 48.49 | 40 | -0.7669 |
| | 9 | 0.035 | 7.53 | 71.85 | 38 | -0.93 |

| | | | | | | |
|---|---|---|---|---|---|---|
| | 9.3 | 0.042 | 6.58 | 73.39 | 36 | -1.570 |
| | 9.6 | 0.059 | 3.27 | 81.23 | 35 | -0.419 |
| | 9.9 | 0.0933 | 3.45 | 62.01 | 25 | -0.684 |
| 2 | 10.2 | 0.084 | 3.21 | 55.95 | 27 | -1.692 |
| | 10.5 | 0.1000 | 6.36 | 100.9 | 27 | -0.706 |
| | 10.8 | 0.084 | 3.30 | 70.30 | 30 | -0.56 |
| | 11.1 | 0.07 | 3.25 | 57.42 | 30 | -0.901 |
| | 11.4 | 0.05 | 3.20 | 60.80 | 35 | -1.6658 |
| | 11.7 | 0.093 | 5.16 | 97.07 | 33 | -0.496 |
| | 12 | 0.055 | 2.74 | 53.67 | 32 | -1.327 |
| | 12.3 | 0.08 | 3.33 | 71.80 | 30 | -2.01 |
| | 12.6 | 0.183 | 3.97 | 110.04 | 27 | -1.01 |
| | 12.9 | 0.247 | 2.18 | 81.77 | 20 | -0.424 |
| | 13.5 | 0.187 | 1.86 | 61.12 | 18 | -0.889 |
| | 13.8 | 0.066 | 3.99 | 97.33 | 42 | -0.448 |
| | 14.1 | 0.052 | 3.82 | 68.19 | 37 | -0.451 |
| | 14.4 | 0.0543 | 3.97 | 58.98 | 37 | -1.119 |
| | 14.7 | 0.070 | 7.39 | 88.73 | 37 | -2.089 |
| | 15 | 0.077 | 4.41 | 110.97 | 35 | -0.727 |
| | 15.3 | 0.089 | 3.19 | 78.87 | 33 | -0.91 |
| | 15.6 | 0.068 | 6.82 | 131.52 | 37 | -0.358 |
| | 15.9 | 0.0421 | 5.36 | 81.07 | 37 | -1.031 |
| | 16.2 | 0.0573 | 5.22 | 88.10 | 38 | -3.830 |
| | 17.4 | 0.074 | 2.42 | 124.21 | 25 | -0.382 |
| | 17.7 | 0.068 | 3.06 | 96 | 35 | -0.915 |
| | 18 | 0.044 | 12.47 | 119.5 | 41 | -0.816 |
| | 18.3 | 0.020 | 7.15 | 84.38 | 45 | -0.70 |
| | 18.6 | 0.01 | 7.21 | 83.11 | 47 | -0.682 |
| | 18.9 | 0.045 | 5.53 | 84.38 | 43 | -0.73 |
| | 19.2 | 0.03 | 6.03 | 79.92 | 45 | -0.723 |
| | 20.1 | 0.036 | 2.92 | 52.71 | 50 | -0.677 |
| | 20.4 | 0.045 | 4.15 | 126.2 | 38 | -0.718 |
| | 20.7 | 0.04 | 4.73 | 75.9 | 37 | -0.69 |
| | 22.2 | 0.061 | 4.83 | 66.22 | 35 | -0.716 |
| | 22.5 | 0.090 | 2.35 | 48.83 | 30 | -0.706 |
| | 22.8 | 0.101 | 2.92 | 63.51 | 30 | -0.73 |
| | 23.1 | 0.0882 | 3.14 | 60.63 | 33 | -0.739 |
| | 23.4 | 0.0407 | 5.73 | 91.13 | 42 | -0.760 |
| | 23.7 | 0.038 | 4.48 | 51.4 | 52 | -0.554 |
| | 24 | 0.054 | 5.54 | 86.978 | 40 | -0.73 |
| | 24.3 | 0.0633 | 3.61 | 53.33 | 35 | -0.65 |
| | 24.6 | 0.0543 | 6.28 | 112.5 | 40 | -0.721 |
| | 24.9 | 0.072 | 5.22 | 89.4 | 37 | -0.72 |
| | 25.2 | 0.07 | 4.29 | 106.79 | 34 | -0.74 |
| | 25.5 | 0.167 | 2.92 | 73.74 | 21 | -0.73 |
| | 25.8 | 0.152 | 1.97 | 57.75 | 20 | -0.72 |
| | 26.1 | 0.163 | 3.29 | 71.9 | 22 | -0.71 |
| | 27.9 | 0.082 | 4.11 | 76.88 | 32 | -0.538 |
| | 28.2 | 0.113 | 1.71 | 38.92 | 22 | -0.679 |
| | 28.5 | 0.115 | 2.96 | 55.93 | 27 | -0.644 |
| | 28.8 | 0.075 | 2.38 | 44.09 | 30 | -0.631 |
| | 29.1 | 0.078 | 1.16 | 30.11 | 27 | -0.629 |
| | 29.4 | 0.143 | 2.28 | 46.48 | 25 | -0.678 |

| | | | | | | |
|---|---|---|---|---|---|---|
| 3 | 29.7 | 0.050 | 3.08 | 76.04 | 5 | -0.795 |
| | 30 | 0.054 | 1.45 | 65.60 | 4 | -0.827 |
| | 30.3 | 0.066 | 3.71 | 110.7 | 10 | -0.88 |
| | 30.6 | 0.041 | 3.24 | 40.40 | 50 | -0.512 |
| | 30.9 | 0.0352 | 4.27 | 51.28 | 43 | -0.574 |
| | 31.2 | 0.057 | 1.41 | 78.83 | 2 | -0.868 |
| | 31.5 | 0.050 | 4.35 | 68.58 | 37 | -0.70 |
| | 31.8 | 0.046 | 3.95 | 50. | 36 | -0.606 |
| | 32.7 | 0.054 | 4.47 | 66.52 | 33 | -0.674 |
| | 33 | 0.027 | 3.94 | 45.30 | 55 | -0.564 |
| | 33.3 | 0.023 | 6.53 | 55.43 | 63 | -0.524 |
| | 33.6 | 0.032 | 5.97 | 72.18 | 45 | -0.626 |
| | 33.9 | 0.033 | 1.81 | 34.13 | 45 | -0.558 |
| | 34.2 | 0.044 | 2.07 | 32.5 | 44 | -0.505 |
| | 34.5 | 0.040 | 3.79 | 53.05 | 40 | -0.644 |
| | 34.8 | 0.018 | 7.24 | 73.32 | 43 | -0.620 |
| | 35.1 | 0.028 | 5.15 | 73.01 | 40 | -0.68 |
| | 35.7 | 0.046 | 2.44 | 39.80 | 35 | -0.61 |
| | 36 | 0.104 | 4.02 | 67.58 | 20 | -0.70 |
| | 36.3 | 0.063 | 4.93 | 121.8 | 45 | -0.681 |
| | 36.6 | 0.097 | 5.64 | 160.29 | 37 | -0.714 |
| 4 | 36.9 | 0.040 | 4.92 | 75.09 | 47 | -0.589 |
| | 37.2 | 0.048 | 15.49 | 174.18 | 42 | -0.687 |
| | 38.1 | 0.059 | 3.86 | 77.40 | 34 | -0.642 |
| | 38.4 | 0.045 | 7.54 | 105 | 21 | -0.701 |
| | 39 | 0.035 | 3.73 | 64.3 | 19 | -0.685 |
| | 39.3 | 0.061 | 3.10 | 57.80 | 18 | -0.68 |
| | 39.6 | 0.029 | 6.45 | 58.29 | 37 | -0.51 |
| | 40.2 | 0.0256 | 3.99 | 41.49 | 60 | -0.470 |
| | 40.5 | 0.0434 | 4.31 | 65.06 | 43 | -0.604 |
| | 40.8 | 0.058 | 3.22 | 62.5 | 40 | -0.651 |
| | 41.4 | 0.029 | 2.43 | 33.99 | 55 | -0.498 |
| | 41.7 | 0.032 | 4.33 | 51.41 | 50 | -0.55 |
| | 43.8 | 0.031 | 8.05 | 79.78 | 50 | -0.575 |
| | 44.1 | 0.045 | 5.26 | 88.86 | 40 | -0.69 |
| | 44.4 | 0.06 | 10.5 | 134.7 | 37 | -0.71 |
| | 44.7 | 0.063 | 7.23 | 100.25 | 37 | -0.7 |
| | 45 | 0.08 | 3.29 | 68.81 | 33 | -0.719 |
| | 45.3 | 0.06 | 3.17 | 54.99 | 35 | -0.68 |
| | 45.6 | 0.023 | 4.65 | 47.42 | 40 | -0.684 |
| | 45.9 | 0.030 | 5.12 | 54.87 | 32 | -0.71 |
| | 46.2 | 0.019 | 3.89 | 37.30 | 50 | -0.680 |
| | 46.5 | 0.0117 | 3.89 | 33 | 55 | -0.66 |
| | 46.8 | 0.013 | 3.50 | 33.7 | 56 | -0.615 |
| | 47.1 | 0.014 | 2.65 | 28.91 | 72 | -0.510 |
| | 47.4 | 0.01 | 3.81 | 34.9 | 66 | -0.50 |
| | 47.7 | 0.01 | 5.05 | 40.87 | 60 | -0.51 |
| | 48 | 0.015 | 3.16 | 31.7 | 90 | -0.394 |
| | 48.3 | 0.03 | 4 | 42.7 | 41 | -0.520 |
| | 48.6 | 0.038 | 4.21 | 54.2 | 40 | -0.6329 |

$\chi_{ARM}$ = ratio of ARM to 79.6; S-ratio is the ratio of IRM at –300mT to IRM at 2500 mT; BoCr is the remanence coercivity; SIRM is the saturated IRM (IRM at 2500mT)

Bivariate plot of SIRM/$\chi_{lf}$ vs. ARM/$\chi_{lf}$ shows clustering of samples is between magnetite and titano-magnetite zone, (Fig. 4.12a) (Maher and Thompson, 1999). SIRM/$\chi_{lf}$ vs $Bo_{Cr}$ plot shows prèsence of magnetic grains in the MD range with Unit-3 samples are in the SP particle range (Bradshaw and Thompson, 1985) shown in figure 4.12b. The plot of SIRM vs. $K_{lf}$ shows an increase in magnetic concentration in Unit 2 and 3 , while Units 1 and 4 have relatively less magnetic concentration (Figure 4.12c) (Thompson and Oldfield, 1986).

In terms of magnetic mineralogy, the IITK drill core is dominated by ferrimagnetic minerals, like magnetite, as indicated by low $Bo_{Cr}$ values throughout the core except a spike in the topmost part which seems to be anomalous. Significant fluctuations in S-Ratio values in upper part of Unit 2 indicates enrichment of anti-ferromagnetic minerals like hematite/goethite at some horizons. The overall magnetite grain sizes are SD-MD indicating coarser magnetite except in Unit-2a and 3a where SP particles are present.

The magnetic susceptibility and mineral magnetic parameters in IITK drill core shows a systematic variations down depth. The top 5m shows very little variations in terms of SIRM and BoCr value indicating low magnetic influx, more stable condition for deposition. In the Unit 1b, a rise in the SIRM value, and corresponding low $Bo_{Cr}$ and low $\chi_{fd\%}$ indicate influx of coarse ferrimagnetic minerals (by fluvial process or by eolian dust). In the Unit-2a, low SIRM and an increase in $\chi_{fd}\%$ indicate the presence of SP particles at the bottom of the unit. The S-ratio shows fluctuation in the values between ferrimagnetic and anti-ferromagnetic minerals. At the top of Unit-2b a high $\chi_{lf}$, $\chi_{fd}\%$ and $\chi_{ARM}$ with comparatively low. SIRM and varying S-ratio is observed from 12.8m to 13.6m indicating presence of SP magnetite. The formation of such SP magnetite is considered to be favored in swampy conditions with high organic activity (Lovely, 1987). However the condition changed from reducing to oxidizing environment in the upper parts (between 10m to 12.8m) as indicated by sharp fluctuations in S-ratio values suggesting periodic wet-dry sequences. The rest of Unit-2b shows periodic high SIRM values with corresponding high $\chi_{lf}$ and low $\chi_{fd}\%$ which indicate detrital ferrimagnetic influx. S-ratio values show variations in values down to 17m, below which it showed no

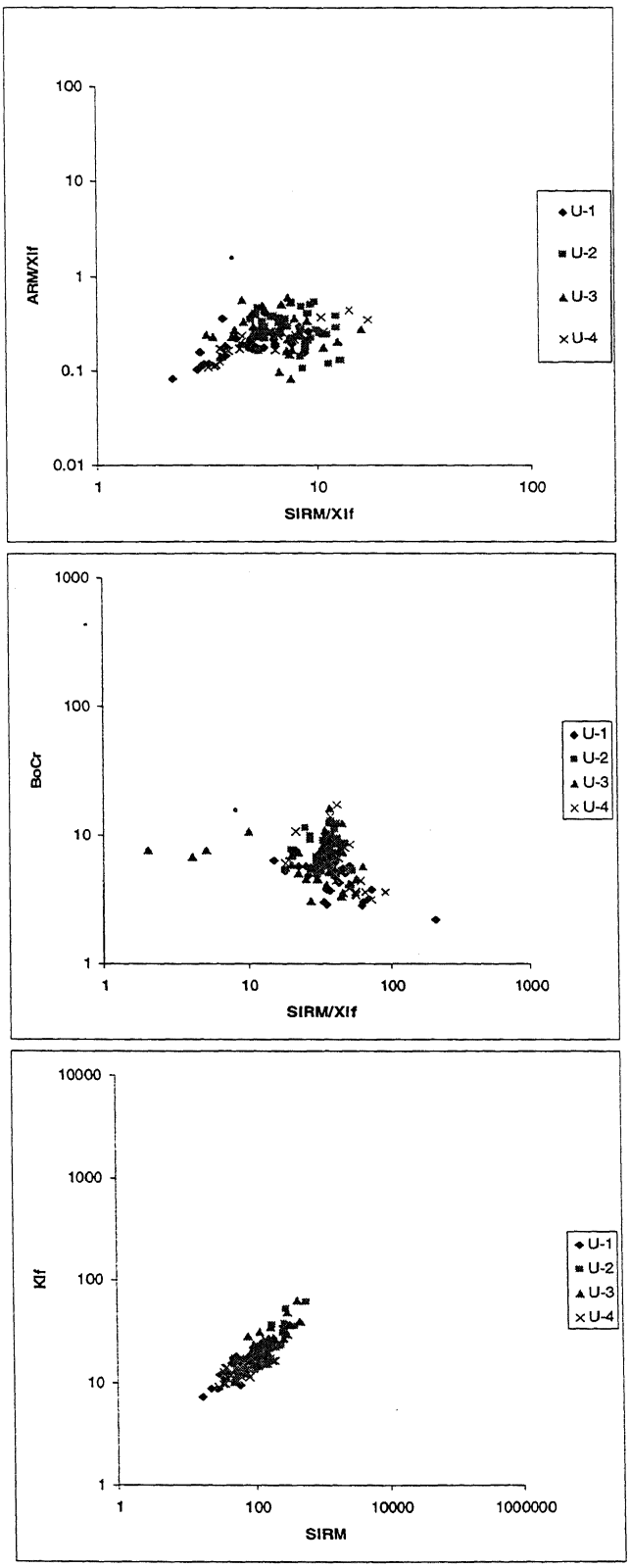


Figure 4.12. Bi-variate plots of magnetic parameters of IITK samples

variation is recorded indicating lesser time for sub aerial exposures and quicker deposition and burial of sediments in comparison to upper horizons. Unit-3a is characterized by a slight increase in SIRM, high $\chi_{lf}$, $\chi_{fd}$% and $\chi_{ARM}$ at the top level, with gradual lowering of values of all parameters below. Unit- 3b shows SIRM peaks at places with high $\chi_{lf}$ and low $\chi_{fd}$% indicating magnetic influx. Small fluctuations of $Bo_{Cr}$ at high SIRM values indicate changes in depositional conditions during burial of sediments. High SIRM peaks are separated by very low SIRM and $\chi_{lf}$ values with slight increase in $\chi_{fd}$% probably suggesting generation of in-situ formation of SP magnetite. Unit 4a shows low SIRM, slightly higher $\chi_{fd}$% and $\chi_{ARM}$, low $Bo_{Cr}$ values once suggesting generation of in-situ magnetite. Unit 4b shows slight increase in SIRM, high $\chi_{ARM}$ and $\chi_{fd}$% at 45m and the values gradually decrease towards the base indicating more stable condition, with no influx of sediments from outside and in-situ formation of magnetite.

### 4.2.5. Data Interpretation

Table 4.12.summarizes the sediementological, mineralogical and magnetic data for the IITK core samples. The IITK core shows no significant changes in grain size and lithology which makes difficult to divide them into distinct facies. The IITK core, as a whole represents a typical overbank sequence dominated by silt-clay intercalations, with occasional presence of coarse silts. The post-depositional changes are more prominent in this section.

*Unit*-1 is the top most horizon, present from 0m to 10m and comprises of silty-clay layers at top, followed by some thin silty patches at the bottom. Overall grain size is fine silt and have high organic content at the top. A dark clay layer present at 5.5m divides the silty-clay layer and silt horizons. High magnetic influx recorded in the silty horizons, indicating high energy conditions, bringing in the magnetic material. The top 5m shows some degree of post-depositional changes indicated by slight rise in $\chi_{fd}$% and S-ratio values.

Unit-2 shows cycles of influx of sediments with intermediate periods of non-deposition/erosion phases. From 10m to 14m , SIRM shows low value, except at 13m,

## Table 4.12: IITK Drill core summary

| Units (Depth in m) | Physical Parameters and mean grain size | Organic Matter content | XRD Bulk minerals | XRD Clay minerals | Magnetic Analysis | Interpretation |
|---|---|---|---|---|---|---|
| 1a (0-5.4) | Silty-clay layer, With concretions | high | Quartz, Feldspar Mica, Calcite | Illite> Kaolinite> chlorite | Low SIRM, low $Bo_{Cr}$ | Stable period, Little detrital Influx (modern Part) |
| 1b (5.4-9.9) | Silt layer with No Concretion, Mica Content increases | | Quartz, Feldspar Mica | Illite> Chlorite> Kaolinite | High SIRM at Silt layers, low $\chi_{fd}$% and high $\chi_{lf.}$ low $Bo_{Cr}$ | Detrtal magnetic influx |
| 2a (9.9-12.8) | Clayey-silt, with Increasing red-Brown clay at Bottom, kaolinit Increases at bottom | 1.5% (low) | Quartz, Feldspar Mica | Illite> Kaolinite> chlorite | Low SIRM, Increase in $\chi_{fd}$% At botoom, S-Ratio fluctuates Between ferrim agnetic and Anti-ferromagn etic value | Dissolution of ferrimagnetic concentration, pedogenic activity (slow sedimentation, arid to humid climate fluctuation)/gleying |
| 2b (12.8 -24.6) | Red-brown clay At top, with Mottling and concretion More silty-clay To Silty at bottom | | Quartz, Feldspar Mica, Calcite | Illite> Kaolinite> chlorite | High $\chi_{lf.}$, $\chi_{fd}$% And $\chi_{ARM}$ with Comparatively low SIRM and varying S-ratio At 13m<br><br>High SIRM Peaks with high $\chi_{lf.}$ and low $\chi_{fd}$% S-ratio showed Little variation After 17m. | In-situ ferrimagnetic Enhancement, generation of SP particles of magnetite with high organic activity- anaerobic condition.<br><br>High detrital magnetic Influx followed by Period of weathering /slow burial rate. High Sedimentation rate below 20m. |
| 3a(24.6-28.5) | Red-brown clay With mottling a The top | 2.3% | Quartz, Feldspar Mica | Illite> Chlorite= Kaolinite | Slight increase In SIRM, high $\chi_{lf.}$, $\chi_{fd}$% and $\chi_{ARM}$ | In-situ magnetic Enhancement and Generation of SP Particles at upper level Anaerobic condition |
| 3b (28.5 -36.6) | Olive-brown cla With silty patche | | Quartz, Feldspar Mica, Calcite | Illite> Chlorite= Kaolinite | High SIRM, Peaks at places with high $\chi_{lf}$ and low $\chi_{fd}$%. At high SIRM peaks, small fluctuations of $Bo_{Cr}$ present | Detrital magnetic Influx at horizons with Intervening erosion phases |
| 4a (36.6 -43.8) | Yellow brown Silty-clay with Thick concretion Zone at bottom | 2.2% | Quartz, Feldspar Mica | Illite> Chlorite= Kaolinite | Low SIRM, High $\chi_{fd}$%. And $\chi_{ARM.}$ low $Bo_{Cr}$ | More stable condition, little input from detrital source, more in-situ weatherin |
| 4b (43.8 -48.6) | Yellow brown Silty-clay with Silty patches | | Quartz, Feldspar Mica | Illite> Kaolinite> chlorite | Slight increase in SIRM, high $\chi_{ARM}$, $\chi_{fd}$% at 45 m, decreasing below | Anaerobic condition, generation of SP particles at 45m. |

## 4.3 Firozpur Drill Core

A summary log of the Firozpur drill core section is shown in the Figure 4.13. At the top 1.5m, alternating silt and very fine sand layers are present. Abundant roots, rhizocretions, some dark nodules and red and brown mottling are also observed. Yellowish brown silty-clay with sparsely distributed concretions is recorded between 1.5m to 2.8m, measured from top. Alternate silt and fine sand layer with very few concretions are present from 3m to 5.23m. A 1.5m thick red fine medium sand layer with abundant pale clay lenses is present from 3.83m to 5.2m. Nearly 5.5m thick yellowish brown micaceous fine medium sand with no concretions is present in the sandy layer. At places few red and brown mottling and some dark nodules are present. At the bottom of the thick sand layer a pale silty clay layer is present between 11.32m to 11.66m. From 12m downwards, yellowish brown silty clay with concretions (average diameter 3-4mm) and red and brown mottling are observed. At the top of the clay layer, few dark nodules are also reported. Red-brown silty clay with abundant red and brown mottling and sparse concretions are common between 14.27 to 15.08m. Concretions are much more frequent between 15.90 to 16.30m and 16.80 to 16.92m with a diameter varying from 3mm to 3cm. A pale yellow clay layer with abundant concretions, and red/brown mottling between 17.75 to 18.26m is followed by a reddish brown silty clay layer with abundant concretions (diameter 3mm to 1.2cm) and red and brown mottling. A silt to fine sand layer with concretions (diameter 2mm to 1.6cm) is present between 19.87m to 20.66m followed by ~60cm thick yellowish-white fine to medium sand layer with sparse concretions. This layer passes to a 1m thick yellowish brown silty-clay layer with concretions (average diameter 5mm to 2cm) and few red and brown mottling is present. The silty-clay layer is thinly laminated with few patches of grayish silt. This layer continues down to ~24m after which drilling was stopped.

### 4.3.1 Litho-Stratigraphic Units

Four stratigraphic units have been identified in the Firozpur core on the basis of physical parameters viz. grain size, texture, and compositional variations. A brief description of the individual units is given below:

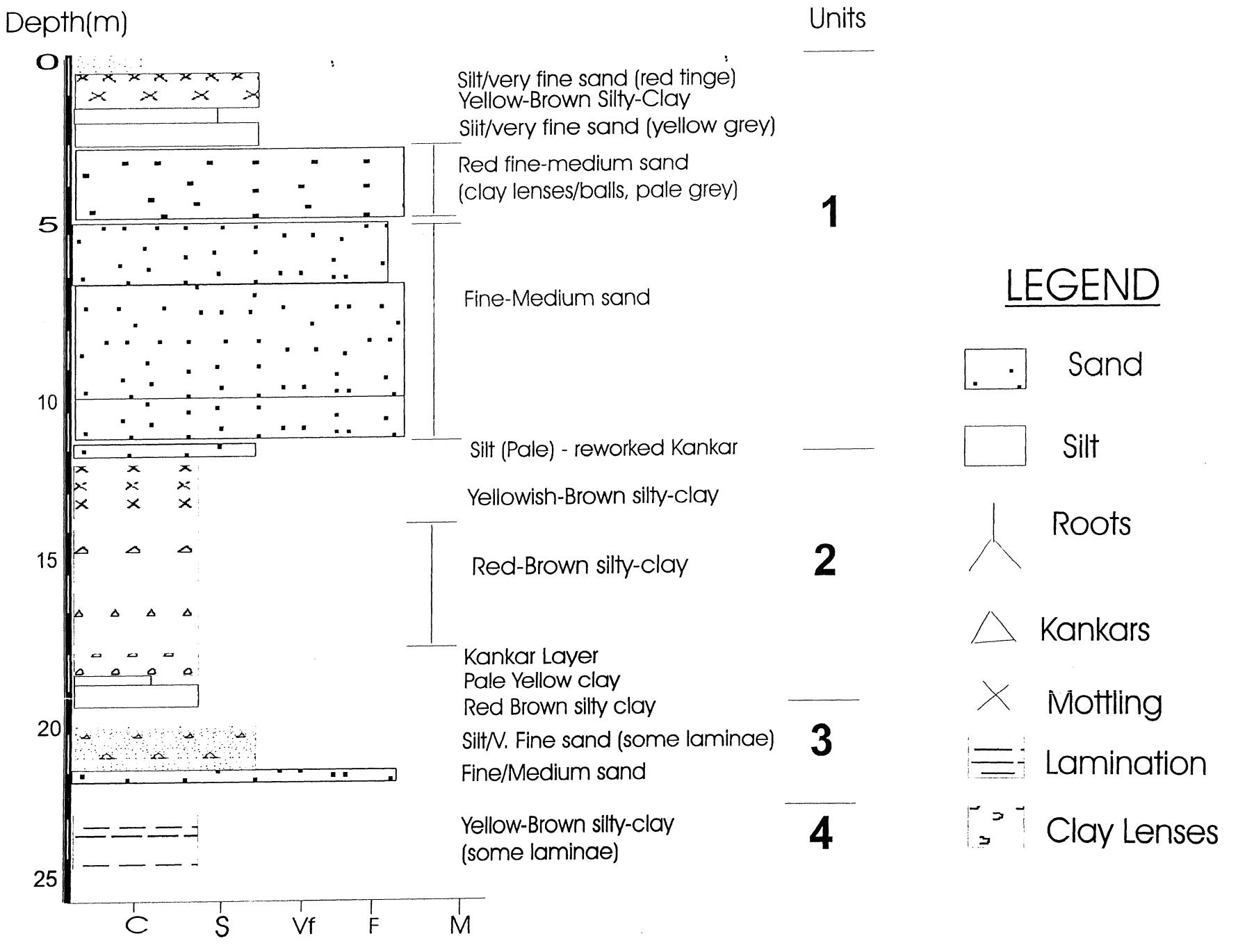


Figure 4.13. Summary of Firozpur drill core

*Unit1* is a 12m thick sandy layer present at the top the core. In the top 1.5m of this unit, an alteration of silt to very fine sand layer with roots, rhizocretions and some dark nodules are present followed by a thin (~1.5m) yellowish brown silty clay layer. The remaining part of this unit consists of fine to medium micaceous sand with red and brown mottling, more reddish in the top part, with pale clay lenses. Sparse kankars (2-3m in diameter) are recorded in the sandy layer.

*Unit 2* (12-19.42m) is a thick silty clay layer, mostly yellowish brown in color with reddish brown silty-clay is present between 14.3 to 15.07m. Two distinct zones of frequent concretions, 3mm-3cm in diameter, are recorded at 15.90-16.30m and 16.80-16.92m. Red and brown mottling is present throughout the unit. A pale yellow clay patch is recorded between 17.75 to 18.20m. The bottom of the Unit 2 is marked by a reddish brown silty clay layer with some kankarswhich are slightly larger than the overlying layer (diameter 1cm to 5cm).

*Unit 3* (19.87-21.25m) comprises of alternation of silt and very fine sand at the top grading to fine to medium sand below. In the lower part of this unit, ~1m thick yellowish white clayey silt layer with intercalation of whitish fine sand is recorded. Concretions with average diameter 5mm to 2cm are present in the silty layers. This layer grades to a thin, yellowish white, fine to medium sand layer with 2-3mm size kankars at the bottom of the unit.

Unit 4 is the lowermost unit starting at 21.25 meters comprising of yellowish brown silty clay with clay laminations (1-2mm thick). Some patches of silt are present between the clay layers. The unit is characterized by red and brown mottling and sparse kankars (diameter 5mm to 2cm) in the top part.

### 4.3.2 Grain size and Organic matter content

The samples were taken from the different units for the grain size analysis. Table 4.13 lists the statistical grain size parameters and Figure 4.14 shows the cumulative frequency distribution for samples from different units at Firozpur drill core.

The mean grain size of the samples varies between fine sand to fine silt. Unit 1 samples vary in mean grain size from coarse silt at the top to very fine sand at the bottom. The Unit 2 sample, represented mainly by clayey silt in the log, shows a mean grain size of medium to fine silt. Grain size is a little coarser in Unit-3 and in the bottom most unit mean size is medium to fine silt. All samples are poorly sorted and positively skewed. Positively skewed distribution indicating finer material present than in a normal distribution, except in the unit-3 where skewness is symmetrical. The kurtosis of the samples were mostly mesokurtic, except in the 3.30m sample where it was very leptokurtic indicating strong peaked curves with good sorting in the central part of the distribution. The unit-4 sample showed platykurtic distribution indicating very flat curves of poorly sorted sediments.

**Table 4.13: Grain size parameters for Firozpur Drill Core samples**

| Depth (m | Units | Mean | Sorting | Skewness | Kurtosis | Interpretation |
|---|---|---|---|---|---|---|
| 3.30 | 1 | 4.91 | 1.88 | 0.394 | 1.62 | Very coarse silt, poorly sorted, very positively skewed and very leptokurtic |
| 8.40 | 1 | 4.48 | 1.48 | 0.45 | 0.992 | Very fine sand, poorly sorted, very positively skewed and mesokurtic |
| 12.90 | 2 | 7.41 | 1.4 | 0.151 | 0.919 | Medium to fine silt, poorly sorted, positively skewed and mesokurtic |
| 19.98 | 3 | 7.6 | 1.415 | 0.098 | 0.652 | Medium silt, poorly sorted, symmetrica and very platykuric |
| 23.32 | 4 | 7.26 | 1.52 | 0.1241 | 1.1 | Medium to fine silt, poorly sorted, positively skewed and mesokurtic |

The $H_2O_2$ reactive organic matter content is high in Unit 2 and 4 (Table 4.14) which are dominated by silty-clay sediments. The highest value of OMC occurs at 16.3m coinciding with the high concentration of concretions at that level. The organic matter content is particularly low in the lower part of the Unit 1 comprising of more silty-fine to medium sand material.

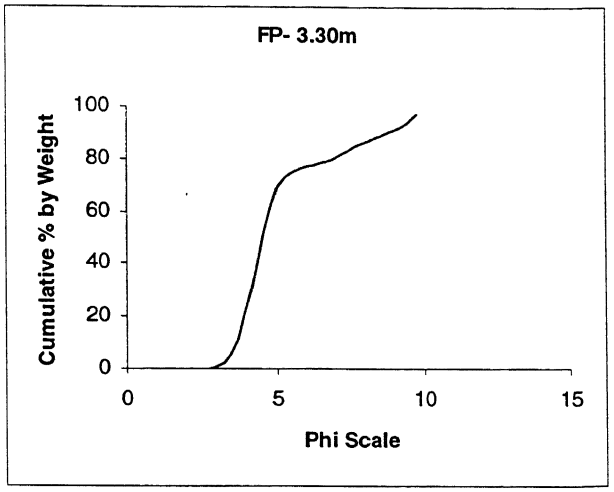


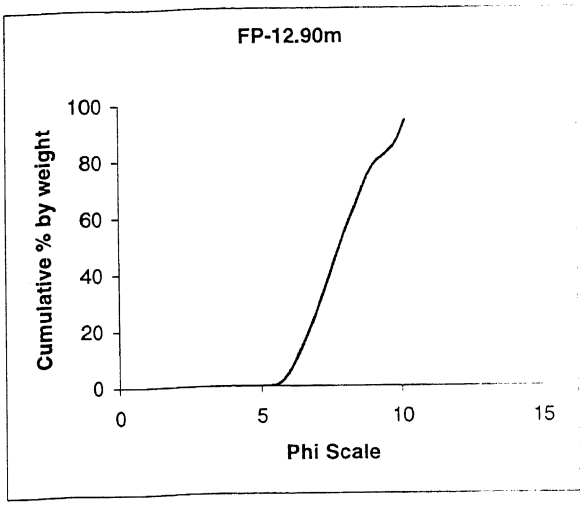


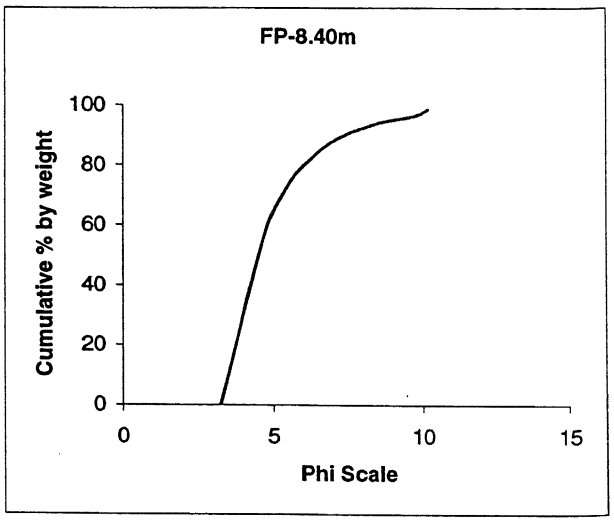


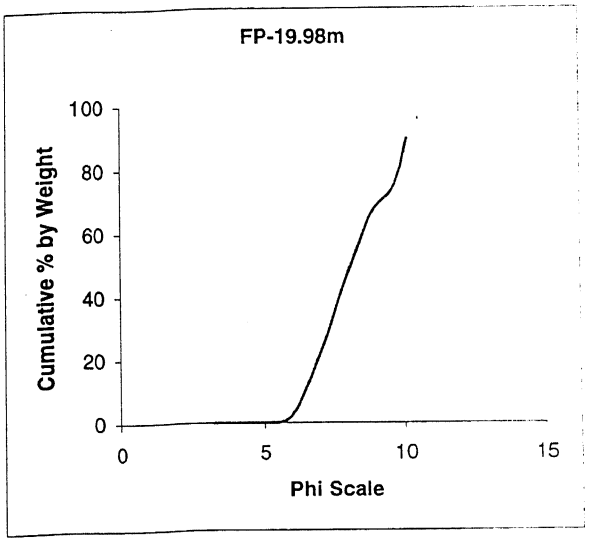


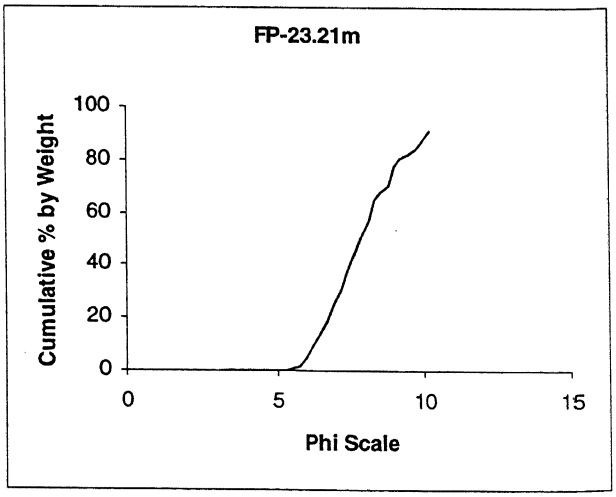


Figure 4.14. Grain size plots for different units of Firozpur drill core

### 4.3.3 Sediment Mineralogy

The bulk mineralogy of core sediments determined by X-ray Diffraction (XRD) is represented by quartz, feldspar, mica, amphibole, calcite in variable amounts (Table 4.14). Amphiboles are present in trace throughout the Unit 1 and in some parts of the Unit 3. Calcite is less abundant in Unit 1, but occurs more frequently in Unit 2. Clay mineral assemblage is represented by Illite, Kaolinite, and Chlorite (Table 4.14).

**Table 4.14: Organic matter and sediment mineralogy for the Firozpur Drill Core**

| Units | Organic Matter (wt%) | Bulk mineralogy | | | | | ogy Units | Clay Mineralogy | | | Concretion mineralogy |
|---|---|---|---|---|---|---|---|---|---|---|---|
| | | Q (3.34Å) | F (3.19 Å) | M (10 Å) | Cc (3.03 Å) | Others | | I (10 Å) | Ch (14.4 Å) | K (3.57 Å) | - |
| 1(n=11) | 2.7 | ++++ | ++ | ++ | + | A++ | 1(n=4) | +++ | ++ | + | - |
| 2 (n=4) | 3.2 | ++++ | ++ | ++ | + | | 2(n=4) | ++++ | ++ | ++ | Calcite |
| 3 (n=1) | 2.2 | +++ | ++ | ++ | + | A+ | 3(n=1) | ++++ | ++ | ++ | Calcite |
| 4 | 2.7 | | | | | | | | | | - |

Q- Quartz, F-Feldspar, M-Mica, Amph- Amphibole, G-Goethite, Cc-Calcite, I-Illite, Chlorite, K-Kaolinite, Mx-Mixed layer clay; Sid- Siderite
++++ High; +++ Moderate; ++ Minor; + Trace

A semi-quantitative estimation of the relative concentrations of the bulk powder and smeared fine fractions based on XRD peak area (Mann and Muller, 1980; Biscaye 1965, Cook, 1975) was conducted and results are shown in Table 4.14 and Fig. 4.15. Quartz is the dominant mineral in all the units comprising more than 80% of the major bulk component. Significantly low quartz content is observed in the upper part of Unit-1 (3.3.0m) and Unit-2. Feldspar is the second most abundant mineral, 10-15% in relative abundance, with a high value of around 36% at the top of Unit 1. Amphiboles are present mostly in the sandy horizons of the Unit 1. Illite, the main clay mineral component, shows a consistent value (~90%) throughout the core with the exception at the bottom of Unit-2. Chlorite and kaolinite are two other components, contributing 6-7% of clay population. Kaolinite is mostly absent in the Unit 1, while an absence of chlorite is recorded from Unit 2. A rise in the illite or soil-mica content along with feldspar content is observed down to 15m. Quartz content is comparatively low below 15m. From 15m to

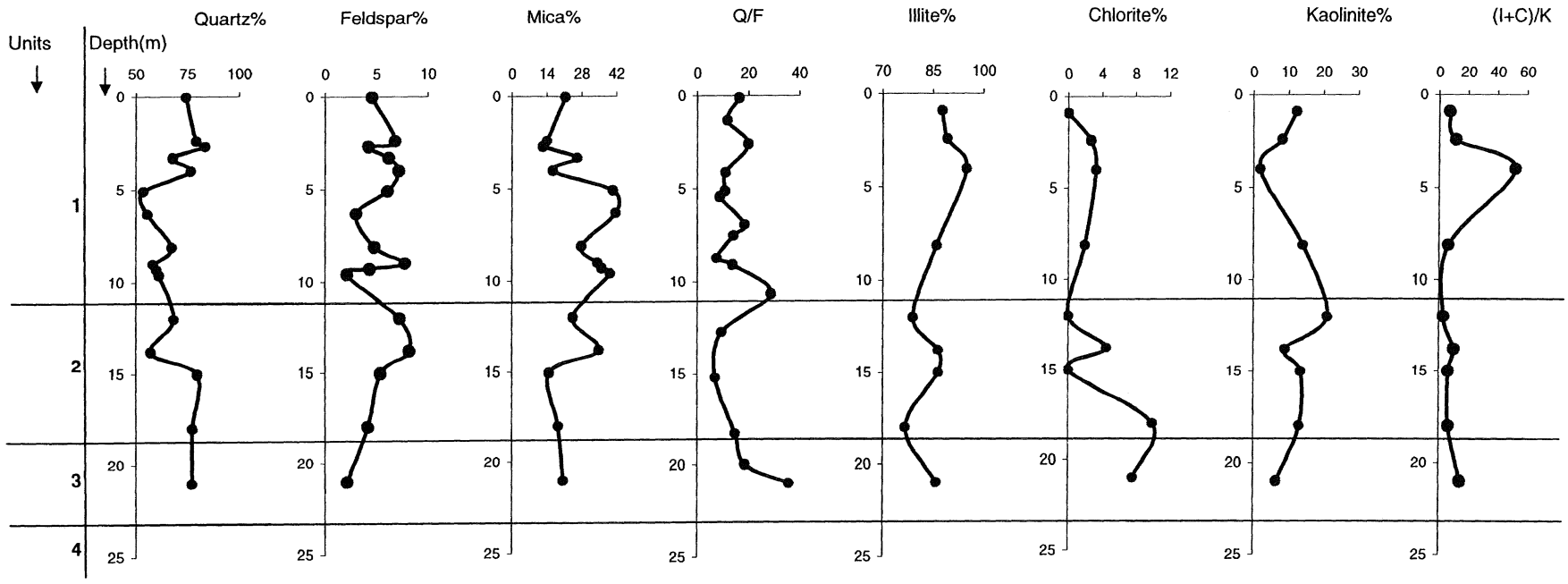


Figure 4.15. bulk and clay mineral abundance in percentage of Firozpur drill core

the bottom of Unit 2, a progressive rise in the quartz content with subsequent decrease in the illite abundance is recorded. The feldspar content also decreases while the (kaolinite + chlorite), mostly kaolinite, content shows progressively higher values. Presences of high feldspar above 15m and subsequent rise in kaolinite percentage at the expense of feldspar indicates significant chemical weathering below 15m. The Q/F ratio showed increase in the values from the top of the Unit 1, reaching a very high value at the bottom of the sandy horizons .The intervening clay horizon shows low quartz content, with subsequent rise in the quartz value in the Unit 3. (Illite + Chlorite)/Kaolinite ratio shows high values in the Unit 1 and 3, while in the Unit 2, it decreases.

**Table 4.15: Relative abundance of minerals computed by normalization in Firozpur Core**

| Bulk powder | | | | | | | Smeared fine fraction | | | | |
|---|---|---|---|---|---|---|---|---|---|---|---|
| Units | Depth (m) | Q% | Felds% | Mica% | Q/F | Units | Depth (m) | Illite% | Chl % | Kaol % | (I+C)/K |
| 1 | 0.03 | 74.14 | 4.56 | 21.29 | 16.25 | 1 | 0.9 | 87.71 | 0 | 12.28 | 7.14 |
| | 2.4 | 79.21 | 6.79 | 14 | 11.66 | | 2.4 | 89.21 | 2.64 | 8.15 | 11.26 |
| | 2.7 | 83.47 | 4.22 | 12.31 | 19.77 | | 4 | 94.85 | 3.25 | 1.89 | 51.9 |
| | 3.3 | 67.74 | 6.2 | 26.05 | 10.92 | | 8.1 | 85.98 | 1.91 | 14.01 | 6.27 |
| | 4 | 76.47 | 7.16 | 16.36 | 10.68 | 2 | 12 | 78.94 | 0 | 21.05 | 3.05 |
| | 5.1 | 53.5 | 6.09 | 40.39 | 8.784 | | 13.8 | 86.48 | 4.5 | 9 | 10.10 |
| | 6.3 | 55.45 | 3.02 | 41.52 | 18.36 | | 15 | 86.48 | 0 | 13.5 | 6.4 |
| | 8.1 | 67.37 | 4.79 | 27.83 | 14.06 | | 18 | 76.74 | 9.97 | 13.08 | 6.62 |
| | 9 | 58.05 | 7.76 | 34.17 | 7.48 | 3 | 21 | 85.88 | 7.62 | 6.5 | 14.38 |
| | 9.3 | 59.73 | 4.35 | 35.9 | 13.73 | | | | | | |
| | 9.6 | 61 | 2.12 | 39.25 | 28.773 | | | | | | |
| 2 | 12 | 68.32 | 7.25 | 24.42 | 9.43 | | | | | | |
| | 13.8 | 57.09 | 8.17 | 34.72 | 6.987 | | | | | | |
| | 15.04 | 79.76 | 5.38 | 14.86 | 14.82 | | | | | | |
| | 18 | 77.41 | 4.18 | 18.48 | 18.519 | | | | | | |
| 3 | 21 | 77.29 | 2.16 | 20.54 | 35.782 | | | | | | |

I-Illite, C-Chlorite, K-Kaolinite

### 4.3.4 Magnetic Susceptibility analysis

Table 4.16 shows the magnetic susceptibility values in the Firozpur drill core. The bulk magnetic susceptibility value ($\chi_{lf}$) and frequency dependent susceptibility values ($\chi_{fd\%}$) are plotted against depth in Figure 4.16a &b. The $\chi_{lf}$ value shows very high values at 9 m and 11.1m, while the rest of the drill core shows uniformly low and consistent values suggesting presence of paramagnetic or anti-ferromagnetic minerals. The high $\chi_{lf}$ value may indicate presence of ferrimagnetic minerals, which needs to be confirmed by

sedimentary magnetic analysis. The $\chi_{fd\%}$ values shows a variation down the depth, with high values between 2-3m level and at 21m level. The high $\chi_{fd\%}$ values indicate the presence of SP particles in the core. The overall grain size is SD-PSD but some SP particles may be present at same intervals. The peaks of high $\chi_{lf}$ peaks correspond to a very low $\chi_{fd\%}$ peaks which indicate the presence of SP domain ferrimagnetic mineral in these horizons.

**Table 4.16: Magnetic susceptibility data for Firozpur Drill core samples**

| Units | DEPTH (m) | Corrected. Weight ($*10^{-3}$kg) | $\chi_{lf}$ ($*10^{-8}m^3$/kg) | $\chi_{hf}$ ($*10^{-8}m^3$/kg) | $\chi_{fd\%}$ |
|---|---|---|---|---|---|
| 1 | 0 | 10.457 | 12.43 | 10.51 | 1.47 |
| | 0.3 | 14.479 | 6.90 | 6.21 | 0.69 |
| | 0.6 | 12.107 | 7.43 | 5.78 | 1.8 |
| | 0.9 | 10.849 | 8.29 | 7.37 | 1.02 |
| | 1.2 | 10.09 | 6.93 | 3.96 | 4.24 |
| | 1.5 | 10.776 | 11.1 | 8.35 | 2.31 |
| | 1.8 | 10.864 | 7.36 | 2.76 | 5.75 |
| | 2.1 | 11.701 | 7.69 | 4.27 | 3.79 |
| | 2.4 | 9.591 | 8.34 | 3.12 | 6.51 |
| | 2.7 | 9.22 | 7.59 | 3.25 | 6.19 |
| | 3 | 13.492 | 6.67 | 4.44 | 2.47 |
| | 3.3 | 11.109 | 6.30 | 4.5 | 2.57 |
| | 3.6 | 13.623 | 6.60 | 4.4 | 2.44 |
| | 3.9 | 13.583 | 8.09 | 5.88 | 2.005 |
| | 4.2 | 11.241 | 6.22 | 3.55 | 3.81 |
| | 4.5 | 9.627 | 8.30 | 5.19 | 3.8 |
| | 4.8 | 11.401 | 9.64 | 6.13 | 3.18 |
| | 5.1 | 10.968 | 10.94 | 7.29 | 3.05 |
| | 5.4 | 14.009 | 8.56 | 7.13 | 1.18 |
| | 5.7 | 10.686 | 14.97 | 11.22 | 2.3 |
| | 6.3 | 12.614 | 16.64 | 12.68 | 1.88 |
| | 8.1 | 12.838 | 15.57 | 11.68 | 1.94 |
| | 8.4 | 12.246 | 21.23 | 18.78 | 0.94 |
| | 9 | 11.644 | 121.9 | 117.65 | 0.30 |
| | 9.3 | 11.306 | 23.88 | 19.45 | 1.637 |
| | 9.6 | 12.648 | 26.88 | 22.92 | 1.162 |
| | 9.9 | 10.64 | 17.85 | 13.15 | 2.473 |
| | 10.2 | 12.976 | 10 | 6.16 | 2.964 |

| | | | | | |
|---|---|---|---|---|---|
| | 10.8 | 14.538 | 13.06 | 8.94 | 2.172 |
| | 11.1 | 9.667 | 44.48 | 38.27 | 1.443 |
| | 11.4 | 10.273 | 16.54 | 11.68 | 2.863 |
| | 12 | 10.431 | 15.33 | 9.58 | 3.595 |
| | 12.3 | 10.007 | 13.99 | 7.99 | 4.282 |
| | 12.6 | 14.208 | 12.66 | 8.44 | 2.346 |
| | 12.9 | 13.444 | 12.64 | 8.18 | 2.625 |
| | 13.5 | 11.171 | 13.42 | 8.05 | 3.58 |
| | 13.8 | 12.82 | 13.26 | 8.58 | 2.753 |
| | 14.1 | 14 | 12.85 | 7.85 | 2.777 |
| | 14.4 | 11.967 | 15.04 | 9.19 | 3.249 |
| 2 | 14.7 | 11.938 | 15.91 | 10.75 | 3.08 |
| | 15 | 12.304 | 15.44 | 9.75 | 2.994 |
| | 15.3 | 9.454 | 12.69 | 8.4 | 3.525 |
| | 15.6 | 13.108 | 12.96 | 9.15 | 2.243 |
| | 15.9 | 8.71 | 13.77 | 8.03 | 4.783 |
| | 16.2 | 10.529 | 12.34 | 8.54 | 2.922 |
| | 16.5 | 8.878 | 14.64 | 9.01 | 4.33 |
| | 16.8 | 10.926 | 16.47 | 11.89 | 2.542 |
| | 18 | 13.316 | 13.51 | 9.76 | 2.086 |
| | 18.3 | 8.285 | 16.89 | 10.86 | 4.310 |
| | 18.6 | 8.804 | 18.17 | 12.49 | 3.549 |
| | 18.9 | 11.142 | 17.05 | 11.66 | 2.834 |
| 3 | 19.2 | 12.183 | 12.31 | 6.56 | 3.830 |
| | 20.1 | 9.13 | 12.04 | 5.47 | 5.97 |
| | 20.4 | 10.251 | 12.68 | 9.75 | 2.251 |
| | 20.7 | 10.171 | 12.78 | 8.84 | 3.02 |
| | 21 | 11.118 | 21.58 | 17.08 | 1.87 |
| 4 | 23.4 | 11.581 | 17.26 | 12.95 | 2.15 |
| | 23.7 | 12.915 | 15.48 | 11.6 | 1.9 |
| | 24 | 10.262 | 14.61 | 9.74 | 3.24 |

$\chi_{fd\%}=\{(\chi_{lf}-\chi_{hf})/\chi_{lf}\} * 100$

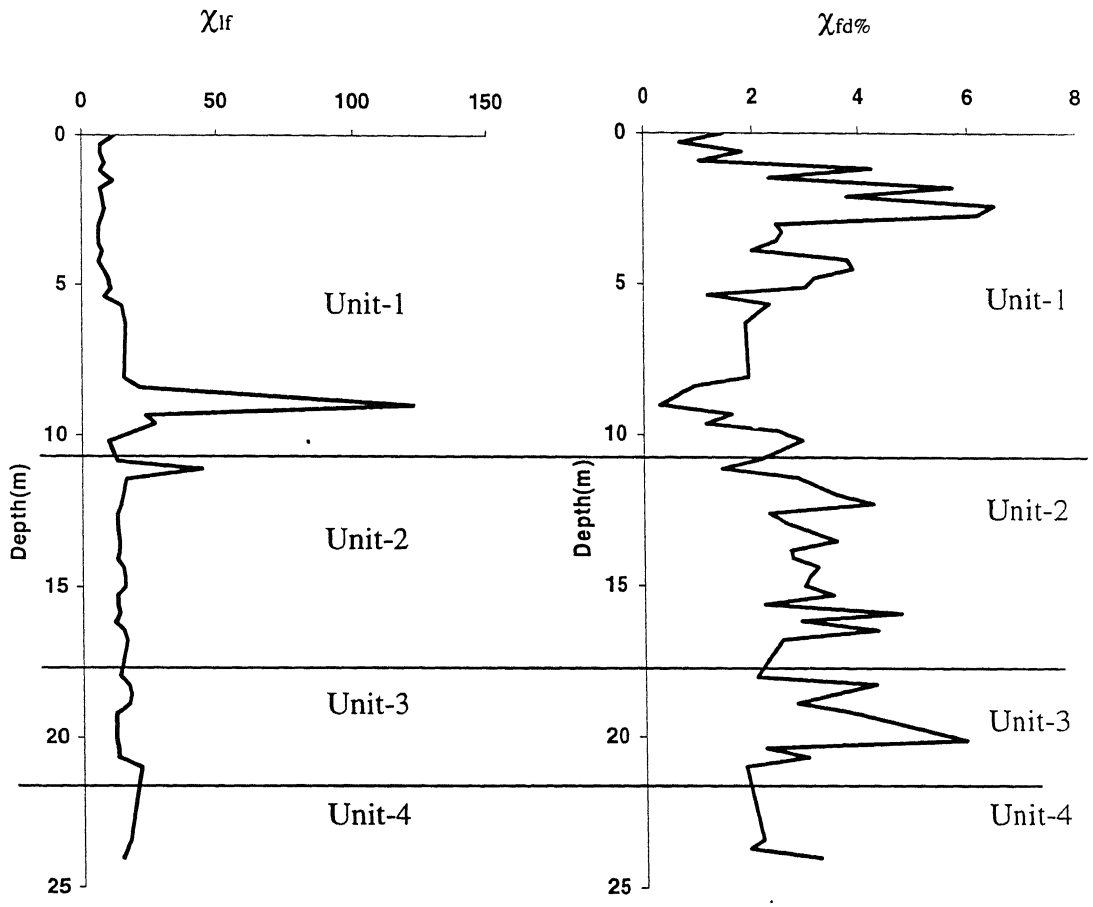


Fig.4.16 a. bulk Magnetic susceptibility ($\chi_{lf}$) plots for Firozpur samples and 4.16b. frequency dependent susceptibility ($\chi_{fd\%}$) for Firozpur samples

### 4.3.5 Data Interpretation

On the basis of lithological, sedimentological, magnetic susceptibility data, the stratigraphic units of the Firozpur drill core can be interpreted in terms of sedimentary facies. Table 4.17 summarizes the sedimentological, bulk, clay mineralogy, susceptibility data for all the units.

The top most unit, *Unit-1* (0-12m), comprises of poorly sorted silty and sandy intercalations in the upper part grading to medium to fine sand below. The top 1.5 m of this unit consists of silt to very fine sand layers with roots, rhizoconcretions and few dark

nodules. The mineralogy of this unit is strongly detrital with quartz and feldspar dominating along with illite and chlorite in the clay fraction. The base of the unit shows two peaks in bulk susceptibility values and suggests influx of detrital ferrimagnetic minerals (coarse grained, MD domain, low $\chi_{fd\%}$ ). This unit represents a dominantly **Channel facies** in the core capped by modern soil with minor pedogenesis.

Unit 2 is dominantly muddy unit consisting of a thick yellowish brown to red brown, poorly sorted, silty-clay sediments with abundant concretions and mottling. Quartz percentage is low and kaolinite is a significant component in the clay fraction. Q/F ratio as well as (I+C)/K ratio are low. Organic matter content is high compared to the other units and is also consistent. Bulk susceptibility values remains uniformly low but $\chi_{fd\%}$ shows a distinct increase indicating presence of SD and SP particles. This unit therefore represents a typical **floodplain deposit** with moderate pedogenesis

*Unit 3* is another sand-dominated unit but the overall grain size is much finer than Unit 1. Concretions with an average diameter of 5mm to 2cm are present in the intercalated silty layers and they decrease in frequency and size in the sandy layers. Organic matter content is low, bulk sucsptibility is consistently low but high $\chi_{fd\%}$ value indicates presence of SP particles the unit. This unit is interpreted as a minor **Channel body or Channel fill** with significant pedogenesis.

Unit-4 is the bottom most unit comprising of poorly sorted, yellowish brown silty clay with clay laminations (1-2mm thick) and sparse concretions. Organic matter content is high with fairly consistent low $\chi_{fd\%}$ and $\chi_{lf}$ values. This unit is also interpreted as a **floodplain deposit**.

**4.17: Summary table for Firozpur drill core**

| Units (Depth in m) | Physical parameters | Organic Matter content | XRD Bulk minerals | XRD Clay minerals | Magnetic Analysis | Interpretation |
|---|---|---|---|---|---|---|
| 1(0-12) | Silt-fine with Sand intercalation To fine medium sand at the bottom, concretions sparse | 2.7 | Quartz, Feldspar, Mica, Amphibole | Illite> Kaolinite> chlorite | Uniformly Low Susceptibility In the top Part High Values at bottom | Major channel Deposit |

| | | | | | | |
|---|---|---|---|---|---|---|
| | | | | | Ferrimagnetic Concentration) with MD magnetic grain | |
| 2(12-19.87) | Silty-clay with abundant Concretions and mottling | 3.2 (high) | Quartz, Feldspar, Mica, calcite | Illite> Kaolinite> chlorite | Uniformly Low Susceptibility With increase in Magnetic Domain size | Floodplain |
| 3(19.87-21.25) | Silt-fine sand Intercalation at top to fine sand at bottom. | 2.2 | Quartz, Feldspar, Mica | Illite> Chlorite =kaolinite | Uniformly Low Susceptibility, SD particles | Small channel Deposit |
| 4 (23.07-24) | Silty-clay with Lamination and concretions | 2.7 | | | Uniformly Low Susceptibility | Floodplain |

## 4.4 Jagadishpur Drill core

A summary log of the Jagadishpur drill core along with OSL ages is shown in the Figure 4.17. At the top 1.6m yellowish brown clayey silt with red and brown mottling and abundant roots are present. Yellowish brown silty clay layers with red and brown mottling are recorded between 2.15m to 3.30m with concretions varying in diameter from 4mm to 1.2cm. This is followed by an alteration of yellowish silt to very fine sand and fine to medium sand down to 9.91m. Silt layers show few red and brown mottling and some of the sand layers have sparse concretions. Few clay patches and a grey clay band is recorded at the bottom of this unit between 8.70-9.91m. This unit passes to a thin patch of silty to fine sand (10.17 to 10.61m) and then to a very thin band of pale yellow clay with sparse concretions (10.61m to 10.82m). Yellow brown silty clay layer with sparse concretions (2-8mm average diameter) and red and brown mottling is present between 11.43m to 13.03m. The silty clay layer was darker and silt rich in the top part grading into paler clay rich bottom part. A thin patch (13cm thick) of micaceous fine sand layer was present below the silty-clay layer. Yellowish silt to very fine sand layer with red and brown mottling was present from 13.14m to 13.99m.Yellowish brown silty clay with no concretions is present between 14.1m to 15.06m. Silt to very fine sand layer with few concretions (3mm to 8mm average diameter) is present from 15.06m to 16.86m. A ~6m

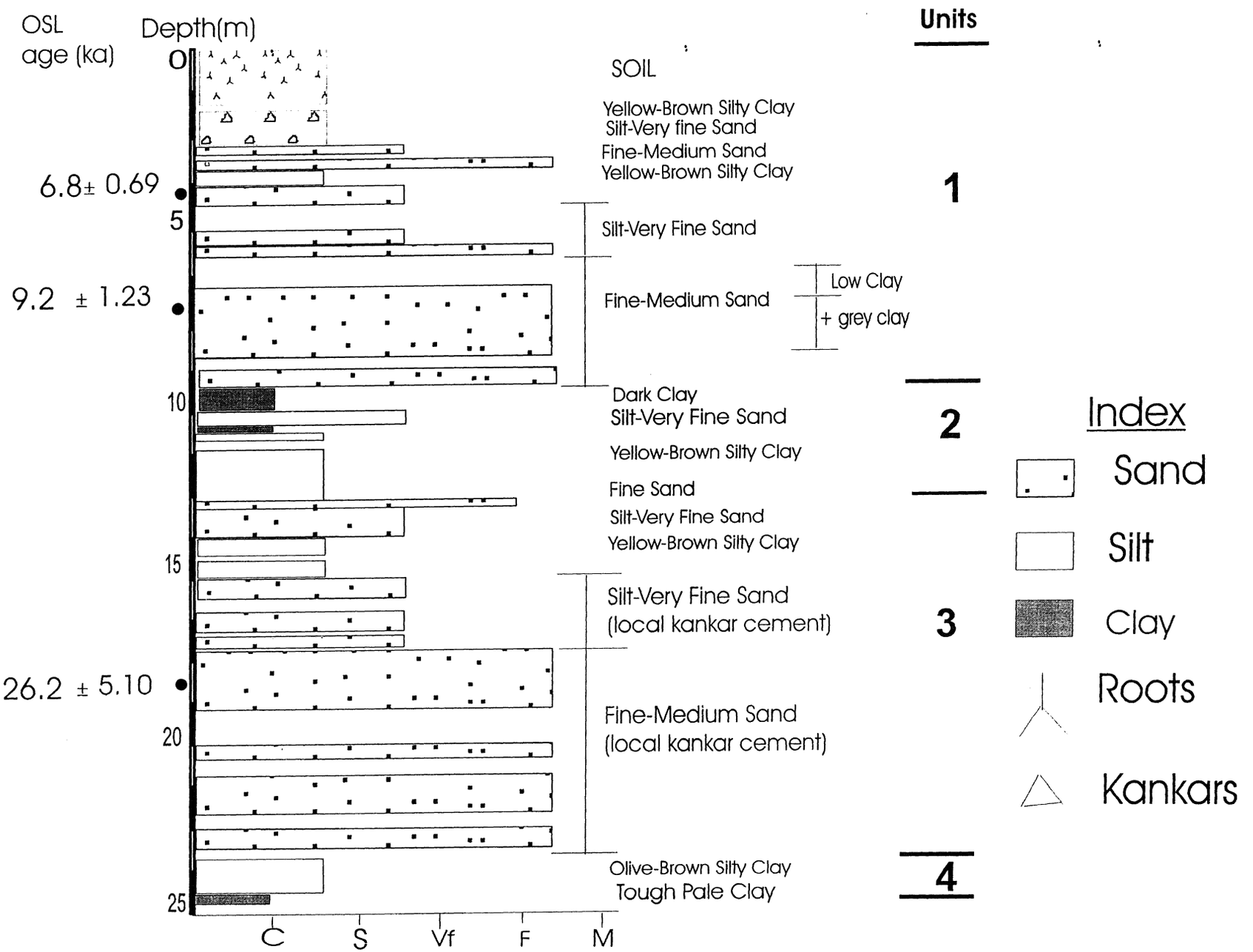


Figure. 4.17. Summary Log of Jagadishpur Core

thick fine to medium micaceous sand layer with red and brown mottling and concretions is recorded at 17.18m followed by a 12cm thick concretion-rich zone which also shows red and brown mottling and dark nodules (2-3mm). The basal parts of the core records olive brown silty clay layers with sparsely distributed concretions (2-4mm average diameter) from 23.05m to 24.65m, and finally, a 10cm thick tough pale clay layer with concretions and red and brown mottling.

### 4.4.1 Litho-Stratigraphic Units

The Jagdishpur core is divided into four different stratigraphic units based on lithological and sediemntological criteria. A brief description of the individual units is given below:

Unit 1 (surface to 9.91m) is represented by thick, fine to medium sand sediments. Top 1.6m is dominated by yellowish brown clayey-silt with some red and brown mottling and abundant roots. Two Yellowish brown silty clay layers with abundant concretions are present from 2.15m to 3.3m and 4.03m to 4.33m separated by a thin patch of silt to fine sand horizon and followed by a ~1.20m thick, yellowish silt to very fine sand layer. The base of the unit is a ~4m thick fine to medium micaceous sand layer. The OSL ages put the base of this unit at ~10ka (Fig.4.17 ).

Unit 2 (9.91-13.03m) is a muddy unit comprised of dark clay to yellow-brown silty-clay with concretions and some red and brown mottling. the only aberration is a thin patch of silt to very fine sand layer between 10.17m to 10.61m with sparse concretions.

Unit 3 (13.03-23.05) is a 10m thick sandy layer with concretions and red and brown mottling. Thin (<1m) layers of yellow brown silty-clay sediments are recorded at some levels. A concretion-rich zone (3mm to 2cm in diameter) along with red and brown mottling and dark nodules (2-3mm) is present in the basal part of the unit between 21.2m and 21.32m. The sand layer at 18.52m in this unit has give an OSL age of 26.2 ± 5.1 ka.

Unit 4 (23.05-24.75m) starts with 1.60m thick olive brown silty clay with concretions (2-4mm average diameter) and red and brown mottling at the top. The basal part of the unit is marked by a 10cm pale, tough clay with red and brown mottling and few small size concretions.

### 4.4.2. Grain size and Organic Matter Content

Table 4.18 lists the statistical grain size parameters and Figure 4.18 shows the cumulative frequency distribution for samples from different units at Jagadishpur drill core. The mean grain size of the samples varies from very coarse silt to fine silt (Udden and Wentworth Scale). Two samples of Unit 1 showed mean grain size varying from coarse silt at the top to coarse to medium silt at the bottom of the unit. The mean grain size of Unit 2 sample fall in medium to fine silt range, while samples from Unit 3 show coarser grain size (mean grain size- very coarse silt). Mean grain size of the Unit 4 sample is medium silt. All samples are poorly sorted and positively skewed. The sample from Unit 3 shows symmetrical skewness. All samples were mesokurtic except the sample at the top most unit of the Unit 1 which is very leptokurtic indicating strong, peaked grain size distribution curve.

**Table 4.18: Grain size parameters for Jagadishpur Drill Core samples**

| Depth (m | Units | Mean | Sorting | Skewness | Kurtosis | Interpretation |
|---|---|---|---|---|---|---|
| 3.3 | 1 | 5.92 | 1.448 | -0.081 | 1.59 | Coarse silt, poorly sorted, positively skewed and very leptokurtic |
| 8.4 | 1 | 5.64 | 1.535 | 0.179 | 0.924 | Coarse silt, poorly sorted, positively skewed and mesokurtic |
| 10.2 | 2 | 7.19 | 1.35 | 0.24 | 0.96 | Medium to fine silt, poorly sorted, positively skewed and mesokurtic |
| 18.3 | 3 | 5.42 | 1.6 | 0.052 | 1.017 | Very coarse silt, poorly sorted, symmetrical and mesokurtic |
| 24 | 4 | 7.07 | 1.374 | 0.195 | 0.995 | Medium silt, poorly sorted, positively skewed and mesokurtic |

The $H_2O_2$ reactive organic matter (Table.4.19) shows a significant decrease down depth in Unit 1. The top silty clay part shows a relatively higher organic matter content compared to the sample taken from sandy horizons of same unit. A decrease in the

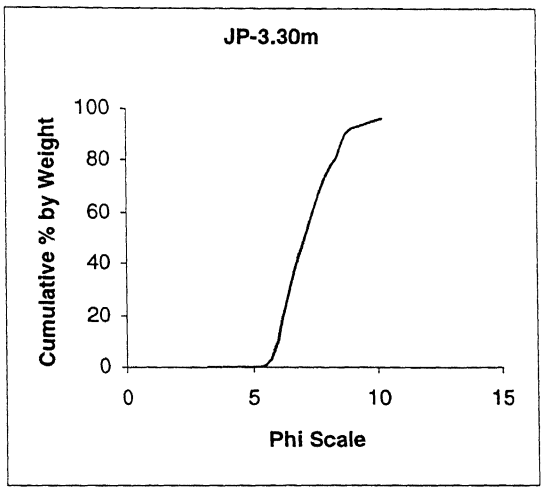


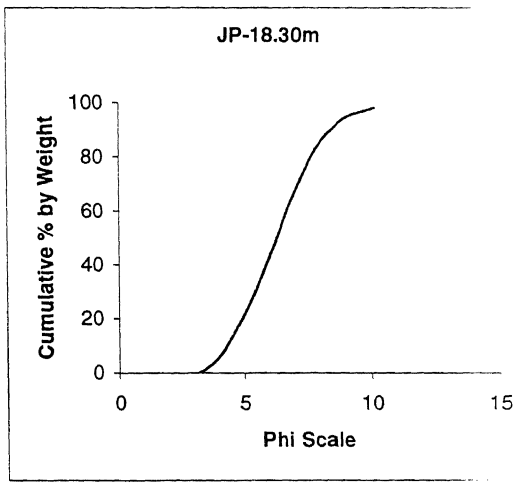


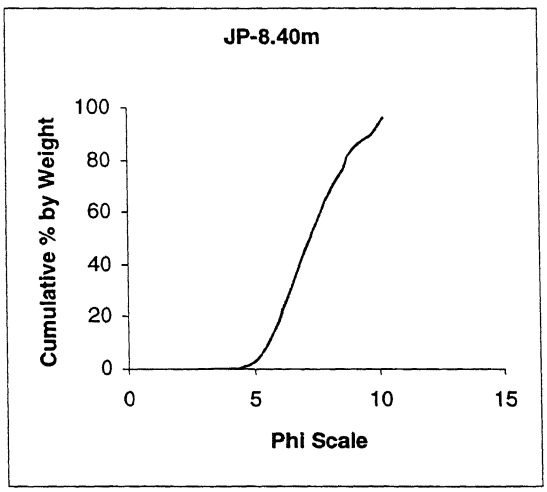


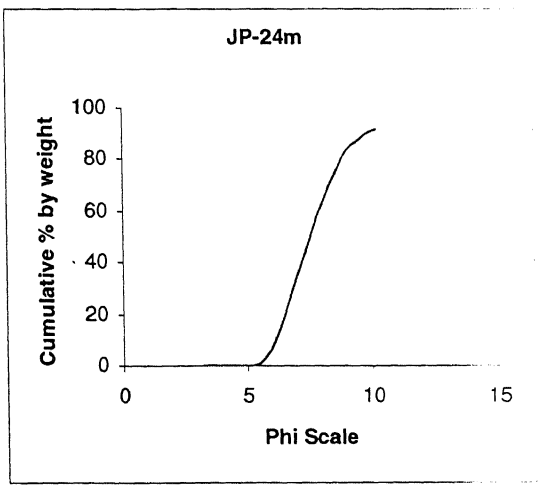


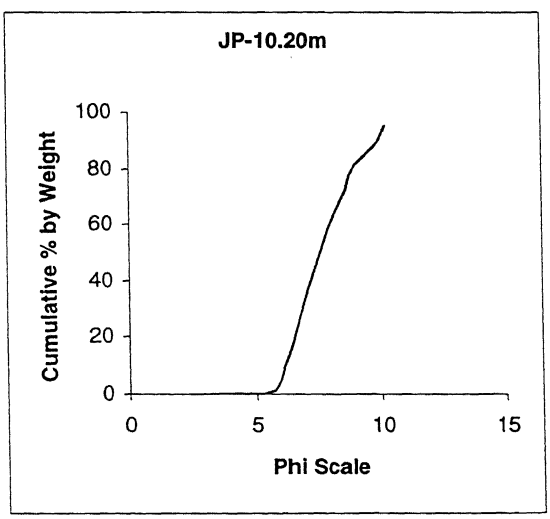


Fig. 4.18. Grain size plots of different stratigraphic units of Jagadishpur samples

The $H_2O_2$ reactive organic matter (Table.4.19) shows a significant decrease down depth in Unit 1. The top silty clay part shows a relatively higher organic matter content compared to the sample taken from sandy horizons of same unit. A decrease in the organic matter content was marked by a low value in Unit 3. Unit 4 shows a comparatively high organic matter content.

### 4.4.3 Sediment Mineralogy

Bulk XRD analysis of sediments shows presence of quartz, feldspar, mica, calcite, and amphiboles as the dominating minerals. Amphiboles are present mostly in the sandy horizons. Major clay minerals are illite, chlorite and kaolinite (Table 4.19). Smectite are absent but a mixed clay (11Å peak) was identified in a few samples. The concretions were mostly calcitic, present in Unit-2 with a decreasing $MgCO_3$ trend down depth (8% at the top to 3 % at bottom) (Chave, 1951).

**Table 4.19: Organic matter and sediment mineralogy for the Jagadishpur Drill Core**

| Units | Organic Matter Content (wt%) | Bulk mineralogy | | | | | logy Units | | | | Concretion mineralogy |
|---|---|---|---|---|---|---|---|---|---|---|---|
| | | Q (3.34Å) | F (3.19 Å) | M (10 Å) | Cc (3.03 Å) | Others | | I (10 Å) | Ch (14.4 Å) | K (3.57 Å | |
| 1(n=10) | 3.1 | ++++ | ++ | +++ | + | A++ | 1(n=6) | ++++ | ++ | + | _ |
| 2(n=2) | 2.2 | +++ | ++ | ++ | + | | 2 (n=2) | ++ | ++ | +++ | calcite |
| 3(n=5) | 1.7 | +++ | ++ | +++ | | A+ | 3(n=2) | +++ | +++ | + | _ |
| 4 (n=1) | 2.5 | +++ | ++ | ++ | | | 4 (n=1) | +++ | ++ | + | _ |

Q- Quartz, F-Feldspar, M-Mica, Amph- Amphibole, G-Goethite, Cc-Calcite, I-Illite, Chlorite, K-Kaolinite, Mx-Mixed layer clay; Sid- Siderite

++++ High; +++ Moderate; ++ Minor; + Trace

The semi-quantitative data on XRD mineralogy presented in Table 4.20 and Figure 4.19 indicates that quartz constitutes more than 85% of the bulk composition. A significant decrease in the quartz content is observed in Unit 1, at 5.1m and 8.7m depth, and again at the bottom of Unit 3 at 19.98m depth. Feldspars constitute around 10% of the bulk composition and a relatively high abundance is recorded at the bottom of Units 1 and 3. Illite is the major mineral (> 80%) in the clay fraction followed by chlorite and kaolinite.

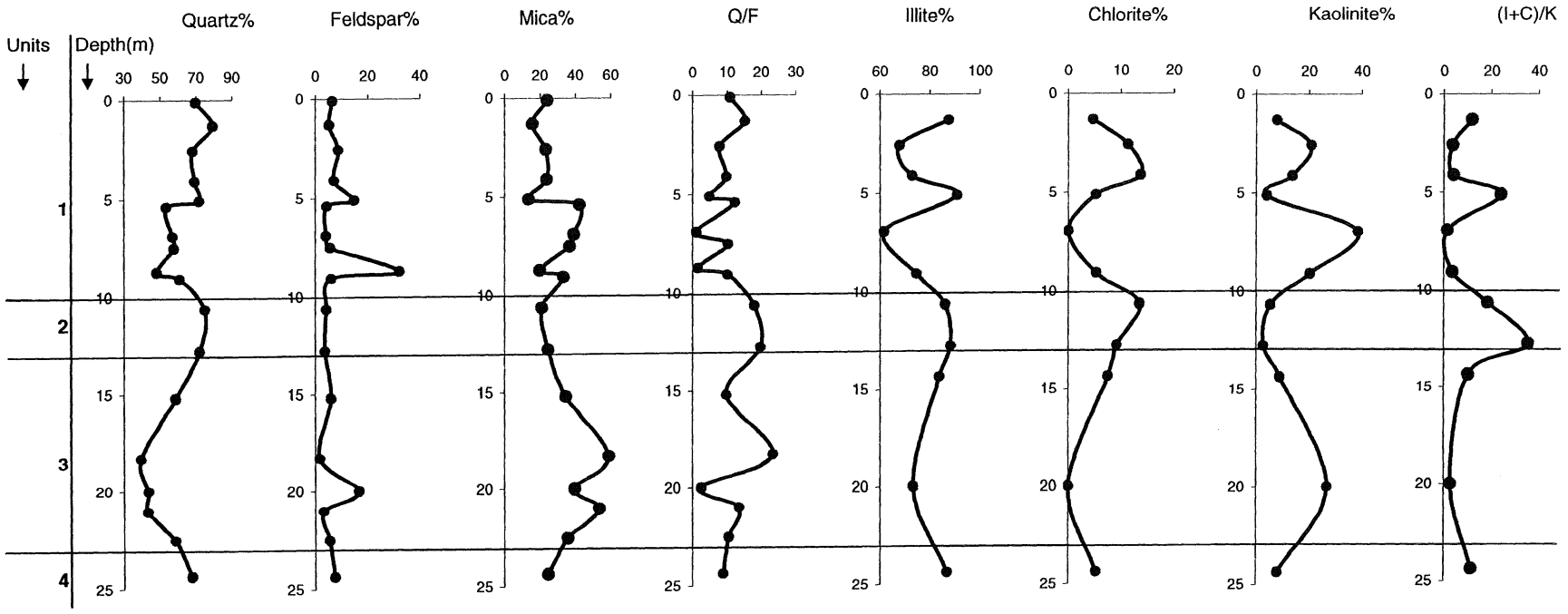


Figure. 4.19. bulk and clay menral abundance of Jagadisgpur drill core

low in Unit1 and 4 but is high in Units 2 and 3. (Illite + Chlorite)/Kaolinite ratio shows a very high value in the unit 2, and we also record a peak in the middle of Unit 1.

**Table 4.20: Relative abundance of minerals at Jagadishpur Core computed by normalization**

| Bulk powder | | | | | | | Smeared fine fraction | | | | |
|---|---|---|---|---|---|---|---|---|---|---|---|
| Units | Depth (m) | Q% | Felds% | Mica% | Q/F | Units | Depth (m) | Illite% | Chl % | Kaol % | (I+C)/K |
| 1 | 0.1 | 69.62 | 6.39 | 23.98 | 10.8 | 1 | 1.3 | 87.5 | 4.68 | 7.81 | 11.8 |
| | 1.3 | 79.13 | 5.21 | 15.65 | 15.1 | | 2.58 | 67.86 | 11.31 | 20.82 | 3.8 |
| | 2.58 | 68.02 | 8.72 | 23.25 | 7.80 | | 4.1 | 72.72 | 13.64 | 13.64 | 4.13 |
| | 4.1 | 69.23 | 7.1 | 23.66 | 9.75 | | 5.1 | 90.78 | 5.2 | 4 | 23.995 |
| | 5.1 | 71.6 | 14.76 | 13.62 | 4.85 | | 6.93 | 61.531 | 0 | 38.46 | 1.59 |
| | 5.4 | 53.43 | 4.36 | 42.19 | 12.2 | | 9.05 | 74.45 | 5.25 | 20.29 | 3.66 |
| | 6.9 | 56.98 | 4.05 | 38.96 | 1.076 | 2 | 10.62 | 86.02 | 13.44 | 5.37 | 18.52 |
| | 7.5 | 57.65 | 5.59 | 36.75 | 10.30 | | 12.75 | 88.14 | 9.12 | 2.74 | 35.49 |
| | 8.7 | 47.99 | 32.1 | 19.9 | 1.49 | 3 | 14.36 | 83.67 | 7.45 | 8.88 | 10.26 |
| | 9.05 | 60.78 | 6.03 | 33.18 | 10.07 | | 19.98 | 73.17 | 0 | 26.82 | 2.72 |
| 2 | 10.62 | 74.86 | 4.18 | 20.94 | 17.90 | 4 | 24.35 | 86.81 | 5.21 | 7.98 | 11.53 |
| | 12.75 | 71.89 | 3.64 | 24.47 | 19.7 | | | | | | |
| 3 | 15.2 | 58.57 | 5.98 | 34.45 | 9.794 | | | | | | |
| | 18.3 | 39.33 | 1.68 | 58.92 | 23.41 | | | | | | |
| | 19.98 | 43.51 | 16.73 | 39.74 | 2.607 | | | | | | |
| | 21 | 43.17 | 3.2 | 53.62 | 13.49 | | | | | | |
| | 22.5 | 58.54 | 5.57 | 35.87 | 10.57 | | | | | | |
| 4 | 24.35 | 67.78 | 7.54 | 24.68 | 8.98 | | | | | | |

I-Illite, C-Chlorite, K-Kaolinite

### 4.4.4 Magnetic Susceptibility Analysis

Table 4.21 shows the magnetic susceptibility values in the Jagadishpur drill core. The bulk magnetic susceptibility value ($\chi_{lf}$) and frequency dependent susceptibility values ($\chi_{fd\%}$) are plotted against depth in Figures 4.20 a & b.

The $\chi_{lf}$ value is uniformly low in this core except for a sharp peak at the base of Unit 1 accompanied with a minima in $\chi_{fd\%}$. The high $\chi_{lf}$ value may indicate presence of ferrimagnetic minerals at that horizon, which needs to be confirmed by magnetic mineralogical analysis. The plot of $\chi_{fd\%}$ with depth shows rapid fluctuations in the top 5m of the core, touches zero at ~9m and then remains low (1-1.5%). The overall magnetic domain is interpreted to be SD-PSD, with some MD grains and notable absence of SP

particles. The high value of $\chi_{lf}$ in the section correspond to very low $\chi_{fd\%}$ suggesting that ferrimagnetic mineral present in those horizon do not fall in SP domain.

**Table 4.21: Magnetic susceptibility data for Jagadishpur drill core samples**

| Units | Depth (m) | Corrected. Weight ($*10^{-3}$kg) | $\chi_{lf}$ ($*10^{-8}m^3$/kg) | $\chi_{hf}$ ($*10^{-8}m^3$/kg) | $\chi_{fd\%}$ |
|---|---|---|---|---|---|
| | 0 | 13.254 | 6.03 | 4.52 | 1.88 |
| | 0.3 | 12.281 | 15.4 | 13.84 | 0.85 |
| | 0.6 | 10.668 | 9.37 | 6.56 | 2.81 |
| | 0.9 | 11.262 | 6.21 | 4.43 | 2.53 |
| | 1.2 | 11.537 | 8.66 | 7.80 | 0.86 |
| | 1.5 | 10.994 | 7.27 | 5.45 | 2.27 |
| | 2.4 | 9.394 | 6.38 | 4.25 | 3.54 |
| | 2.7 | 11.04 | 5.43 | 4.52 | 1.50 |
| | 3 | 11.228 | 6.23 | 5.34 | 1.27 |
| | 3.3 | 10.212 | 4.89 | 3.91 | 1.95 |
| | 3.6 | 10.294 | 12.62 | 11.65 | 0.74 |
| | 4.2 | 7.708 | 6.48 | 5.189 | 2.59 |
| | 4.5 | 9.536 | 3.14 | 2.09 | 3.49 |
| | 5.4 | 12.754 | 14.8 | 14.11 | 0.41 |
| 1 | 6.9 | 11.881 | 6.73 | 5.89 | 1.05 |
| | 7.2 | 11.747 | 4.25 | 3.40 | 1.70 |
| | 7.5 | 10.917 | 5.49 | 4.58 | 1.52 |
| | 7.8 | 10.224 | 20.53 | 19.56 | 0.465 |
| | 8.1 | 10.039 | 25.89 | 24.90 | 0.38 |
| | 8.4 | 12.717 | 40.89 | 40.89 | 0 |
| | 8.7 | 11.751 | 63.82 | 62.96 | 0.11 |
| | 9.6 | 11.743 | 25.54 | 24.69 | 0.28 |
| | 9.9 | 9.73 | 16.44 | 16.44 | 0 |
| | 10.2 | 9.585 | 22.95 | 21.9 | 0.47 |
| 2 | 10.5 | 9.107 | 9.88 | 9.88 | 0 |
| | 10.8 | 11.12 | 12.58 | 11.69 | 0.64 |
| | 11.7 | 10.626 | 14.11 | 14.11 | 0 |
| | 12 | 9.49 | 9.48 | 8.42 | 1.17 |
| | 12.3 | 8.516 | 8.219 | 8.21 | 0 |
| | 12.6 | 9.111 | 9.87 | 8.78 | 1.21 |
| | 12.9 | 9.641 | 9 | 9.33 | 1.03 |
| 3 | 13.2 | 11.27 | 9.41 | 14.19 | 0.52 |
| | 13.5 | 11.84 | 9.5 | 16.04 | 0.42 |
| | 13.8 | 12.156 | 9.33 | 11.51 | 0.54 |
| | 14.1 | 10.207 | 10 | 14.69 | 0 |
| | 14.4 | 12.61 | 9.47 | 14.27 | 0.4 |

| | | | | | |
|---|---|---|---|---|---|
| | 14.7 | 11.83 | 10 | 17.75 | 0 |
| | 15 | 12.152 | 9.41 | 13.16 | 0.48 |
| | 15.3 | 12.381 | 8.75 | 5.65 | 1.00 |
| | 16.8 | 9.37 | 9.64 | 28.81 | 0.38 |
| | 17.4 | 12.786 | 9.09 | 7.82 | 0.7 |
| | 17.7 | 13.419 | 10 | 14.15 | 0 |
| | 18 | 12.591 | 8.75 | 5.55 | 0.99 |
| | 18.3 | 13.007 | 8 | 3.075 | 1.53 |
| | 19.8 | 12.936 | 9.61 | 19.32 | 0.29 |
| | 20.1 | 11.223 | 9.47 | 16.03 | 0.46 |
| | 21 | 14.586 | 9.33 | 9.59 | 0.45 |
| | 21.3 | 13.103 | 9.23 | 9.15 | 0.58 |
| | 21.6 | 12.448 | 9.28 | 10.44 | 0.57 |
| | 22.2 | 12.443 | 9.5 | 15.26 | 0.40 |
| | 22.5 | 12.549 | 9.33 | 11.15 | 0.53 |
| 4 | 23.1 | 11.169 | 8.88 | 7.16 | 0.99 |
| | 23.4 | 12.18 | 9.28 | 10.67 | 0.58 |
| | 23.7 | 11.544 | 9.16 | 9.52 | 0.72 |
| | 24 | 13.22 | 8.88 | 6.05 | 0.84 |
| | 24.3 | 11.565 | 8.75 | 6.05 | 1.08 |
| | 24.6 | 12.58 | 8.46 | 8.74 | 1.22 |

$\chi_{fd\%} = \{(\chi_{lf} - \chi_{hf}) / \chi_{lf}\} * 100$

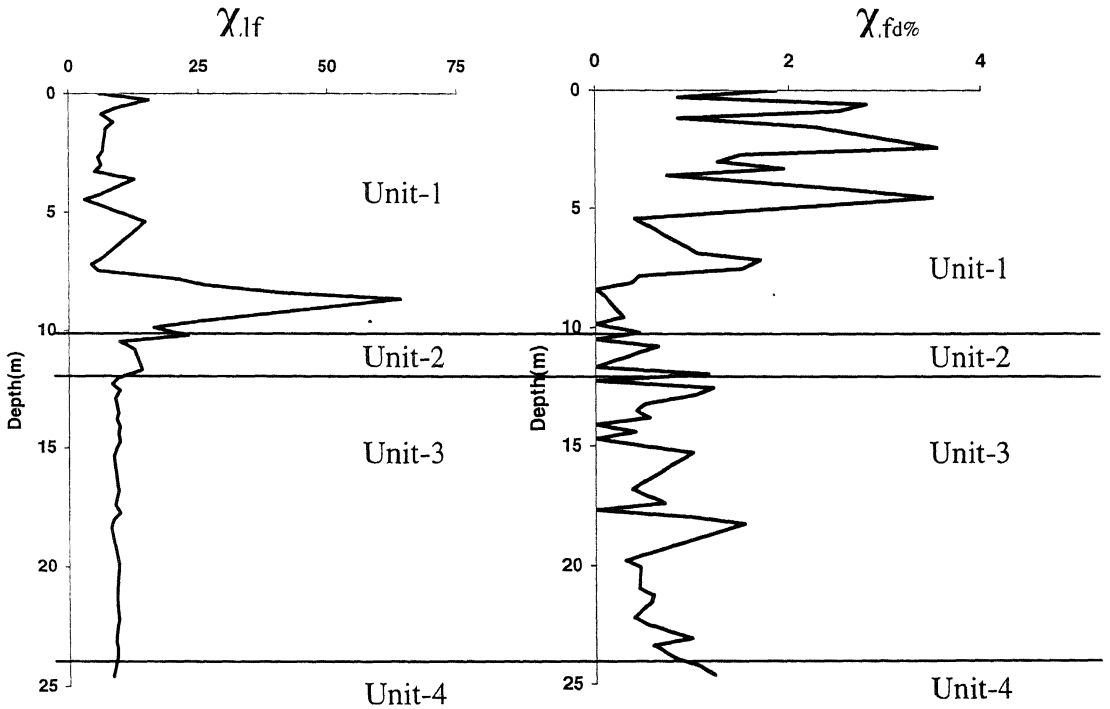


Figure.20a. bulk Magnetic susceptibility ($\chi_{lf}$) & b. frequency dependent susceptibility ($\chi_{fd\%}$ plots for Jagadishpur samples

### 4.4.5 Data Interpretation

The overall facies interpretation of the Jagdishpur core is very similar to that of Firozpur core. A summary table is given in table 4.22. Unit-1 is a dominantly sandy unit representing a **channel facies** capped by modern soil. Sand is quartz rich and becomes micaceous in the lower part of the unit. The lower part is also very high in bulk susceptibility indicating influx of coarse-grained detrital ferrimagnetic minerals as reflected from very low $\chi_{fd\%}$. On the contrary, the rapid fluctuations in $\chi_{fd\%}$ in the upper part suggests some finer magnetic minerals but the consistently low $\chi_{lf}$ values rule out any significant concentration of ferrimagnetic SP particles, like magnetite.

Similar to Firozpur, the underlying Unit-2 is a **floodplain deposit** consisting of silty clay sediments with thin dark clay bands, concretions, red/brown mottling and higher organic matter content than the overlying sandy facies. Bulk and clay mineralogy do not show any significant variation in this unit. Both $\chi_{lf}$ and $\chi_{fd}$ values remain low indicating absence of ferrimagnetic particles and the overall coarse-grained (PSD-MD) influx of magnetic minerals.

Unit-3 is another major sand facies, ~10m thick, interpreted as a **channel deposit**. A distinct concretion zone (if pedogenic) at ~21m may reflect a minor discontinuity in deposition of this unit. Minor pedogenesis is reflected from higher abundance of kaolinite. The magnetic characteristics are different from the upper sand unit and both $\chi_{lf}$ and $\chi_{fd\%}$ remain low indicating absence of ferrimagnetic minerals and dominance of paramagnetic minerals generally in PSD-MD domain.

Unit-4 is the bottom most muddy unit the base of which was not reached in the core. This unit is also interpreted as a **floodplain deposit** with minor pedogenesis manifested as mottling and sparse concretions. The magnetic properties characterize the magnetic minerals to be paramagnetic falling in PSD domain.

## Table 4.22 : Summary table for Jagadishpur drill core

| Units (Depth in m) | Physical Parameters and mean grain size | Organic Matter content | XRD Bulk minerals | XRD Clay minerals | Magnetic Analysis | Interpretation |
|---|---|---|---|---|---|---|
| 1(0-12) | Silty-clay at the Top to sandy at Bottom, fining up sequence | 3.1 (High in the Silty-clay) | Quartz, Feldspar ,mica, amphibole | Illite> Kaolinite> chlorite | Very low Susceptibility In upper level, Very high In sandy Horizons (possibly ferrimagnetic) . At Upper silty -clay presence of SD-PSD particles | Channel deposit |
| 2(12-19.87) | Clay to silty-clay | 2.2 (High in the clay | Quartz, Feldspar, calcite | Illite> Chlorite> kaolinite | No variation in Susceptibility and PSD-MD grains | Floodplain deposit |
| 3(19.87-21.25) | Silty-clay to fine To medium sand at bottom | 1.7 (Low in the Sandy Horizon) | Quartz, Feldspar, amphibole | Illite> Kaolinite> chlorite | Uniform Susceptibility, Coarse magnetic grains | Channel deposit |
| 4 (23.07-24) | Olive brown Silty clay (fine Grain size) | 2.5 (high) | Quartz, Feldspar, mica | Illite> kaolinite≥ chlorite | No variations In Susceptibility Coarse magnetic grains | Floodplain deposit |

## 4.5 Discussion

Stratigraphical and sedimentological data for Bithur cliff section along the Ganga river and three cores in the valley fills and floodplain have already been presented in the preceding sections. Thick sand bodies, separated by floodplain muds present in Firozpur and Jagadishpur cores testify multiple phases of channel activity at these sites and confirm them to be valley-fill deposits. A well developed floodplain mud unit at the Firozpur site indicates a period of discontinuity/shift in channel. The Bithur section represents a proximal floodplain setting with thick accumulation of floodplain mud at the bottom. However, the presence of swampy and eolian deposits at the top of the floodplain mud indicates a depositional discontinuity when the floodplain was detached from the main channel. The IITK site represents a distal floodplain environment throughout the ~86ka period having no major sand body in the top 50m of alluvial stratigraphy and the sediments indicate moderate weathering and digenetic activities.

The floodplain deposits at all locations, marked by the presence of kankars, red-brown mottling and rhizoconcretions, indicate a moderate to intense degree of pedogenesis, although individual soil profiles are difficult to identify. Presence of anti-ferromagnetic minerals and an increase in relative abundance of kaolinite in floodplain mud with respect to other minerals reflect variation in degree of pedogenic activity (Sangode and Kumar, 2001). The onset of inter-bedded swampy and eolian deposits at the top of the floodplain mud at Bithur represents a period of major discontinuity. The anaerobic environment in swamps with high organic content has encouraged the formation of SP magnetite (Maher, 1998; Lovely, 1987). The lower part of the swamp deposits are characterized by lesser kaolinite perhaps due to poorly drained conditions (Grim, 1953; Chamley, 1989) but a higher kaolinite abundance and antiferromgnetic minerals in the top part of the swamp deposits indicate more leaching and sub-aerial exposure (Eriksson and Sandgren, 1999). Such periodic water logging and subsequent dry phase encourage gleying process and release of iron from the parent minerals (Borgaard, 1997). The IITK drill site shows a moderate degree of pedogenic activity, particularly in the upper part of Unit-2 accompanied by slow sedimentation rate. The site

shows periodic influx of sediments with intermediate period of post-depositional/weathering phases.

Comparison of the Bithur section and other three drill core locations in terms of their OSL and $^{14}C$ ages indicates a collateral development of area with lateral facies variations. The similarity of ages (~26 ka) between lower sandy horizons at Jagadishpur and lower units of the Bithur section indicates a close relationship between these two locations in terms of stratigrpahic development. The Jagadishpur and Firozpur sites represent the sites of major channel deposition from 26ka to 6 ka. The top sand body at Jagadishphur indicates an age of 6-8 ka, which marks the age of channel abandonment at this site. The Bithur section developed as proximal floodplain deposit during this period with a major detachment phase perhaps during the LGM period when the rivel level was low. This interpretation is based on the age dates and is supported by the decline in the monsoonal intensity between ~30ka and LGM (Prell and Kutzbach, 1987). Comparison with proxy records of monsoon intensity suggest the detachment reflects decreased precipitation around Last Glacial Maximum (Marine Isotope Stage 2) during 20 ka period (Swain et al., 1983, Overpeck et al., 1996). During this time period, the river gradually shifted towards south-west from the Jagadishpur location to the present day position. During 6 ka the river completely abandoned its channel at Jagadishpur and came to the present location. High monsoonal precipitation during 5.5 ka probably increased discharge of the river relative to sediment load and may have promoted cliff-line incision (Overpeck et al., 1996). The balance between discharge and sediment load within the channel strongly influences the energy available for erosion and depending on this balance, the river could incise.

The IITK site represents accumulation of floodplain mud for more than 86 ka with varying rates of sedimentation. The lower parts of the core (below 20m) reflect a very rapid filling (2.5mm/year) but in the upper 20m, sedimentation rate is very slow (0.8mm/year), a value very close to the floodplain sedimentation rate of 1mm/year (Bloom, 1978).

My results are at variance with the available understanding of the region developed by earlier workers on various accounts. Firstly, the present-day position of the Ganga river is at least 6ka old as opposed to ~1ka proposed by Srivastava et al. (2002). The estimate by Srivastava et al (2002) was based on OSL date of ~1ka of the surface deposits of the scroll deposits within the meander loop. It is possible that the material dated by them represents a later flood deposit or channel fill. It may be noted that the area around Jagadishpur and Firozpur gets flooded occasionally even today. Secondly, Srivastava et al (2002) suggested that climatic factors may not have been a dominant factor in incision and considered that neotectonic activity to be the main reason for incision and cliff development in line with the earlier workers (Singh and Rastogi, 1973; Singh and Bajpai, 1989; Singh, 1996). However, the absence of any major subsurface faults or lineaments in the present area (except the alignment of the river itself which is a manifestation of cliff development) suggests little or no tectonic control for the development of the bank-section at Bithur. My chronological data and stratigraphic framework suggests that the climate must have been the dominant factor in the vertical and lateral facies variation in the region. Hydrological changes in the river regime induced by climatic fluctuations have certainly been the dominant controls of stratigraphic development and incision at Bithur. The channel abandonment phase at Jagadishpur and Firozpur and continued floodplain accumulation at IIT Kanpur are supported by chronological data and monsoonal intensity variation during the last 30 ka.

# Chapter 5

## Summary and Conclusions

The present work has focused on parts of the Ganga plain around Kanpur-Bithur region, Uttar Pradesh representing the Central Ganga plain with a major objective of establishing stratigraphic framework and depositional environment in the region. Three shallow subsurface drill cores (at IIT Kanpur, Jagadishpur and Firozpur) and one exposed section (at Bithur) have been studied. Integrated laboratory and field techniques were employed to study all sections. Detailed stratigraphic logging of exposed section and the drill cores was followed up by mineralogical and environmental magnetism studies. Sediment mineralogy was studied using powder X-ray diffraction for bulk samples and heating and glycolation experiments for the clay fraction. Environmental magnetic studies involved the measurement of magnetic susceptibility and magnetic mineralogical studies through induced magnetizatioin experiments. The major conclusions of this work are as follows:

1. The Bithur section shows an intercalation of floodplain, swamp and eolian facies, while Jagadishpur and Firozpur section represent thick channel facies separated by thin floodplain deposits. The IITK site does not record any sandy horizon for top 50m, indicating a more distal floodplain environment in recent times.
2. The alluvial succession at all sites is marked by strong discontinuities manifested in moderate pedogenesis and calcrete development in exposed sections and drill cores. Data on clay mineralogy and magnetic mineralogy of the sediments support this interpretation. The proximal site such as the Bithur has been 'attached' and 'detached' to the main river during the last ~25-30 ka and the detachment phases are represented by swamp or eolian facies over the floodplain.
3. Sediment mineralogy of the fine fraction has provided important information regarding the provenance of sediments and pedogenic environment. An illite-dominant assemblage and complete absence of smectite is in contrast with the alluvial sediments in the southern plains e.g. Kalpi section at the Yamuna river, ~80km south

of Kanpur where abundant smectite and vermiculites have been recorded (Banerjee, 2002).

4. Relative abundance of kaolinite in comparison to illite and chlorite serves as a good indicator of degree of chemical weathering. For example, the top part of Unit-2 at Bithur and at IITK site are interpreted as zone of leaching and chemical weathering and the interpretation is also supported by the magnetic data. The high abundance of kaolinite in some horizons are also marked with presence of antiferromagnetic minerals, due to sub-aerial exposure and leaching condition indicating soil forming process.
5. Magnetic mineralogy of the alluvial sediments in this region is dominated by ferrimagnetic minerals, like magnetite, mainly in SD-PSD domain size with few SP particles. Antiferromagnetic minerals, like hematite/goethite are also recorded but in lesser abundance.
6. Magnetic mineralogy of Bithur and IITK section shows very similar characteristics in term of magnetic minerals. Similarly, the Firozpur and Jagdishpur cores show striking similarities in susceptibility profiles.
7. It is inferred that the magnetic minerals in the sediments may have been derived from the breakdown of hornblende and garnet which is present as heavy minerals in the unaltered horizons of the section and profiles. The deeper sandy aquifers in this region, supposedly unaltered, have been reported to contain significant quantities of hornblende and garnet (Gokhale, 1971) which could serve as a major source of iron during pedogenic alteration of sediments.
8. Geochronological data (OSL and $^{14}C$ ages) suggest that Jagadishpur and Firozpur were sites of active channel deposition between ~26 ka and 6ka and the area around Bithur kept accumulating floodplain sediments through overbank flooding. During this phase, the river level went down, perhaps during the Last Glacial Maximum (LGM) period represented by development of swamp and eolian facies. Around 6 ka, the depocenter of the river shifted from the Jagdishpur-Firozpur to the preset-day position at Bithur.
9. The river started incising the valley at Bithur in response to increased water budget between 5-6 ka thereby producing the high cliffs at Bithur. It is concluded that the

south-west migration of the Ganga river and the ensuing incision section at Bithur are produced by an interplay of hydrological and climatic conditions rather than by tectonic processes. Further, the present-day position of the Ganga river at Bithur is ~6ka old in contrast to the residence time ~1ka proposed by earlier workers.

10. The area around IIT Kanpur, which forms an upland area today, remained in the distal floodplain setting at least since ~86ka albeit with varying rates of sedimentation.

This work has provided significant new understanding to the alluvial stratigraphic development and post-depositional changes. Some recommendations for the future work are as follows:

1. The differentiation between stratigraphic development, sediment source and pedogenic processes between the Ganga plains (a dominant northern supply of sediments) and the Yamuna plains (a mixed sediment supply from northern and southern source) must be developed more rigorously.
2. Petrographic and geochemical work on concretions could provide valuable information on pedogenic processes and coupled with carbon and oxygen isotope data, climatic fluctuation in the region may be picked up.
3. Additional work on magnetic mineralogy on the cores utilized in this work and additional cores from the Yamuna plains could also provide information on sediment source and post-depositional alteration. More in-depth understanding of the magnetic phases supported by Mossabauer Spectroscopy would be required for confirmations of the minerals.

# References

Agarwal, A.K., Rizvi, M.H., Singh, I.B., Kumar, A., Chandra, S (1992), "Carbonate deposits in Ganga plain", In: Terra Incognita (ed. I.B.Singh), Lucknow University, pp. 35-43.

Babu, G.P. (2003), "Geomorphic characterization and evolution of the Ganga-Yamuna interfluve: a remote sensing approach", unpublished M.Tech thesis, IIT Kanpur. 105 pp.

Bajpai, V.N (1989), "Surface and subsurface evidence of neotectonics and the aquifer disposition in central Gangetic alluvial terrain of Kanpur-Unnao region in Uttar Pradesh, India", Journal of the Indian Society of Remote Sensing, vol. 17, No. 2, pp. 47-53.

Bajpai, V.N. and Gokhale, K.V.G.K. (1986), "Hydrogeomorphic classification of the marginal Gangetic alluvial plain in Uttar Pradesh, India, using satellite imageries", Journal of Geological Society of India, vol. 28, pp. 9-20.

Banerjee, A (2002), "Mineralogy and geochemistry of sediments at an incised bank of river Yamuna near Kalpi", unpublished M.Tech thesis, IIT Kanpur, 57 pp.

Barthes, V., Pozzi, J.P., Vibert-Charbonnel, J.P., Thibal, J., Melieres. M.A (1999), "High-resolution chrono-stratigraphy from downhole susceptibility logging tuned by paleoclimatic orbital frequencies", Earth and Planetary Science Letters, vol. 165, pp. 97-116.

Bazylinski, D.A. and Moskowitz, B.M. (1997), "Microbial biomineralization of magnetic iron minerals : microbiology, magnetism and environmental significance", In: Geomicrobiology : Interactions between Microbes and Minerals (J.F.Banfield and K.H Nealson, eds.), Reviews in Mineralogy, vol. 35, pp. 181-223.

Berger, A. (1988), "Milankovitch theory and climate", Reviews in Geophysics, vol. 26, pp. 624-657.

Biscaye, P.E. (1965), "Mineralogy and sedimentation of recent deep sea clay in the Atlantic Ocean andadjacent seas and Oceans", Society of America Bulletin , vol.76, pp. 803-831.

Bloemendal, J. and DeMenocal, (1989), "Evidence for a change in the periodicity of tropical climate cycles at 2.4Myr from whole-core magnetic susceptibility measurements", Nature, vol. 342, pp. 897-900.

Bloom, A.L (1978), Geomorphology, Prentice-Hall of India Pvt. Ltd, pp 510.

Blum, M.D. and Tornquist, T.E. (2000), "Fluvial responses to climate and sea-level changes: a review and look forward", Sedimentology, vol. 46, pp.2-48.

Borgaard, O.K. (1997), "Composition, properties and development of Nordic soils", In: Geochemical process, weathering and groundwater recharge in catchment, (Saether O.M. and Decariat, P. eds.), Balkema, pp. 21-75.

Carllisle, D. (1983), "Concentration of uranium and vanadium in calcretes and gypcretes", In: Geological Society London Special Publication, R.C.L.Wilson (eds.), pp. 185-195.

Chamley, H, (1989), Clay sedimetology, Springer-Verlag, Berlin, pp.618.

Chaturvedi, A.K and Raymahashay, B.C. (1981), "Groundwater chemistry and formation of carbonate concretions in alluvial soils", Journal of Geological Society of India, vol. 22, pp. 331-335.

Chave, K.E. (1952), "A solid solution between calcite and dolomite", Journal of Geology, vol. 60, pp.190-192.

Cook, H.E., Johnson, P.D., Matti, J.C., Zemmels, I. (1975), "Methods of sample preparation and X-ray diffraction data analysis", Initial reports of the Deep Sea Drilling Projects, vol. XXVIII, pp. 999-1007.

Dalan, R.A. and Banerjee, S.K. (1998), "Solving archaeological problems using techniques of soil magnetism", Geoarchaeology, vol. 13, pp. 3-36.

Dasgupta, S., Mukhopadhyay, M., Nandy, D.R. (1987), "Active transverse features in the central portions of the Himalaya", Tectonophysics, vol. 136, pp. 255-264.

Dasgupta, S. (1993), "Tectono-geologic framework of the eastern Gangetic foredeep", Geological Survey of India special publication, vol. 31, pp. 61-69.

Dewey, J.F. and Bird, J. M. (1970), "Mountain belts and new global tectonics", Journal of Geophysical Research, vol. 40, pp. 695-707.

Eriksson, M.G. and Sandgren, P (1999), "Mineral magnetic analyses of sediment cores recording recent soil erosion history in Central Tanzania", Palaeogeography, Palaeoclimatology, Paleoecology, vol. 152, pp. 365-383.

Evans, M.E. and Heller F. (2003), Environmental magnetism, Academic press, California, pp 299.

Flanders, P.J. (1994), "Collection, measurement and analysis of airborne magnetic particulates from pollution in the environment", Journal of Applied Physics, vol. 75, pp. 5931-5936.

Gibling, M.R., Tandon, S.K., Sinha, R., Jain, M. (in press), "Modern interfluve and their expression in the late Quaternary records of the southern Gangetic plains".

Gokhale, K.V.G. K (1971), "A case study for hydro-geological investigations in planning for ground water explorations", In: Symposium in water resources, held at IISC, Bangalore, pp. B11-1 – 11-7.

Grim R.E. (1953), Clay mineralogy, Mcgraw Hill Book Company, New York, pp. 384.

Jain, V. and Sinha, R. (2003), "River systems of the Ganga plains and their comparison with Siwaliks: a review", Current Science, vol. 84, pp. 1025-1033.

Jelinowska, A.P., Tucholka, F., Gasse, F., Frontes, J.C., (1995), "Mineral magnetic record of environment in Late Pleistocene and Holocene sediments, Lake Manas, Xinjiang, China", Geophysical Research Letters, vol. 22, pp. 953-956.

Karbassi, A.R. and Shankar, R. (1994), "Magnetic susceptibility of bottom sediments and suspended particulates from Mulki-Pavanje river, estuary and adjoining shelf, west coast of India", Journal of Geophysical Research, vol.99, pp. 10207-10220.

Lean, C.M.B. and McCave, I.N. (1998), "Glacial to interglacial mineral magnetism and palaeocanographic changes at Chatham Rise, SW Pacific Ocean", Earth and Planetary Science Letters, vol.163, pp. 247-260.

Lovely, D.R., Stolz, J.F., Gordon N.L., Elizabeth, J.P. (1987), "Anaerobic production of magnetite by a dissimilatory iron-reducing microorganism", Nature, vol. 330, pp. 252-254.

Maher, B. A. and Thompson, R. (1995), "Paleorainfall reconstructions from pedogenic magnetic susceptibility variations in the Chinese loess and paleosols", Quaternary Research, vol. 44, pp. 383-391.

Maher, B.A. (1988), "Magnetic properties of some synthetic submicron magnetite", Geophysical Journal, vol. 94, pp. 83-96.

Maher, B.A. (1998), "Magnetic properties of modern soil and Quaternary loessic paleosols : Paleoclimatic implications, Palaeogeography, Palaeoclimatology, Paleoecology, vol. 137, pp. 25-54.

Maher, B.A. (2003), "Magnetic mineralogy of soils across Russian Steppe: climatic dependence on pedogenic magnetite formation", Palaeogeography, Palaeoclimatology, Paleoecology, vol.201, pp. 321-341.

Mann, U. and Muller, G (1980), X-ray mineralogy of deep sea drilling project Legs-51 through 53, Western North Atlantic, Initial reports of the Deep Sea Drilling Projects, vol. LI,LII,LIII, pp. 721-729.

Mullins, C.E. (1977), "Magnetic susceptibility of the soil and its significance in soil science – A review", Journal of Soil Science, vol. 28, pp. 223-246.

Overpeck, J., Anderson, D., Trumbore, S (1996), "The southwest Indian monsoon over the last 18000 years", Climate dynamics, vol. 12, pp.213-225.

Peck, J. A. J.A., King, J.W, Colman, S.M., Kravchinsky V.A (1994), "A rock-magnetic record from Lake Baikal, Siberia: Evidence for late Quaternary climate change", Earth and Planetary Science Letters, vol. 122, pp.221-238.

Prakash, B. and Kumar, S. (1991), "The Indo-Gangetic Basin", In: Tandon S.K., Pant, C. C. and Casshyap, S.M. (eds.) Sedimentary Basins of India, Proceedings of the seminar held at Department of Geology, Kumaun University, Nainital, Gyanodaya Prakashan, Nainital, India, pp. 147-170.

Prell, W.L. and Kutzbach, J.E. (1987), "Monsoon variability over the past 150,000 years", Journal of Geophysical Research, vol.92, pp. 8411-8425.

Radhakrishnamurty C. (1985), "Identification of titanomagnetites by simple magnetic techniques and application to basalt studies", Journal of Geological Society of India, vol. 26, pp. 640-651.

Rao, M.B.R. (1973), "The subsurface geology of the Indo-Gangetic plains", Journal of the Geological Society of India, vol. 14, pp. 217-242.

Sangode, S.J., Bloemendal, J., Kumar, R., Ghosh, S.K. (2001), "Plio-Pleistocene pedogenic changes in the Siwalik Paleosols : A rock magnetic approach", Current Science, vol. 81, pp. 387-392.

Sangode, S.J., Suresh, N., Bagati, T.N. (2001), "Godavari source in the Bengal fan sediments: results from magnetic susceptibility dispersal pattern", Current Science, pp. 660-663.

Sangode, S. J. and Kumar R. (2003), "Magnetostatrigraphic correlation of the late Cenozoic fluvial sequences from NW Himalaya, India, Current Science, vol.84, pp. 1014-1024.

Schumm, S.A. (1993), "River response to base level change: Implications for sequence stratigraphy", The Journal of Geology, vol.101, pp. 279-294.

Seimnuilk, V and Searle, D.J. (1985), "Distribution of calcrete in Holocene coastal sands in relationship to climate, southwestern Australia", Journal of Sedimentary Petrology, vol.55, pp. 86-95.

Sinha R. and Jain, V. (2002), "Quaternary geomorphology of the upper and middle Ganga plains", In: Tandon S.K. and Thakur B.C. (eds.), Special volume on Quaternary Geology of India, Manisha Publications, pp.117-142.

Srivastava, P., Parkash, B., Sehgal, J.L., Kumar. S. (1994), "Role of neotectonics and climate in development of the Holocene geomorphology and soils of the Gangetic plains between the Ramganga and Rapti rivers", Sedimentary Geology, vol. 94, pp. 129-151.

Srivastava, P., Sharma, M., Singhvi, A.K (2002), "Luminescence chronology of incision and channel pattern changes in the river Ganga, India", Geomorphology, vol. 51, No. 4, pp. 259-268.

Srivastava, P., Singh, I.B., Sharma, S., Shukla, U.K., Singhvi, A.K. (2003), "Late Pleistocene-Holocene hydrologic changes in the Interfluve areas of the central Ganga plain, India", Geomorphology, vol. 54, pp. 279-292.

Swain, A.M., Kutzbach, J.E., Hastenrath, S. (1983) "Estimates of Holocene precipitation for Rajasthan, India, based on pollen and lake level data", Quaternary Research, vol. 19, pp. 1-17.

Tandon S.K. and Kumar S. (1999), "Semi arid-arid zone calcretes: a review", In: Fluvial geomorphology workshop, IIT Kanpur (2000), pp. 352.

Tucker, M. (1988), Techniques in sedimentology, Blackwell Scientific Publication, Oxford, pp. 394.

Valdiya, K. S. (1976), "Himalayan transverse faults and folds and their parallelism with subsurface structures of North Indian plains", Tectonophysics, vol.32, pp. 353-386.

Verosub, K.L. and Roberts, A.P. (1995), "Environmental magnetism: past, present and future", Journal of Geophysical Research, vol. 100, pp. 2175-2192.

Wadia, D.N. (1975), Geology of India, 4th edition, Tata McGraw Hill, New Delhi.

Wright, V.P. and Tucker, M.E. (1991), "Calcretes: an introduction", In: Calcrete: International Assoc. Sedimentogists Reprint Series 2, pp.1-22.